Antiferromagnetic Materials: Characterisation techniques

Bryan Gallagher, Nottingham University

Experimental techniques which can be used to characterize AF materials.


Exclusive Jewellery for Pets- Combined with the power of Magnets!
MagnetAnimal
Energise your pet

Dr. Bakst Magnetic Shoe Inserts

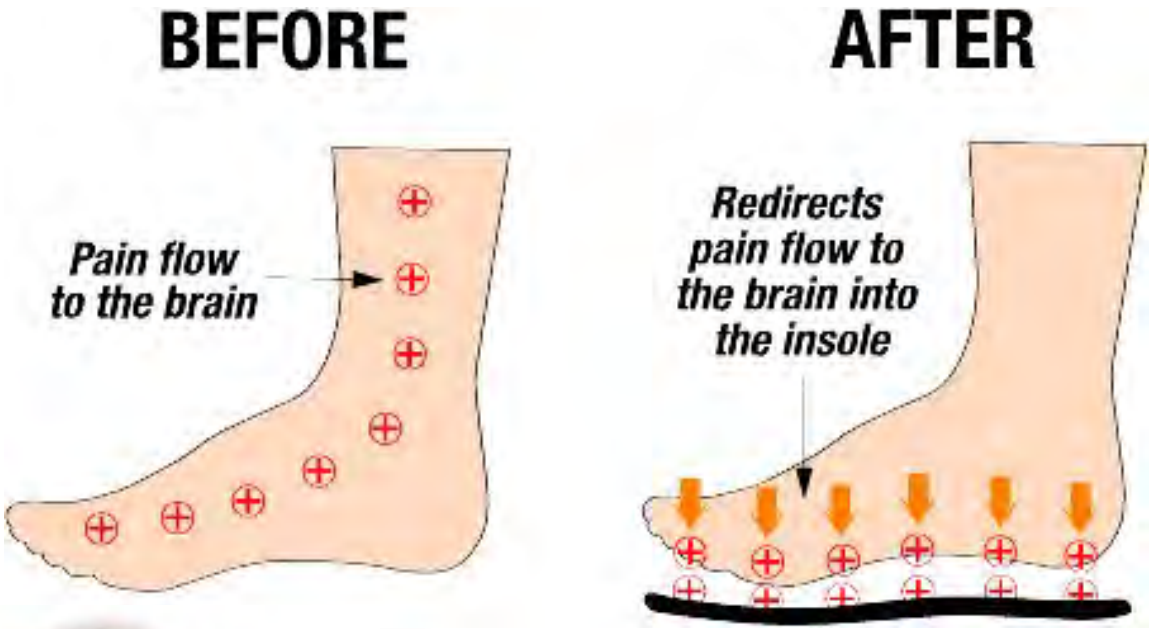

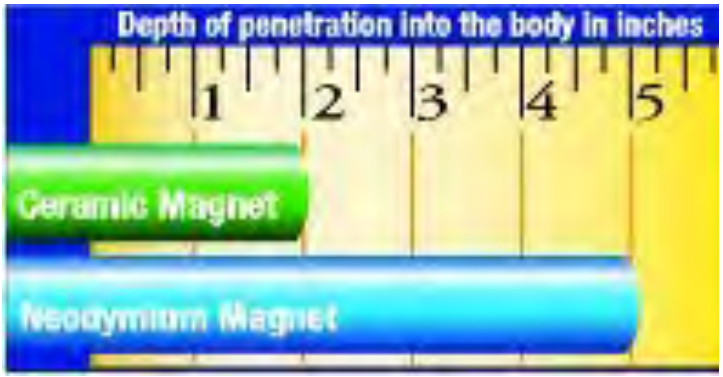

https://www.amazon.com/Dr-Bakst-Magnetic-Shoe-Inserts/dp/B00N3IPCBI?th=1

Talk Contents

1. Materials Growth

Molecular Beam Epitaxy (MBE)

Richard Campion 9.30 Friday

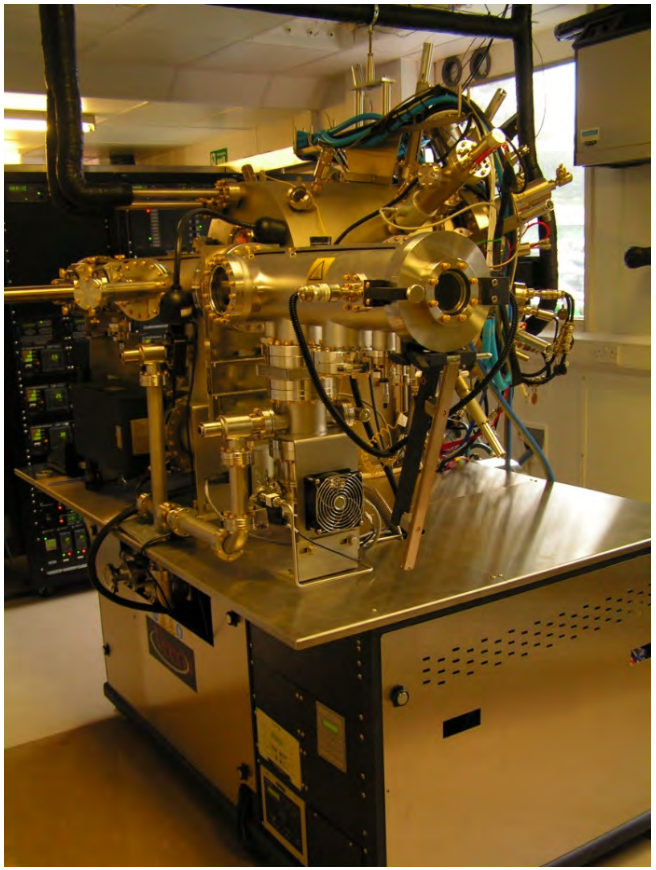

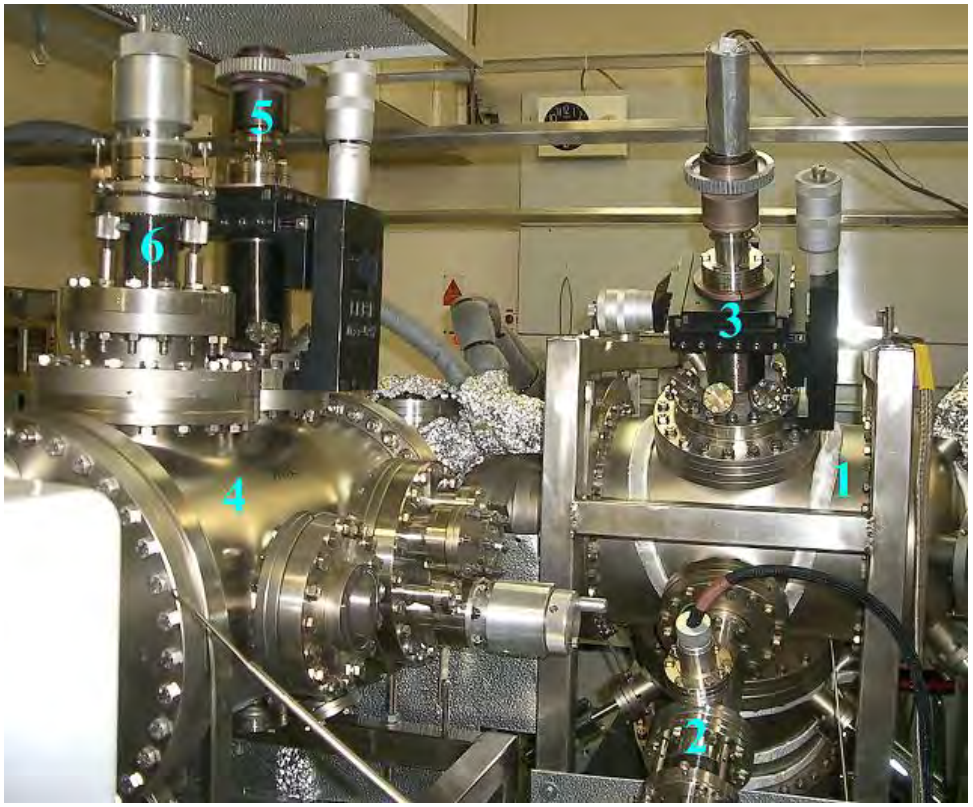

Molecular Beam Epitaxy

Can achieve (with regular calibrations)

- Very good epitaxy
- Very good control of stoichiometry
- Accurate growth temperature control
- Monolayer by monolayer growth
- Abrupt interfaces

In situ monitoring of crystal structure

Reflection high energy electron diffraction (RHEED)

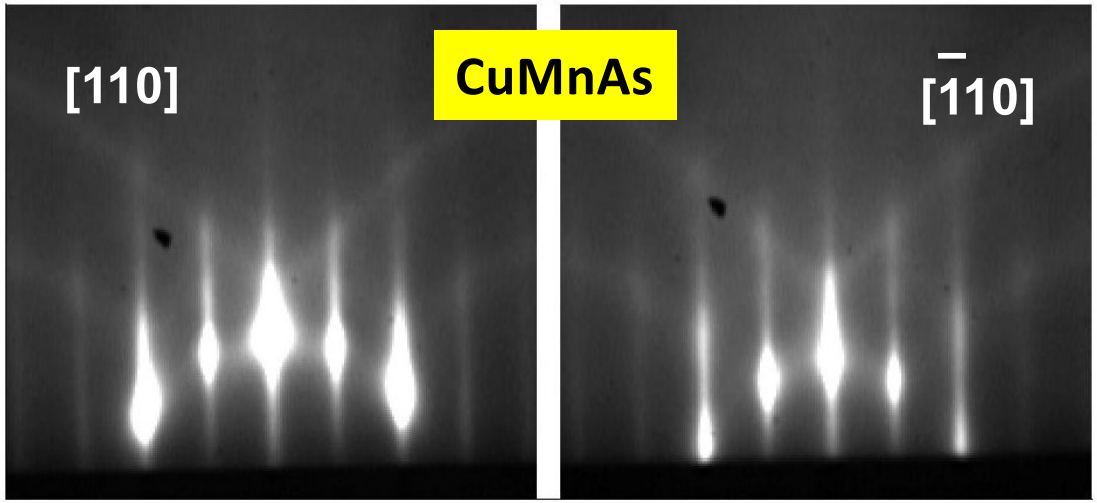

Very slow
Very expensive

Good for materials structurally compatibly with commercial semiconductors

Limited number of elements in a specific machine

Sputter Deposition Facilities

- Very flexible
- Relatively fast and low cost
- Can achieve close to epitaxial growth
- Very wide range of elements
- Can co-deposit from multiple sources
- Can sputter in reactive gas (O_2) or from composite targets (e.g. MgO)

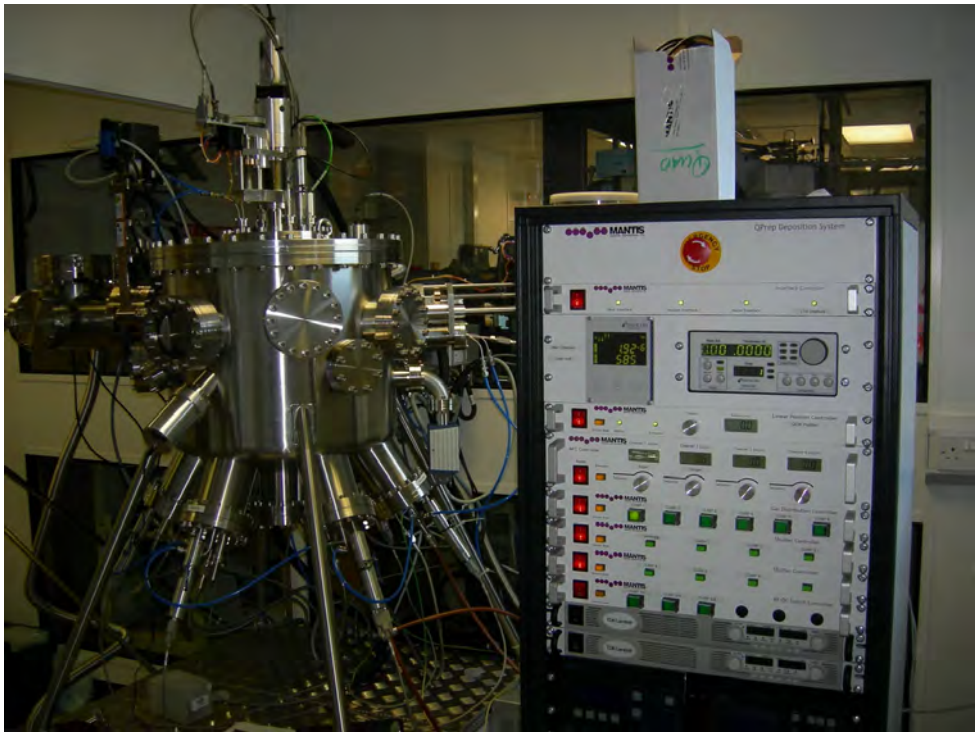

Good to have access to MBE and sputtering

2.1 Structural Characterisation: X-Ray Diffraction (XRD)

- **X-ray diffraction can reveal crystallographic structure.**
- **Want x-ray wavevector, $k \approx$ reciprocal lattice vector, $G \approx 10^{10}$ m^{-1}.**
- **For $k = 10^{10}$ m^{-1} x-ray energy is $\varepsilon = 21$ keV.**
- **Scattering almost elastic since $\varepsilon >>$ phonons and magnons energies (~25meV at room temperature).**

Phillips X-Pert high-resolution X-ray diffractometer

Elastic X-Ray Scattering

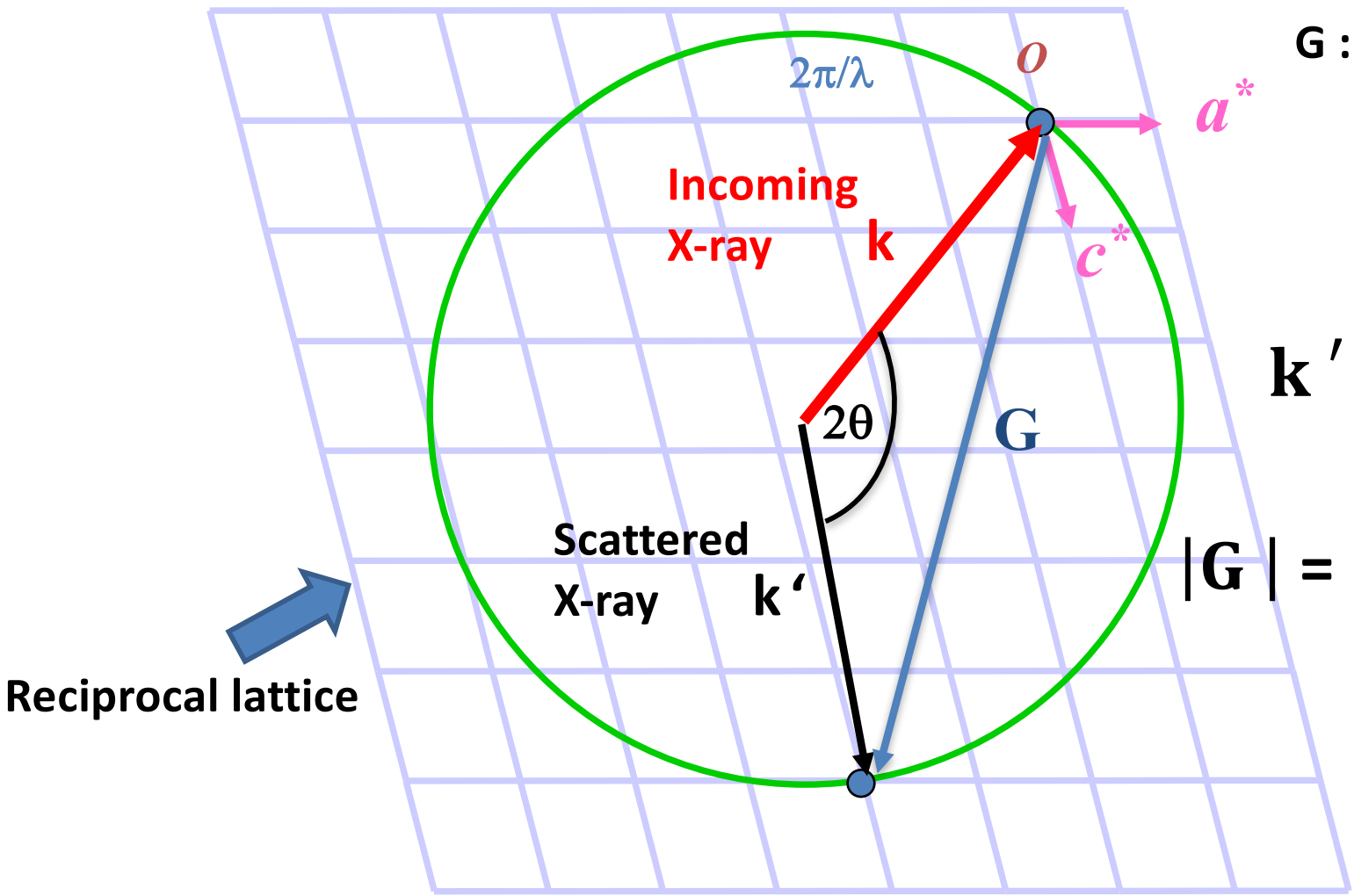

G : reciprocal lattice vector

$$\mathbf{k}' = \mathbf{k} + \mathbf{G}$$

$$|\mathbf{G}| = 2\sin(\theta)|\mathbf{k_n}|$$

Bragg's Law in Reciprocal Space (Ewald Sphere)

X-ray Scattering Amplitude

$$A(\boldsymbol{Q}) \propto \int \rho(\boldsymbol{r})\exp[i\boldsymbol{Q}.\boldsymbol{r}]d\boldsymbol{r} \propto \sum_{j} f_j(\boldsymbol{Q})\exp[i\boldsymbol{Q}.\boldsymbol{r_j}]\sum_{T}\exp[i\boldsymbol{Q}.\boldsymbol{r_j}]$$

$\boldsymbol{Q}$ scattering vector $\rho(\boldsymbol{r})$: electron charge density $f_j(\boldsymbol{Q})$ atomic structure factor
T translation vectors

Inverse problem: infer real space structure from reciprocal space structure

Peak Positions → Translational symmetries
Atom positions in basis

Peak Intensities → Atom types in basis
Order / disorder

Peak Widths → Extent of periodicity
crystallite size / film thickness

X-ray diffraction from NaCl crystal

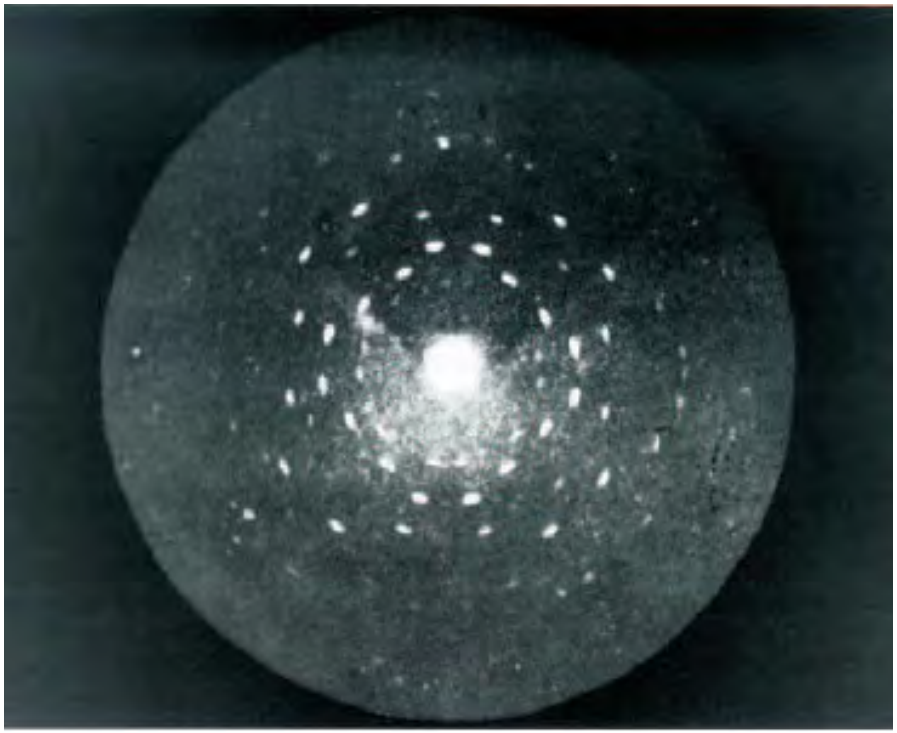

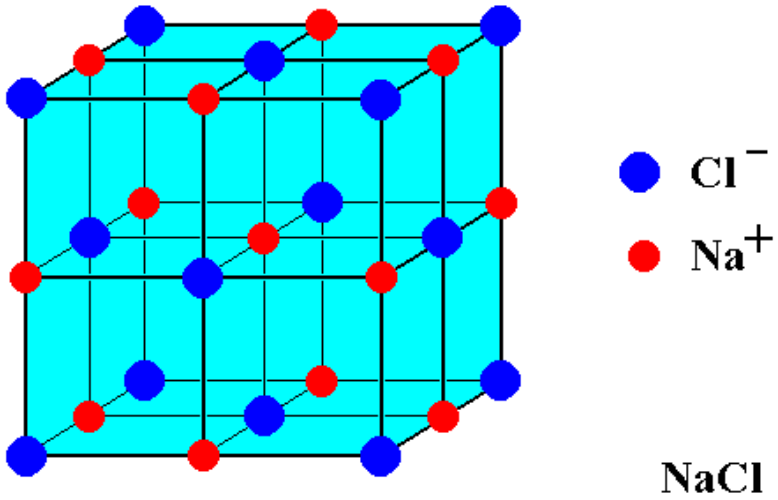

One of the first diffraction photographs taken M. von Laue in 1912

Crystal structure determined from Laue pattern by W. H. and W. L. Bragg in 1913

X-ray diffraction from protein Myoglobin

Image: ~3000 diffraction spots → positions of ~ 3000 atoms in protein

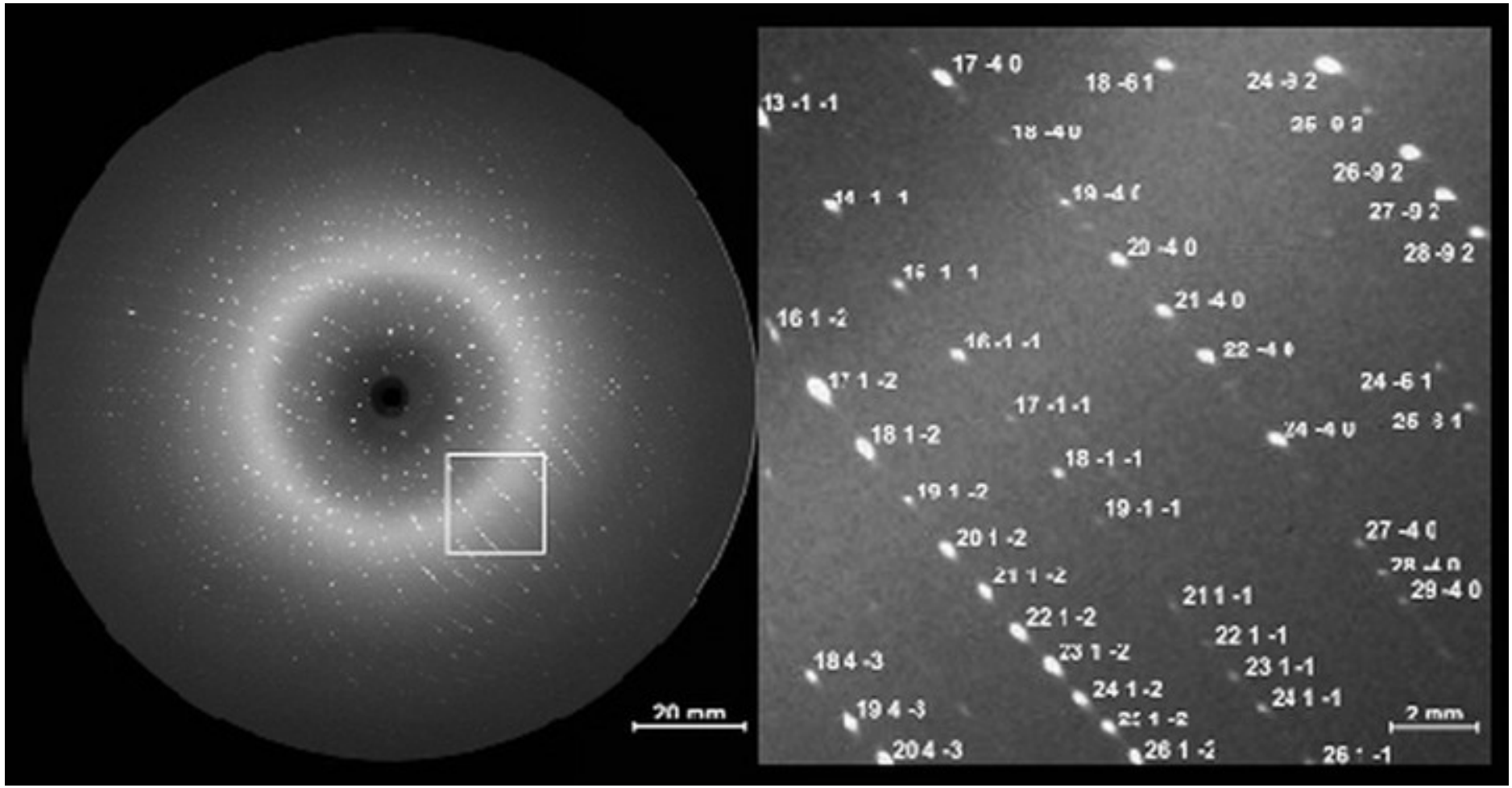

Myoglobin

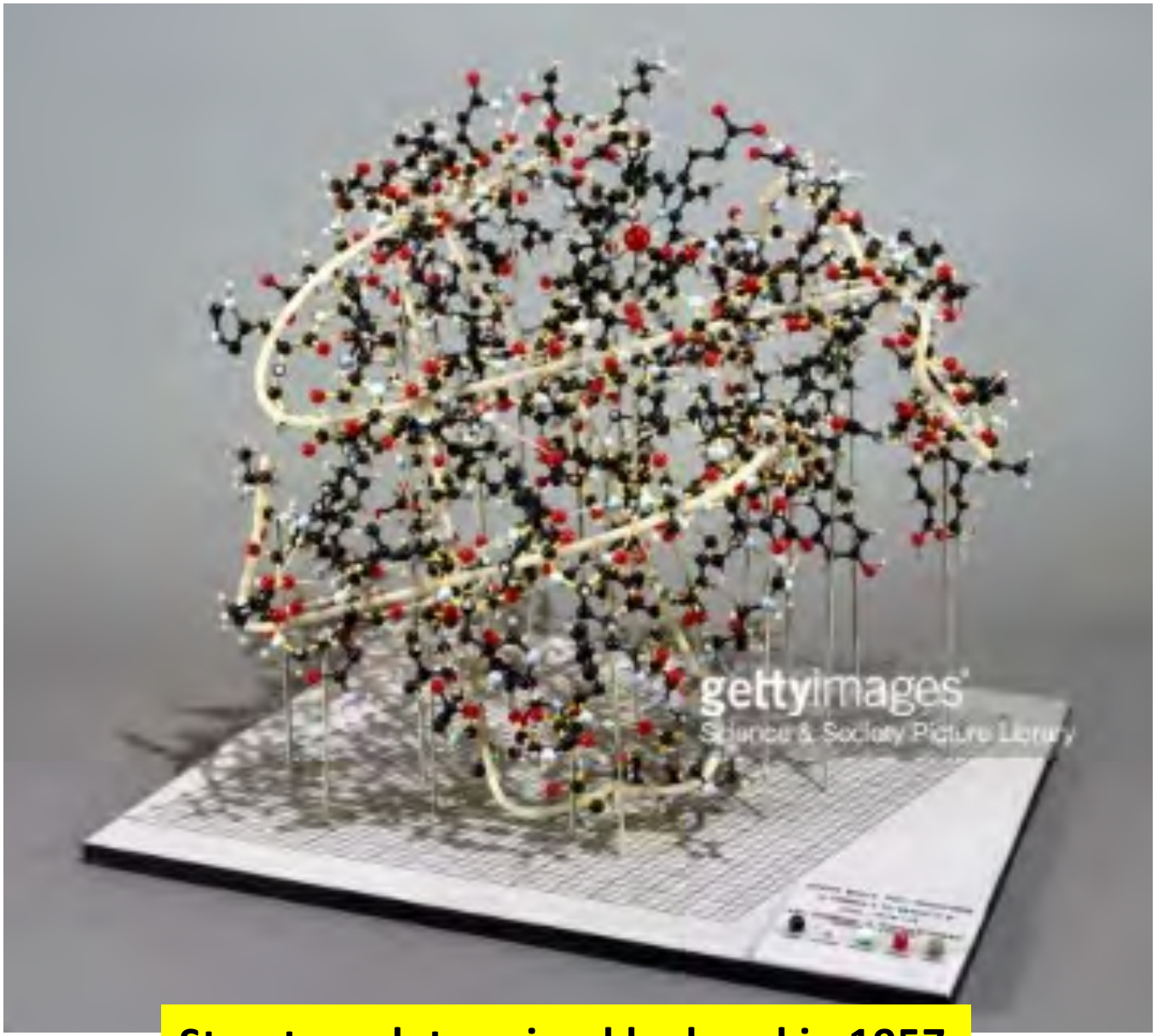

Structure determined by hand in 1957

AF CuMnAs Grown on (100) GaAs or GaP

Structure resolution: Cu_2Sb type structure Tetragonal P4/nmm
a = b = 3.820 A c= 6.318 A

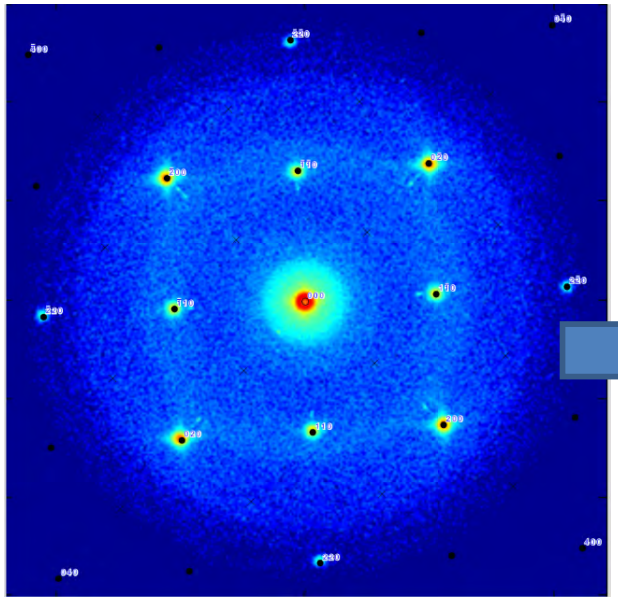

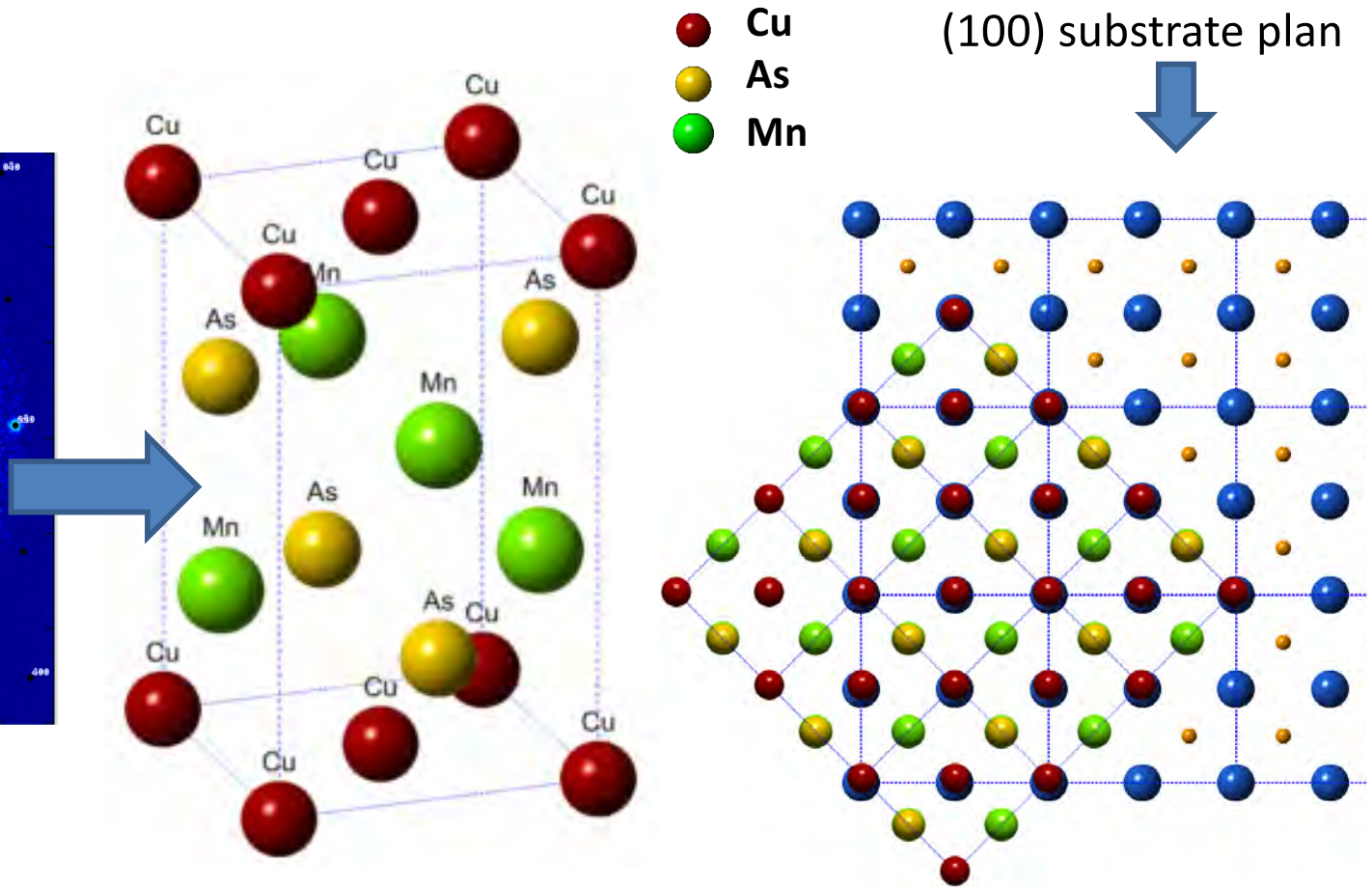

Wadley, Jungwirth, Marti, Zelezny *et al Nat. Commun. (13) DOI: 10.1038/ncomms3322*

Crystal quality of CuMnAs

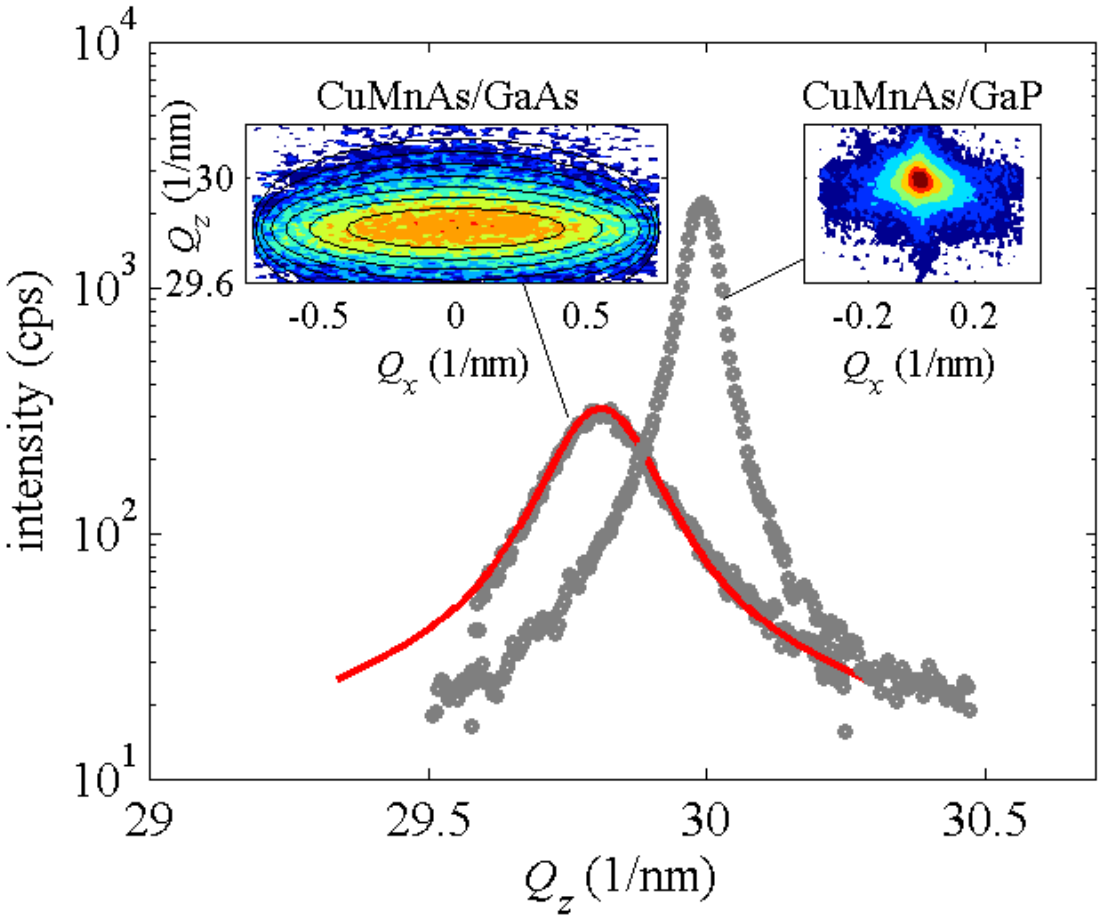

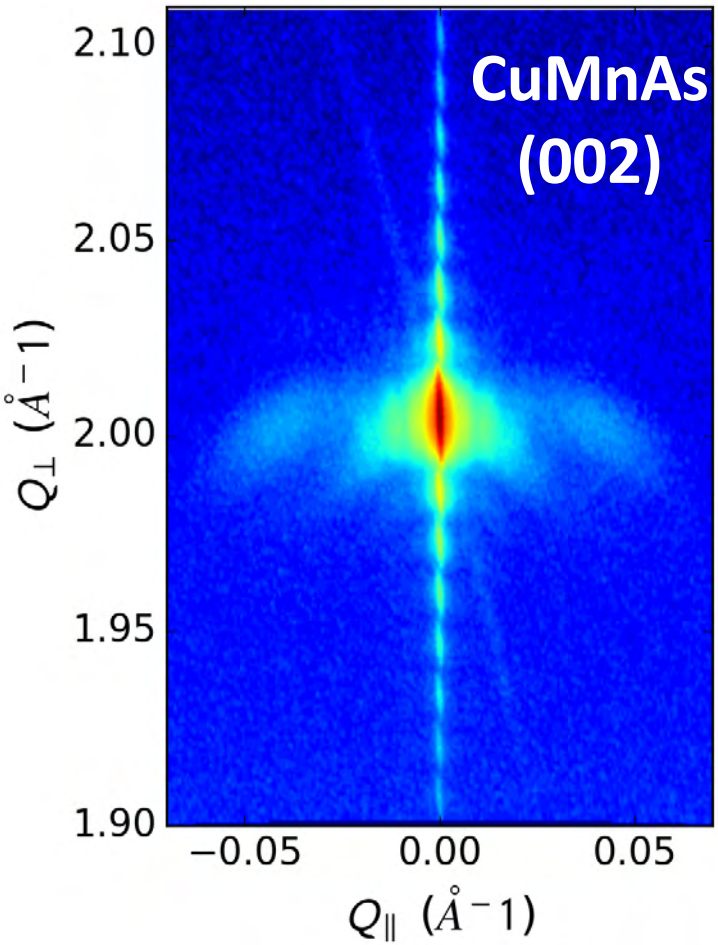

- **Narrower peaks** on better lattice matched GaP substrate: **Higher quality**
- Relaxed mosaic block structure on GaAs
- Fully strained on GaP

Wadley, Jungwirth, Marti, Zelezny *et al Nat. Commun. (13) DOI: 10.1038/ncomms3322*

FM (Ga,Mn)As Grown on GaAs

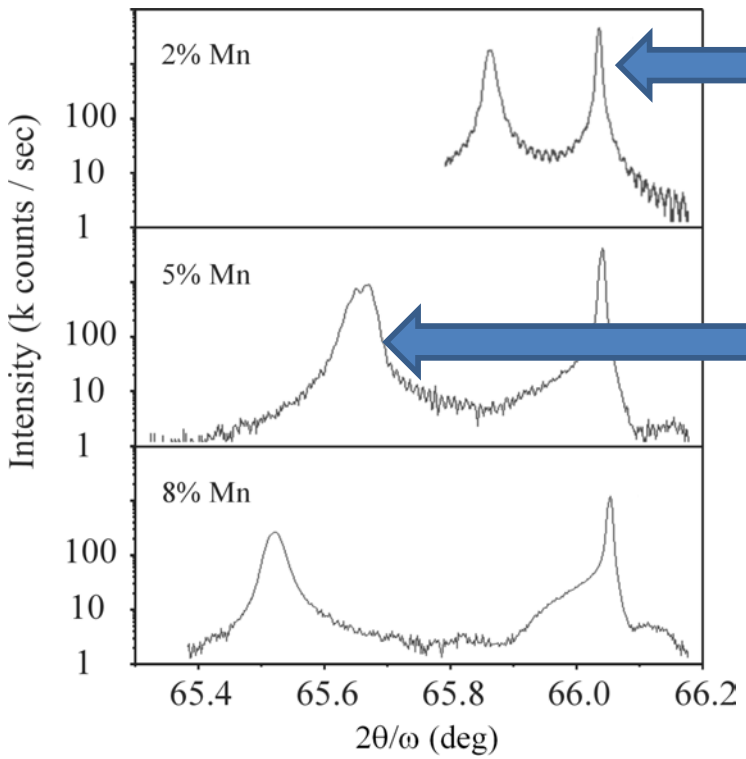

GaAs substrate

(Ga,Mn)As film

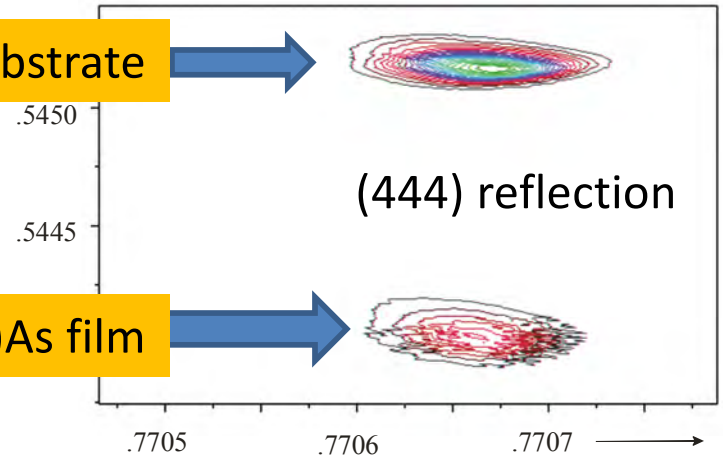

Vertical alignment → film fully strained

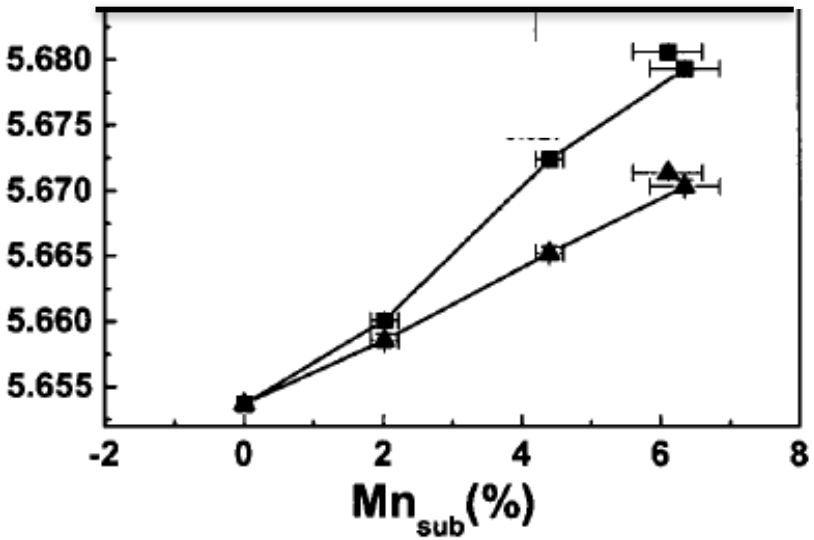

Expansion of the out of plane lattice constant with Mn concentration (as grown and annealed samples)

Zhou et al App Phys Lett ***86****, 071902 (2005)*

Kiessig fringes from thin films

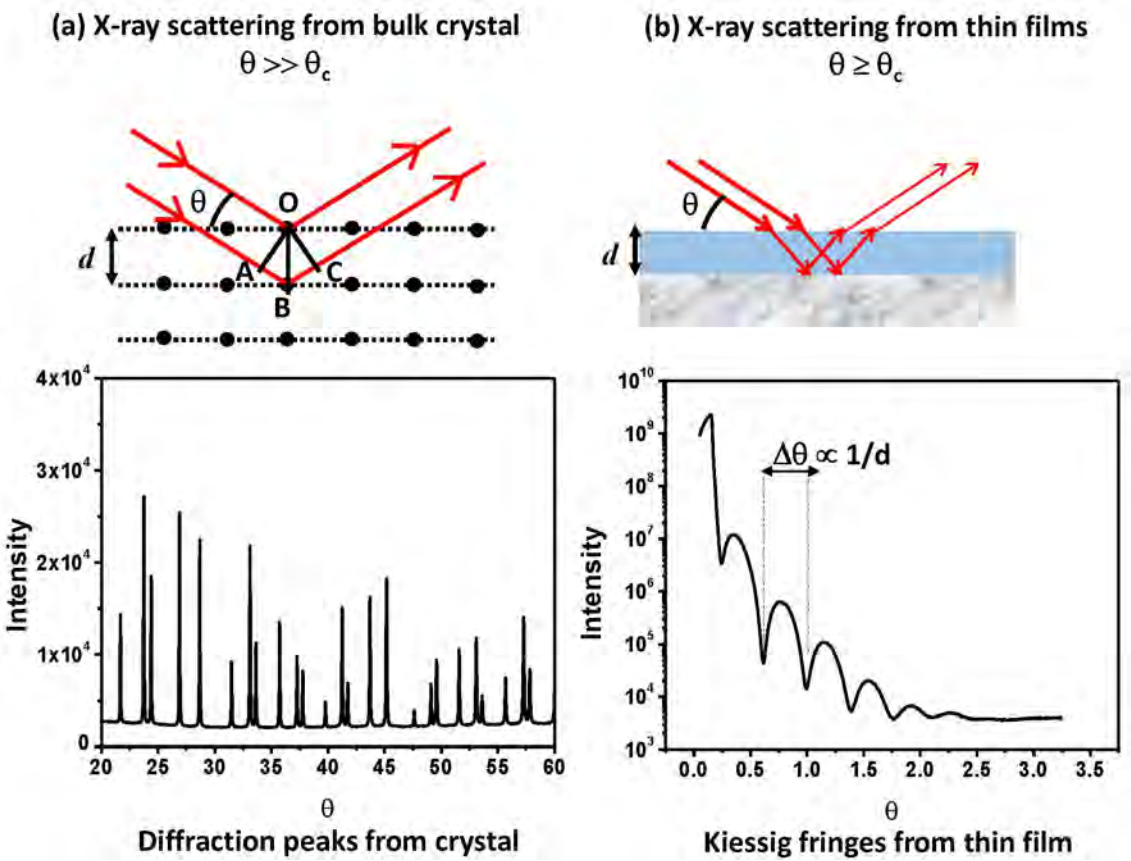

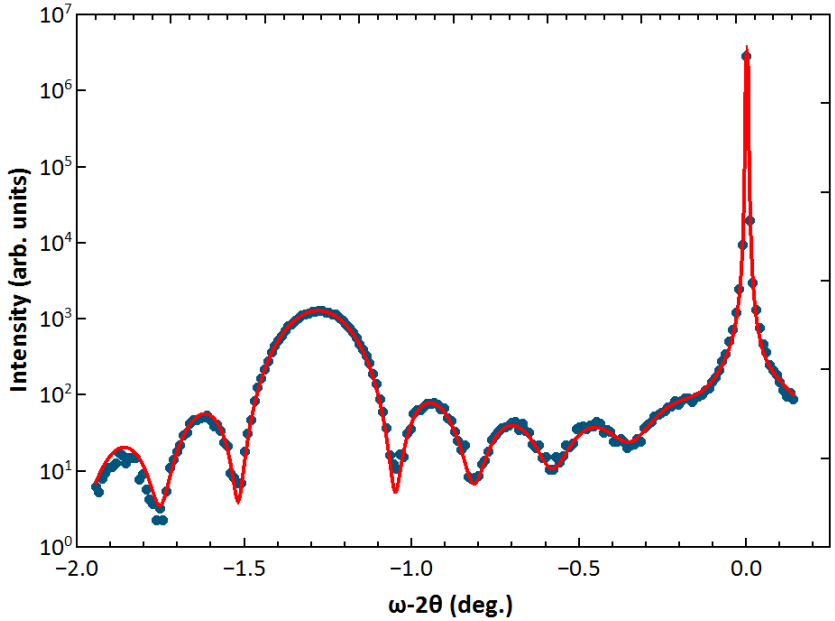

Symmetric 004 reflection from 22.5 nm epitaxial film of $Si_{1-x}Ge_x$ with x = 49% on a Si(001) substrate

FM / AF FeRh thin film

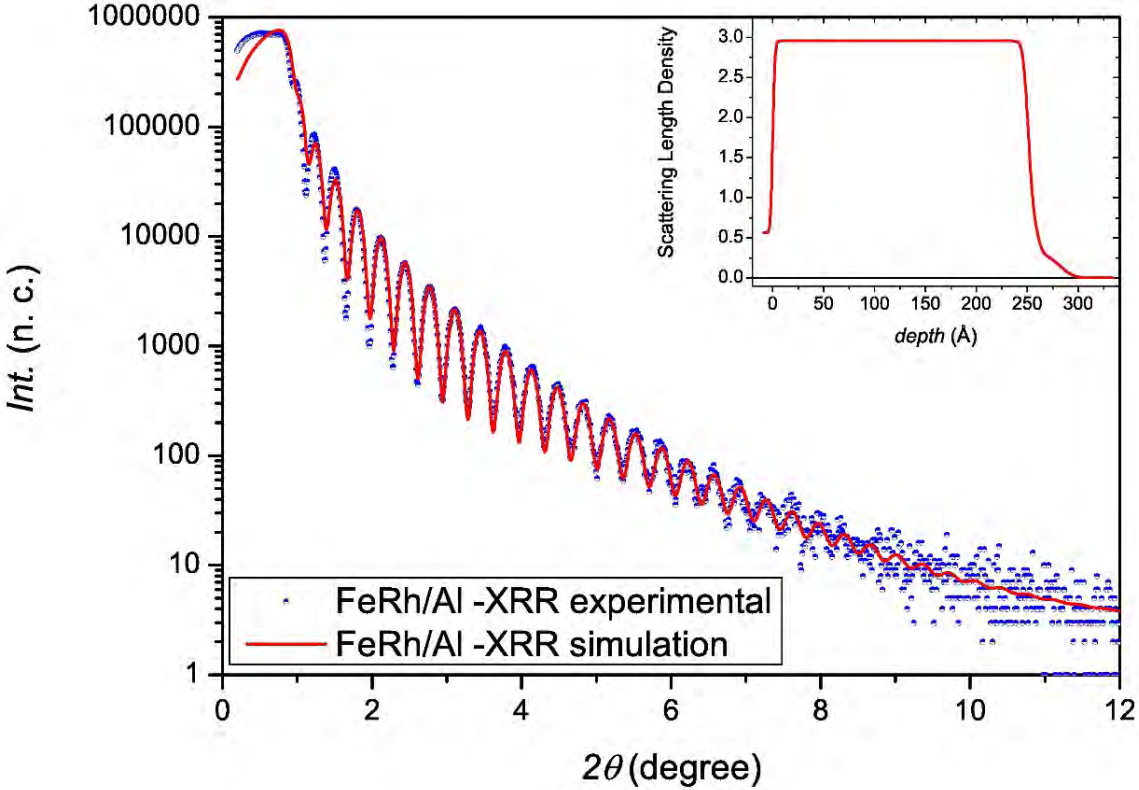

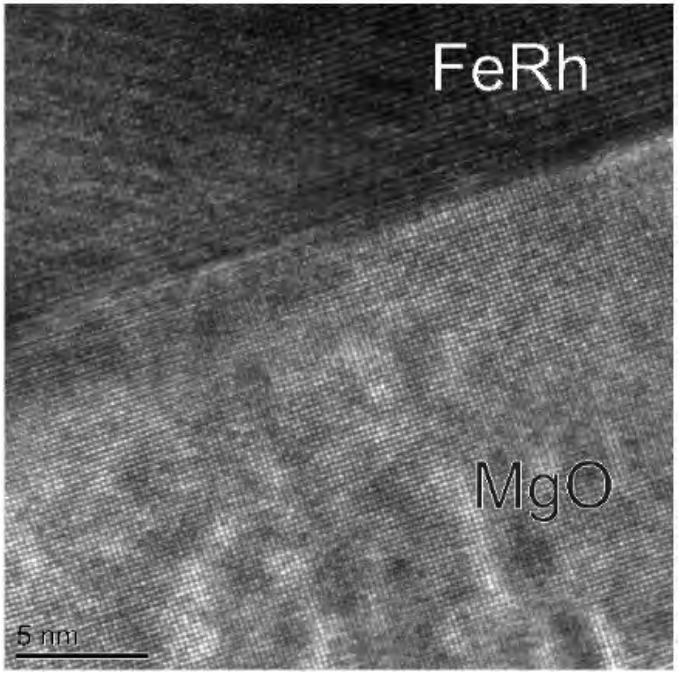

X-ray reflectometry spectrum from a 25 nm thick FeRh epilayers capped with polycrystalline Al. The solid line is a fit using the FeRh density profile of the insert.

Le Graët, ….. Marrows, et al Journal of Visualized Experiments (JoVE), no. 80, e50603. (2013)

3.2 Structural Characterisation: Transmission Electron Microscopy (TEM)

Element (Z)-resolved TEM image of CuMnAs

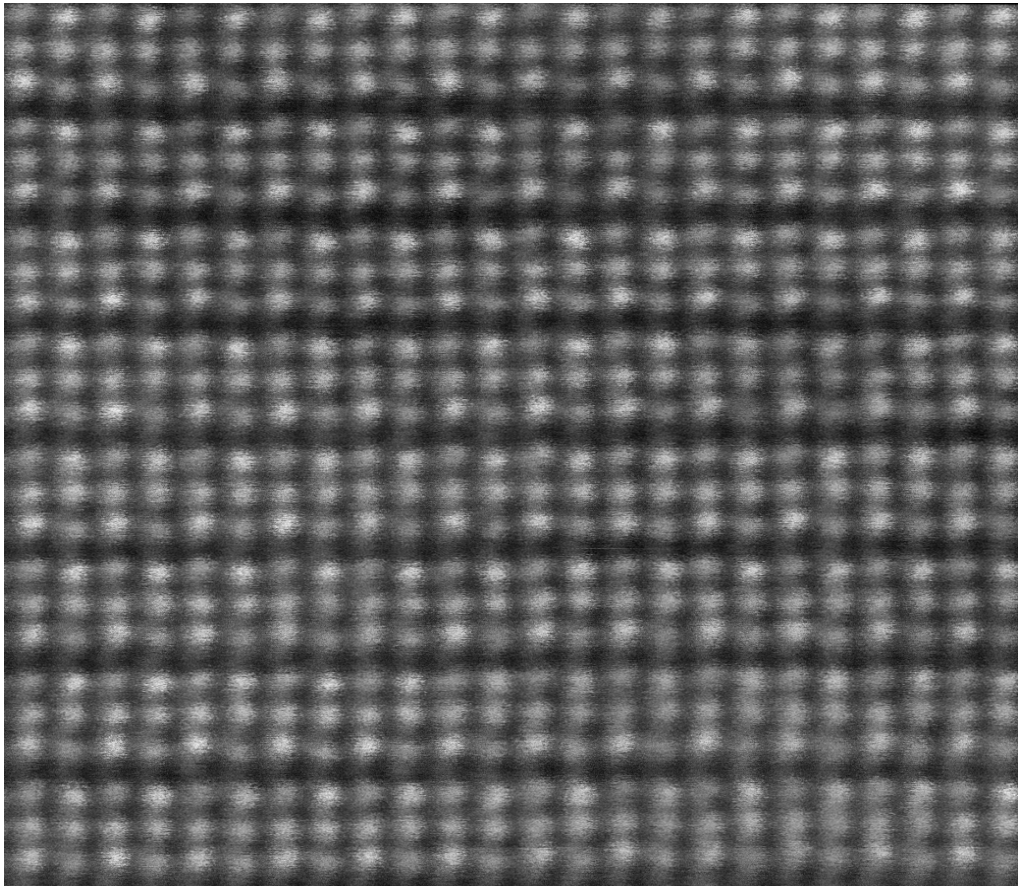

Remember samples ~100 nm thick.

Jaume Gasquez, Oakridge NL

CuMnAs TEM- Comparison to model

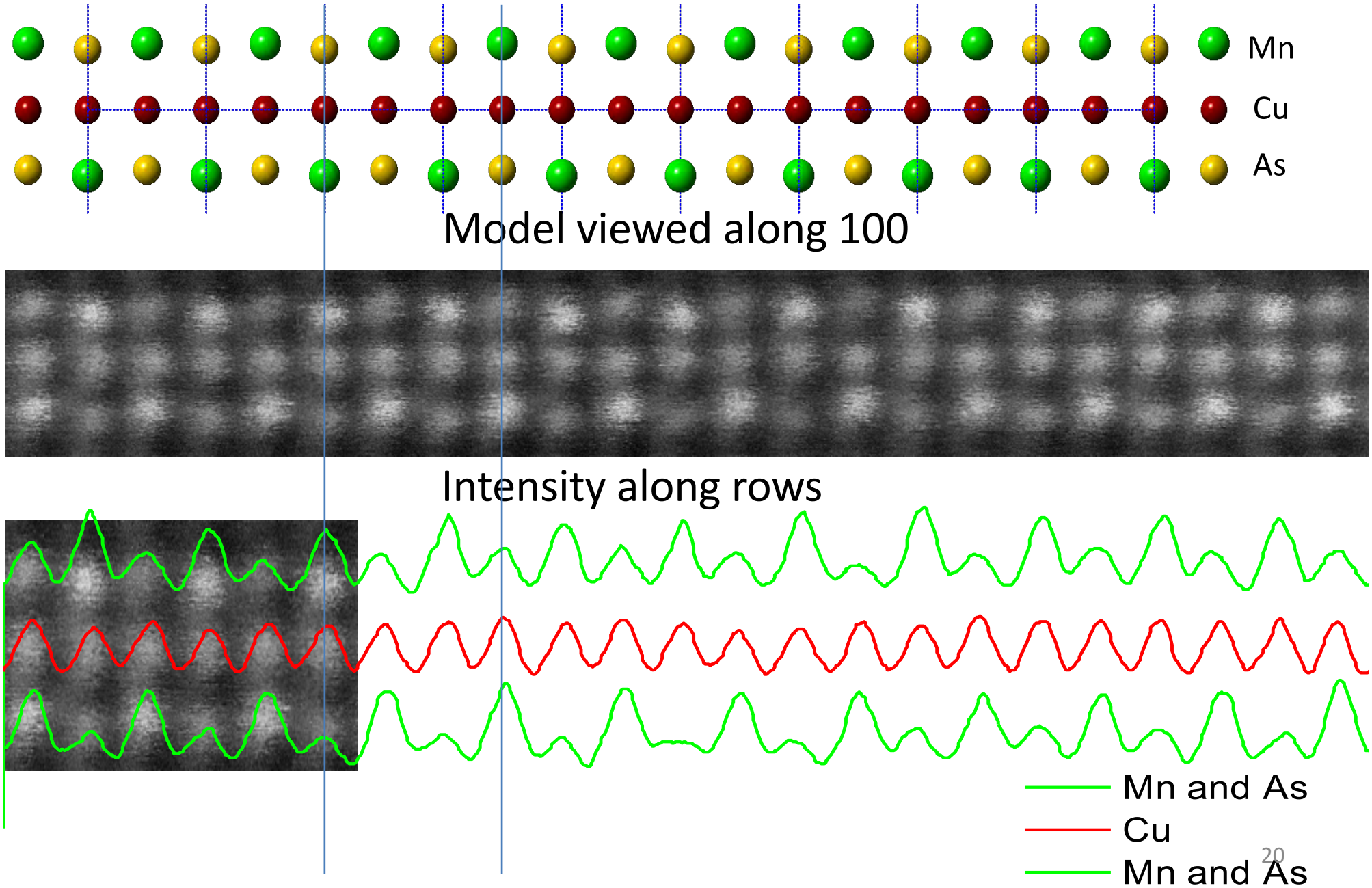

CuMnAs: Anti-phase boundary defects

Arise from steps in the substrate

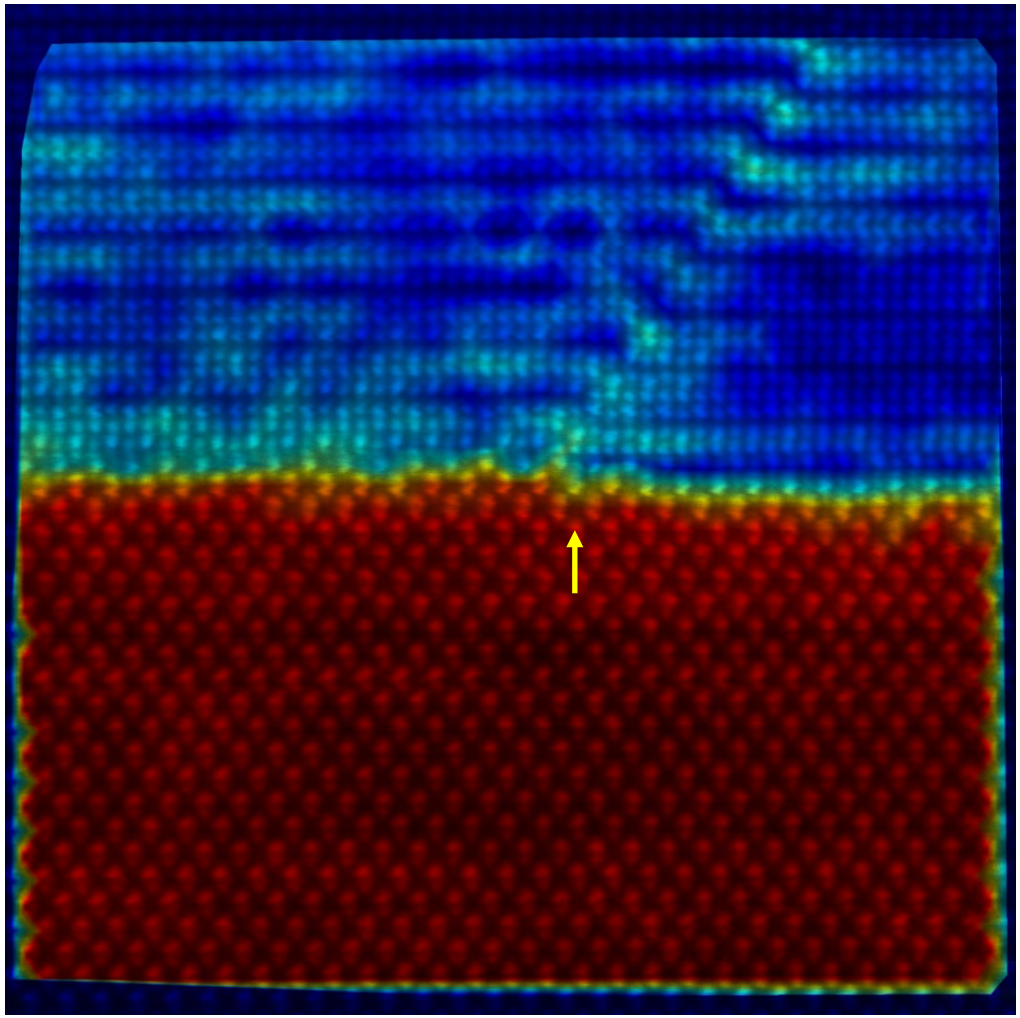

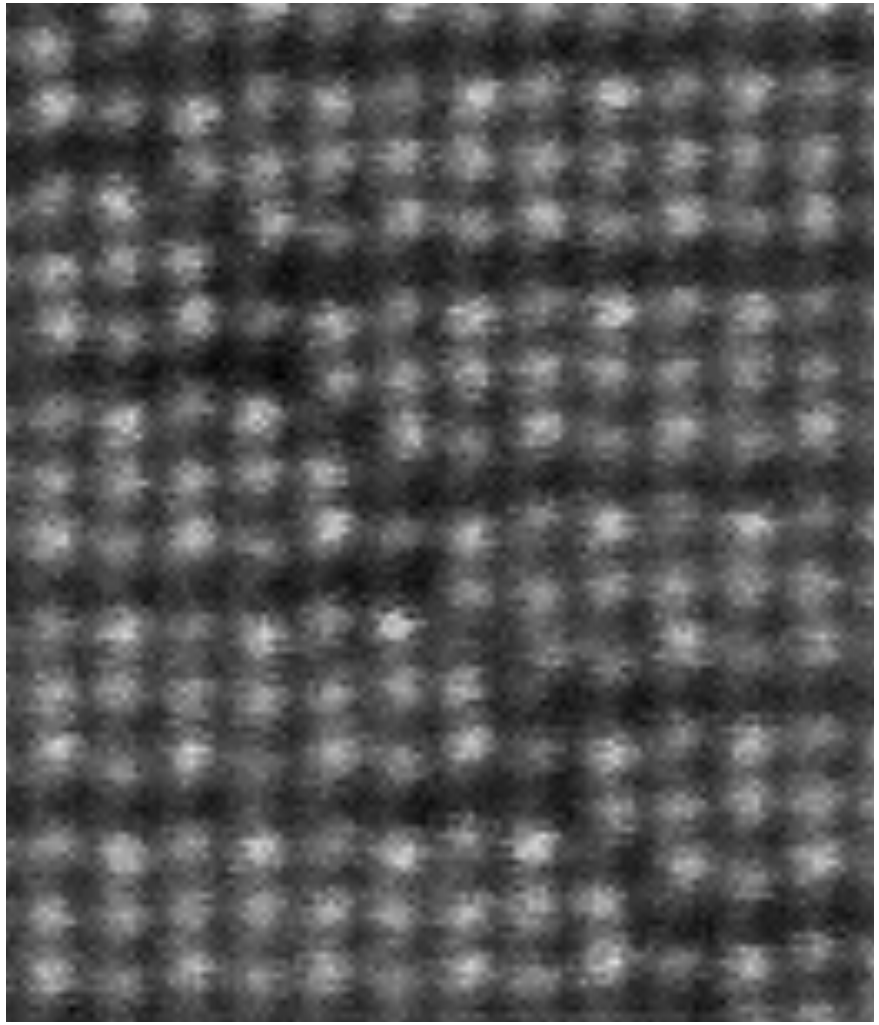

TEM experts

3.1 Magnetic Characterisation: Neutron Scattering

- **Elastic neutron scattering can reveal magnetic structure.**
- **Inelastic neutron scattering can measure dispersion of phonons and magnons.**
- **Want neutron wavevector, $k_n \approx$ reciprocal lattice vector, $G \approx 10^{10}$ m^{-1}.**
- **For $k_n = 3 \times 10^{10}$ m^{-1} neutron energy is ε_n= 25meV $\approx$ kT @ T $\approx$ 300K (Thermal neutrons).**
- **Thermal neutrons have energies $\approx$ phonons and magnons.**

X-ray Scattering

- **X-rays scattered by electrons of atoms. Atomic structure factor f(Q) ~ Z, atomic number.**

- **Size of atoms ≈ neutron wavelength: scattering factor f (Q) decreases as $|Q|$ increases.**

X-rays: Scattered intensity ~ Z^2. Hard to 'see' light elements.

Neutron Nuclear Scattering

- **Neutrons scattered by nuclei (strong force).**
- **Size of nuclei ≈ 10^{-5} x neutron wavelength.**
- **Nuclear scattering factor (b) for neutrons is ≈ independent of scattering wavevector q. Irregular variation with atomic number and isotope.**

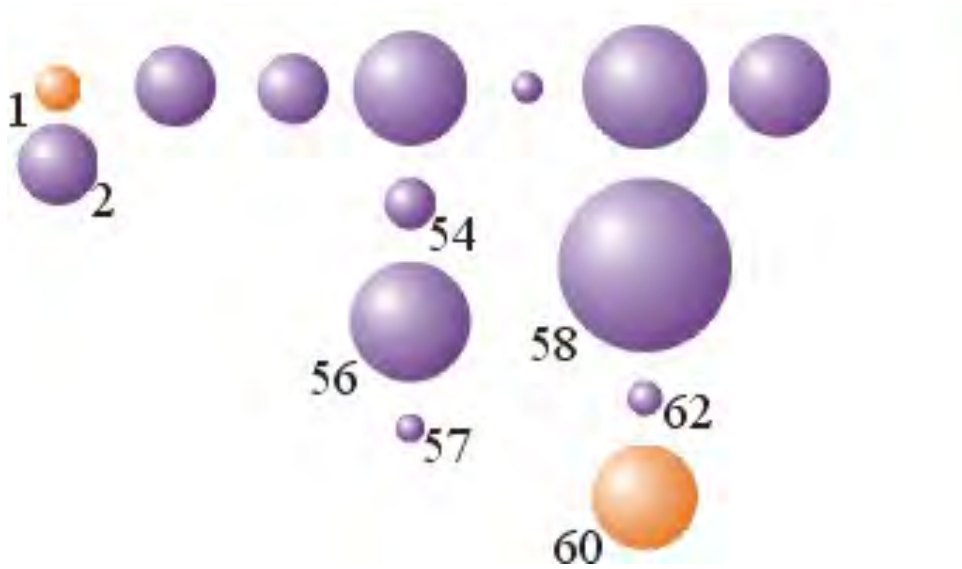

Neutrons: Sensitive to light elements. Isotope dependent: can vary contrast by isotope substitution.

Neutron Magnetic Scattering

- **Neutrons scattered by magnetic moments.**
- **Spin and orbital moments of atom associated with outer electrons.**
- **Magnetic scattering factor for neutrons is strongly dependent on scattering wavevector Q.**

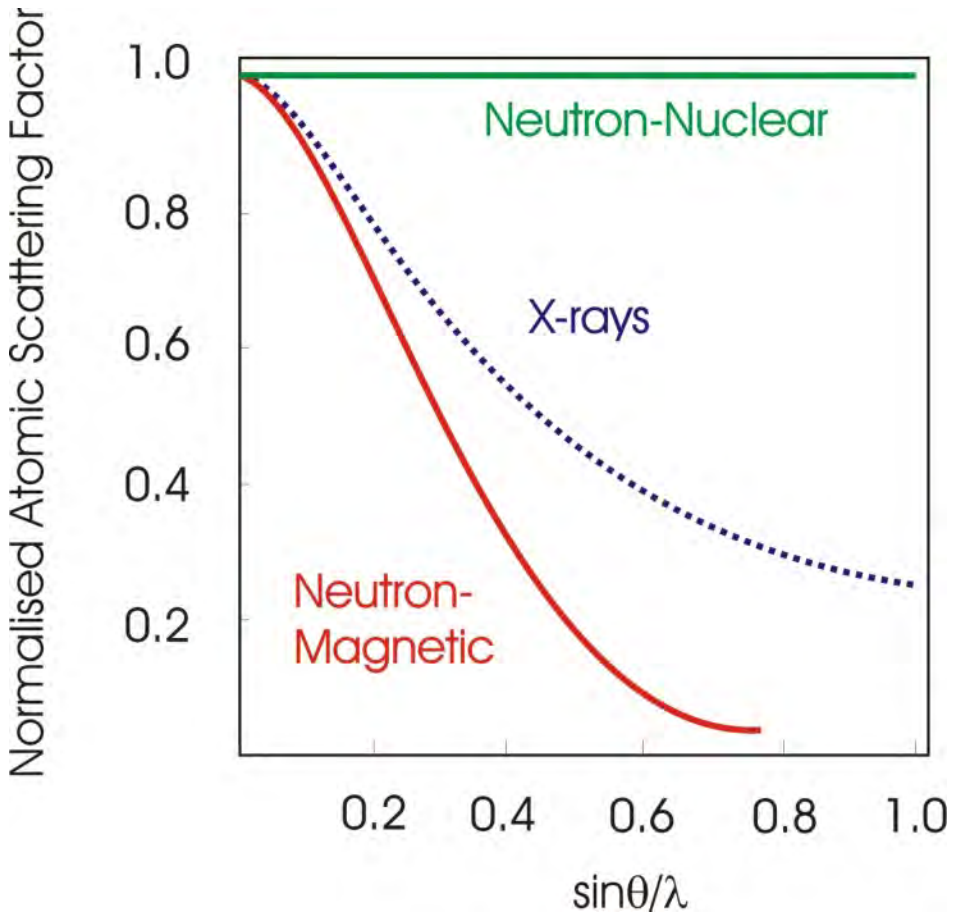

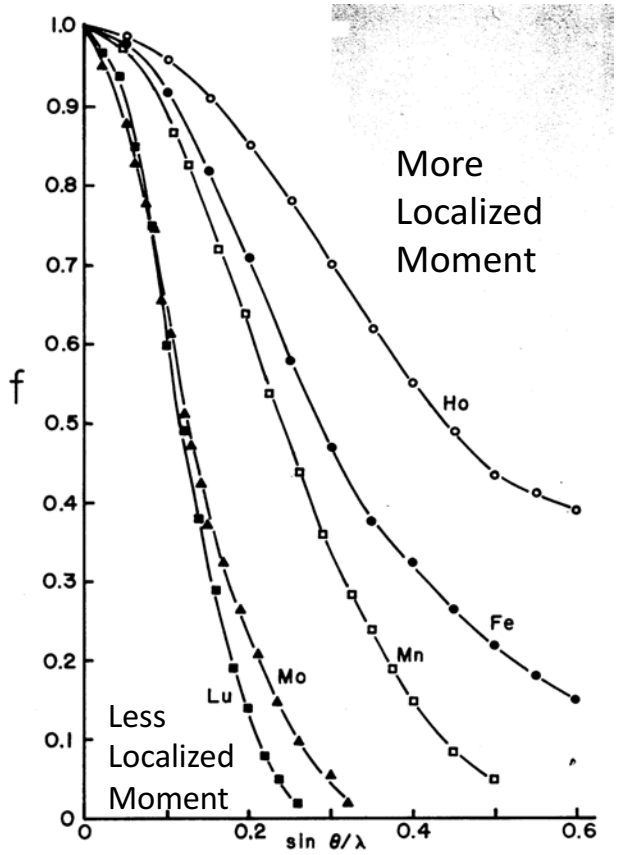

Neutron Diffraction: MnO (T_N = 116 K)

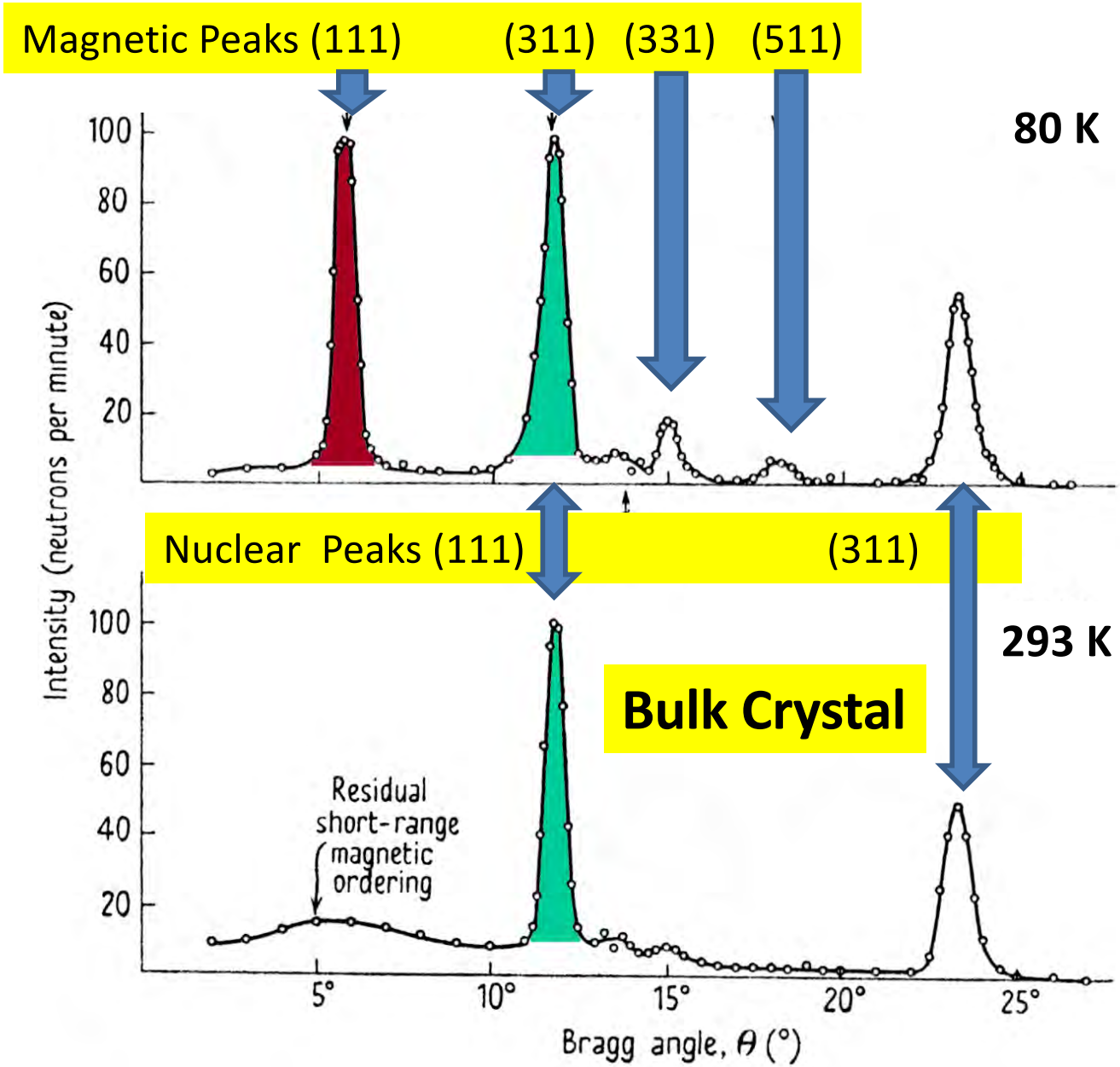

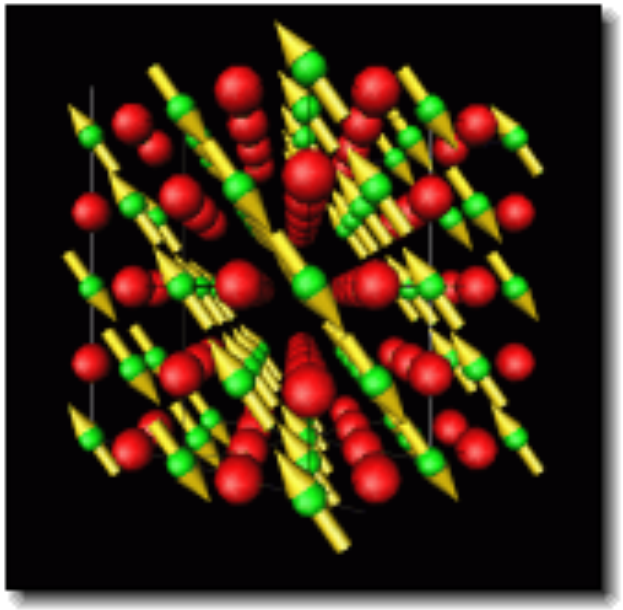

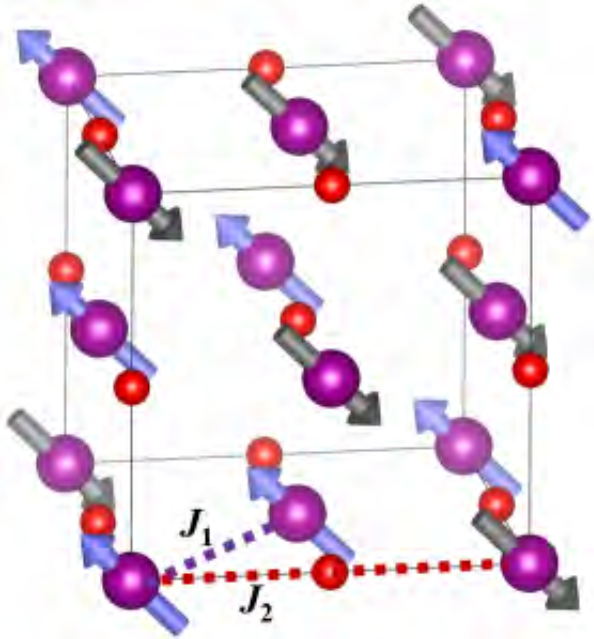

1949 Shull : first direct demonstration of AF order.

Neutron Diffraction: CuMnAs

Structurally forbidden in plane (100) diffraction peak.

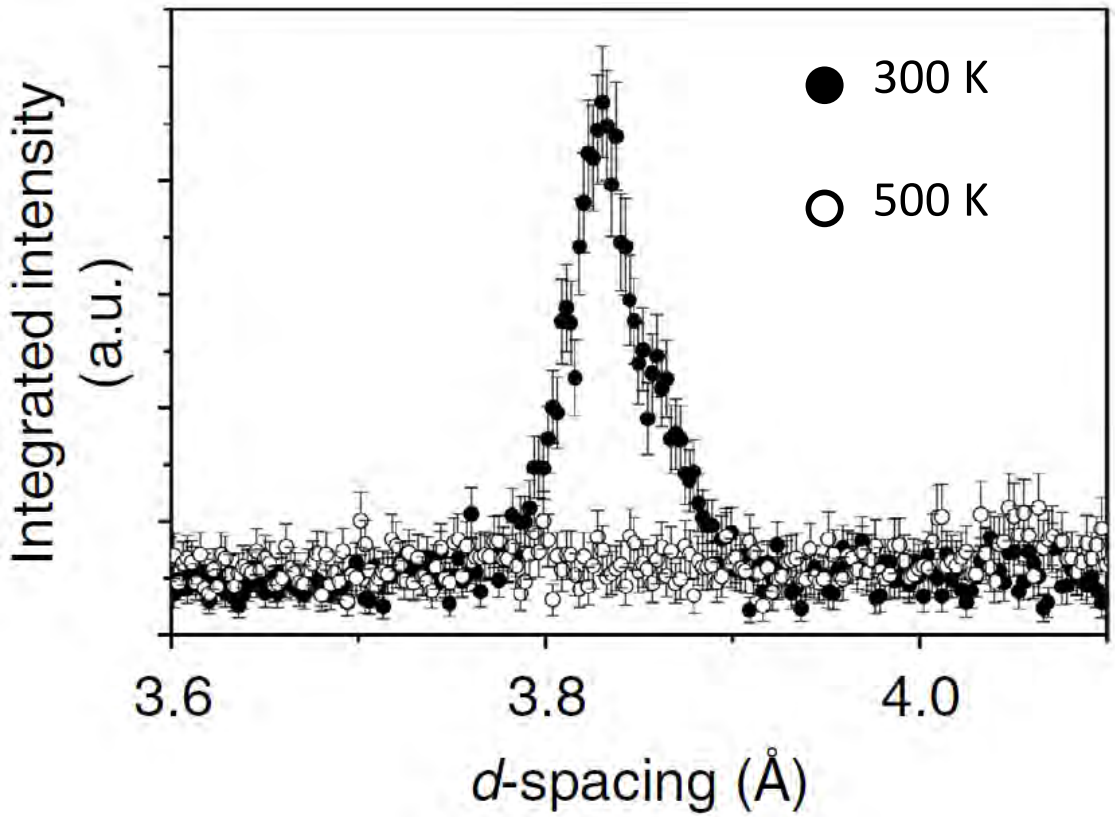

Thin Film

Structural peaks such as (002) as strong at 500K

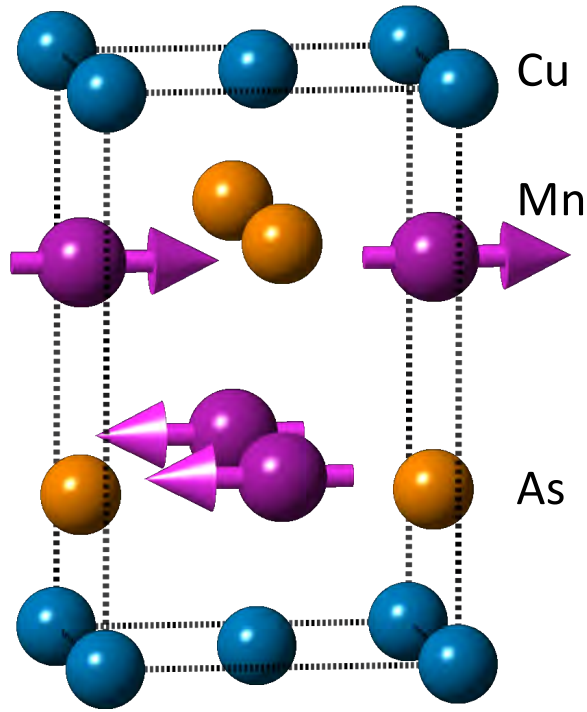

- **AFM ordering with same dimensions as the structural unit cell**
- **Collinear layered antiferromagnet with spin axis in the *ab* plane**
- **Mn moment ≈ 3.6μ_B**

Neutron Diffraction: CuMnAs

Thin Film

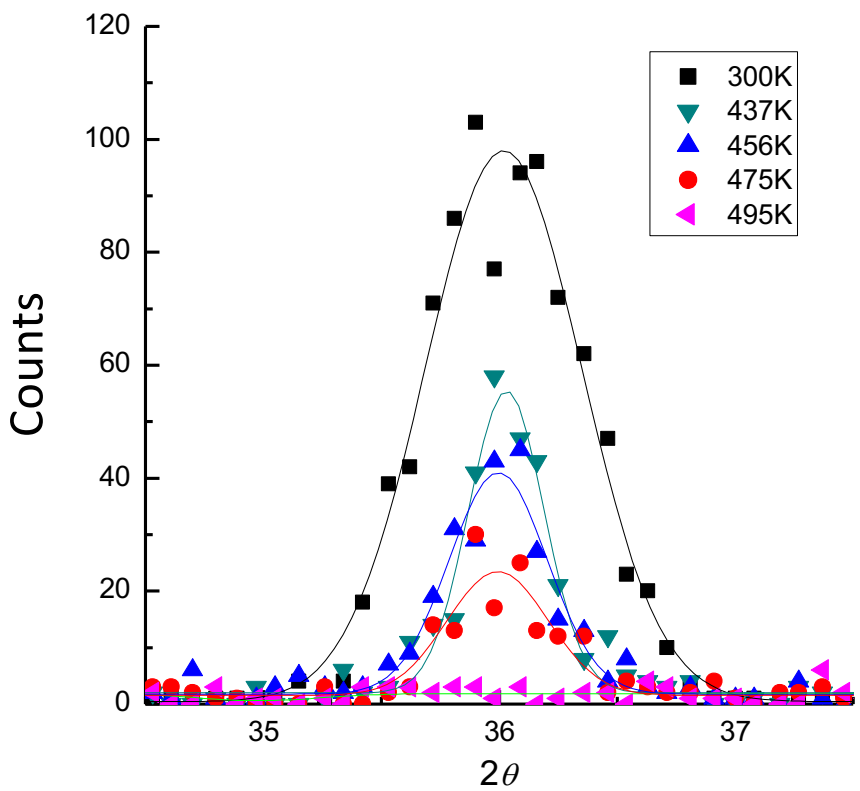

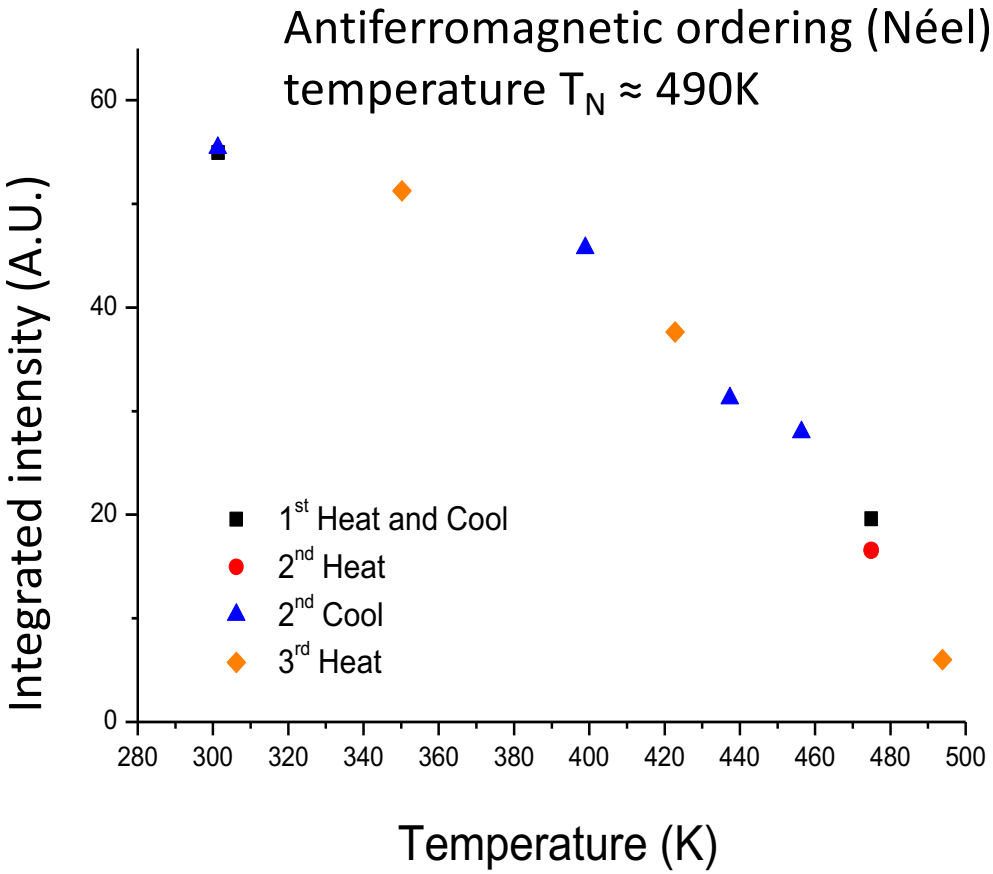

3.2 Magnetic Characterisation: Magnons

Inelastic Neutron Scattering

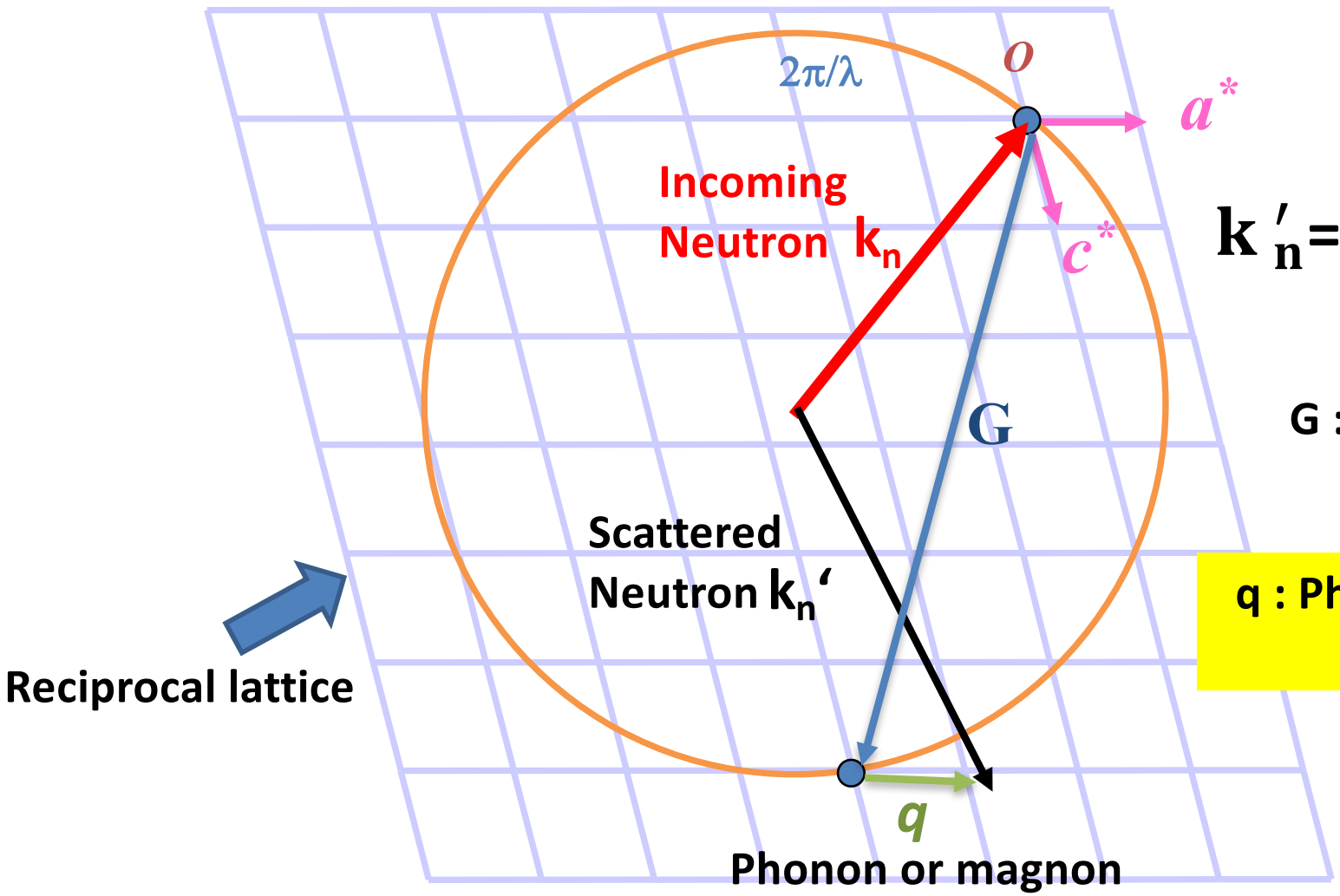

$$\mathbf{k}'_n = \mathbf{k}_n + \mathbf{G} + \mathbf{q}$$

G : reciprocal lattice vector

q : Phonon or Magnon wavevector

Phonons: 1D Harmonic Diatomic Chain

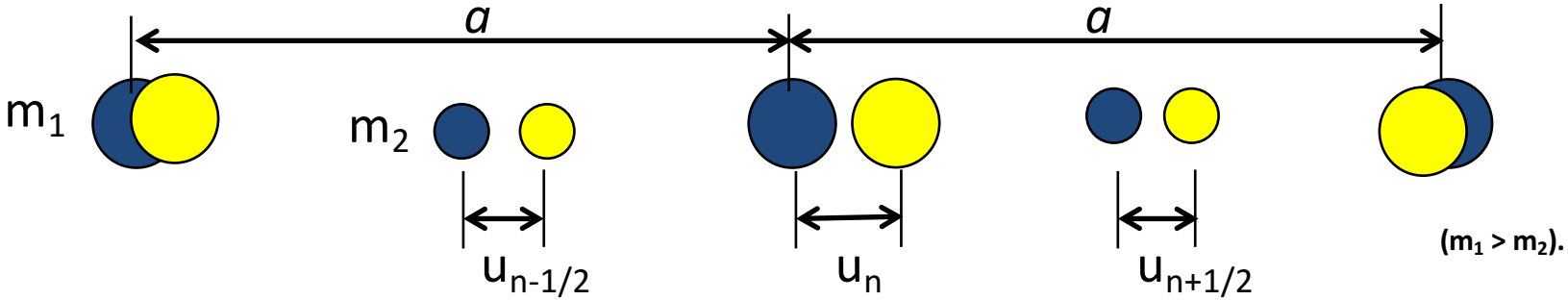

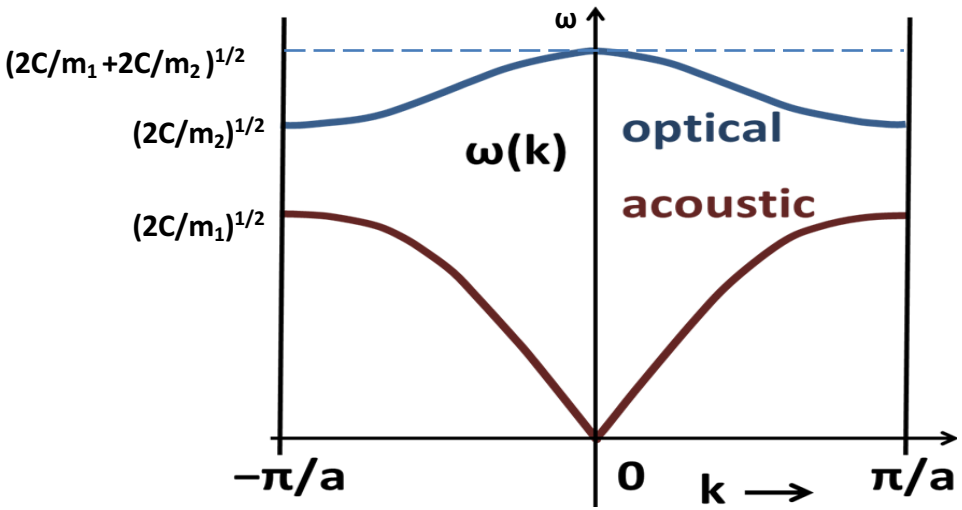

Dispersion relations for Ge (Kittle)

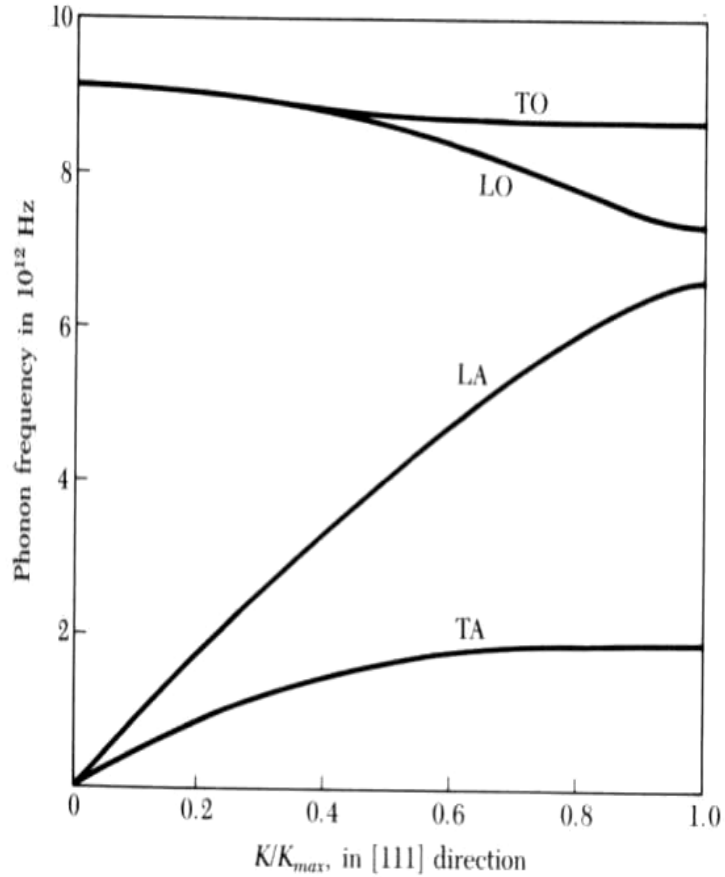

Antiferromagnetic material

Ferromagnetic Magnons / Spin Waves

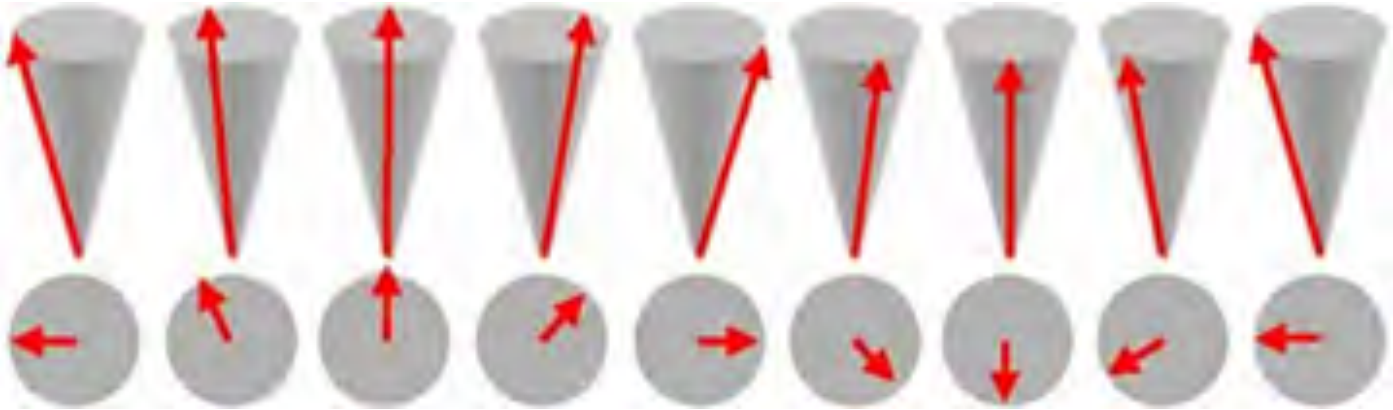

1D linear response, nearest neighbour exchange.

Without anisotropy

$$\hbar\omega = 2E_{ex}(1 - \cos(ka))$$

$$\hbar\omega \approx E_{ex}a^2k^2 = \mathrm{D}k^2 \quad \text{for small k}$$

Energies per moment. D: spin wave stiffness

With uniaxial anisotropy

$$\hbar\omega \approx E_{an} + \mathrm{D}k^2 \quad \text{for small k}$$

For k = 0 $\quad \hbar\omega \approx E_{an}$

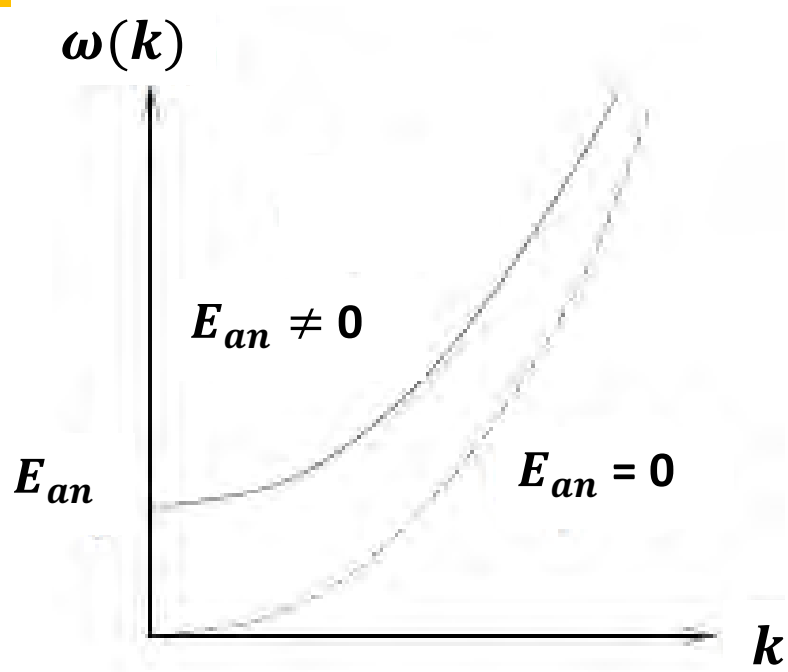

Ferromagnetic Magnons

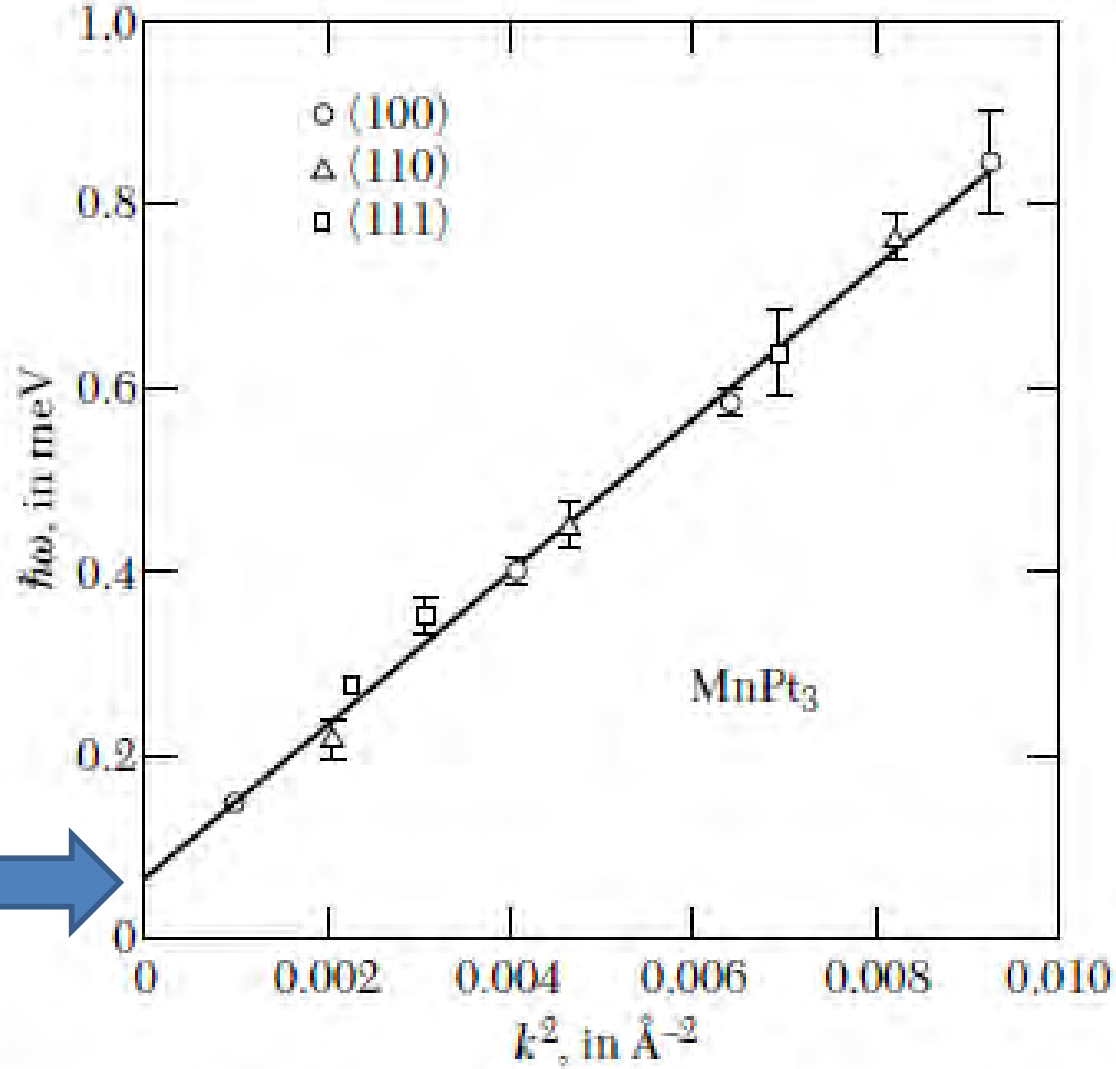

Non zero
E_{an}~ 70μeV

Kittle

Antiferromagnetic Magnons / Spin Waves

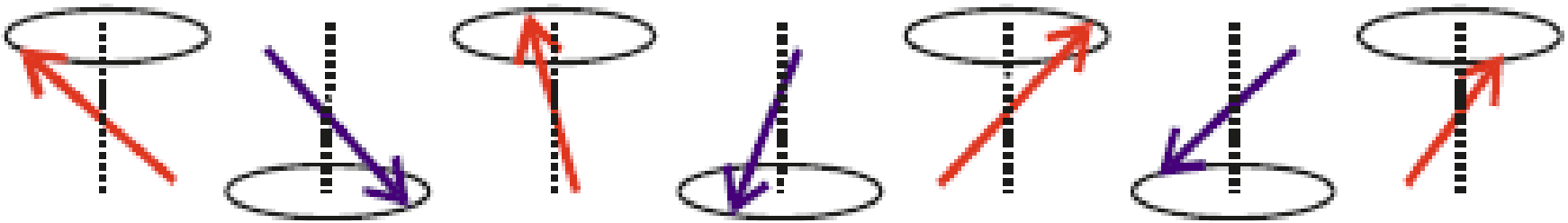

1D linear response, nearest neighbour exchange.

Without anisotropy

$$\hbar\omega = E_{ex}|\sin(ka)| \approx E_{ex}ak \quad \text{for small } k$$

With uniaxial anisotropy

$$\hbar\omega \approx \sqrt{2E_{ex}E_{an} + E_{an}^2 + \left(E_{ex}ak\right)^2} \quad \text{for small } k$$

For k = 0

$$\hbar\omega \approx \sqrt{2E_{ex}E_{an} + E_{an}^2} \approx \sqrt{2E_{ex}E_{an}}$$

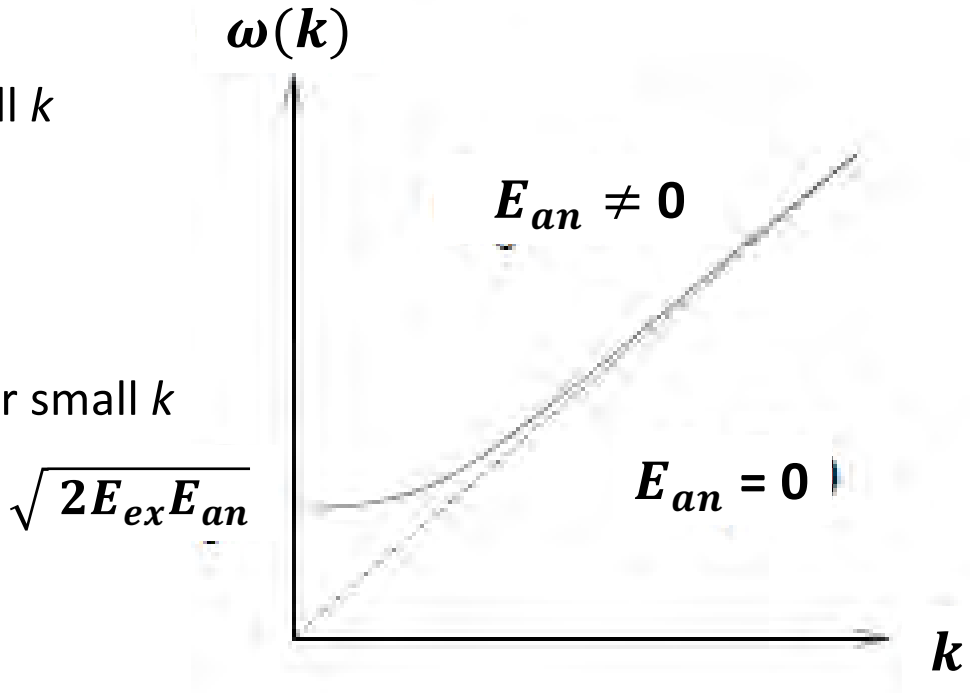

Antiferromagnetic Magnons

$\sqrt{2E_{ex}E_{an}}$ ~ 1meV

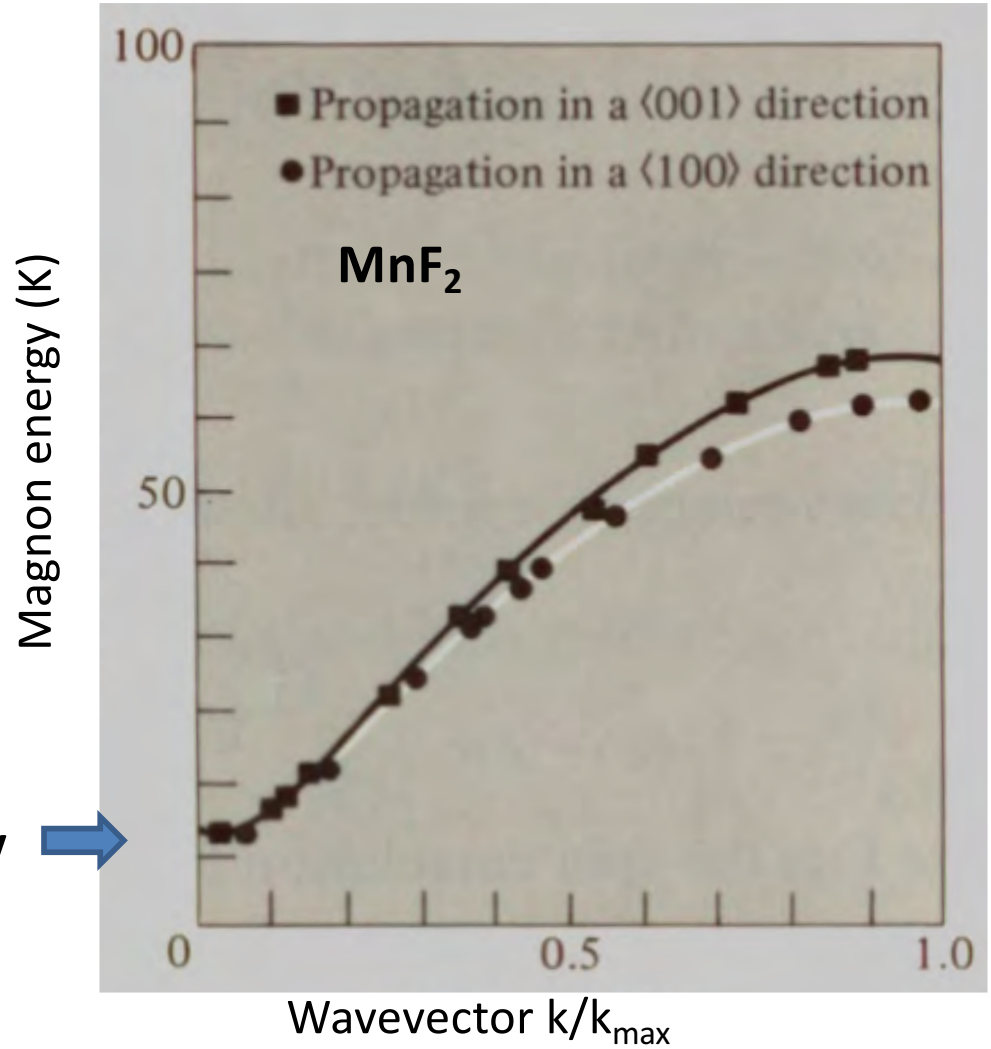

Antiferromagnetic Magnons

Highly anisotropic magnon dispersion in Ca_2RuO_4: evidence for strong spin orbit coupling

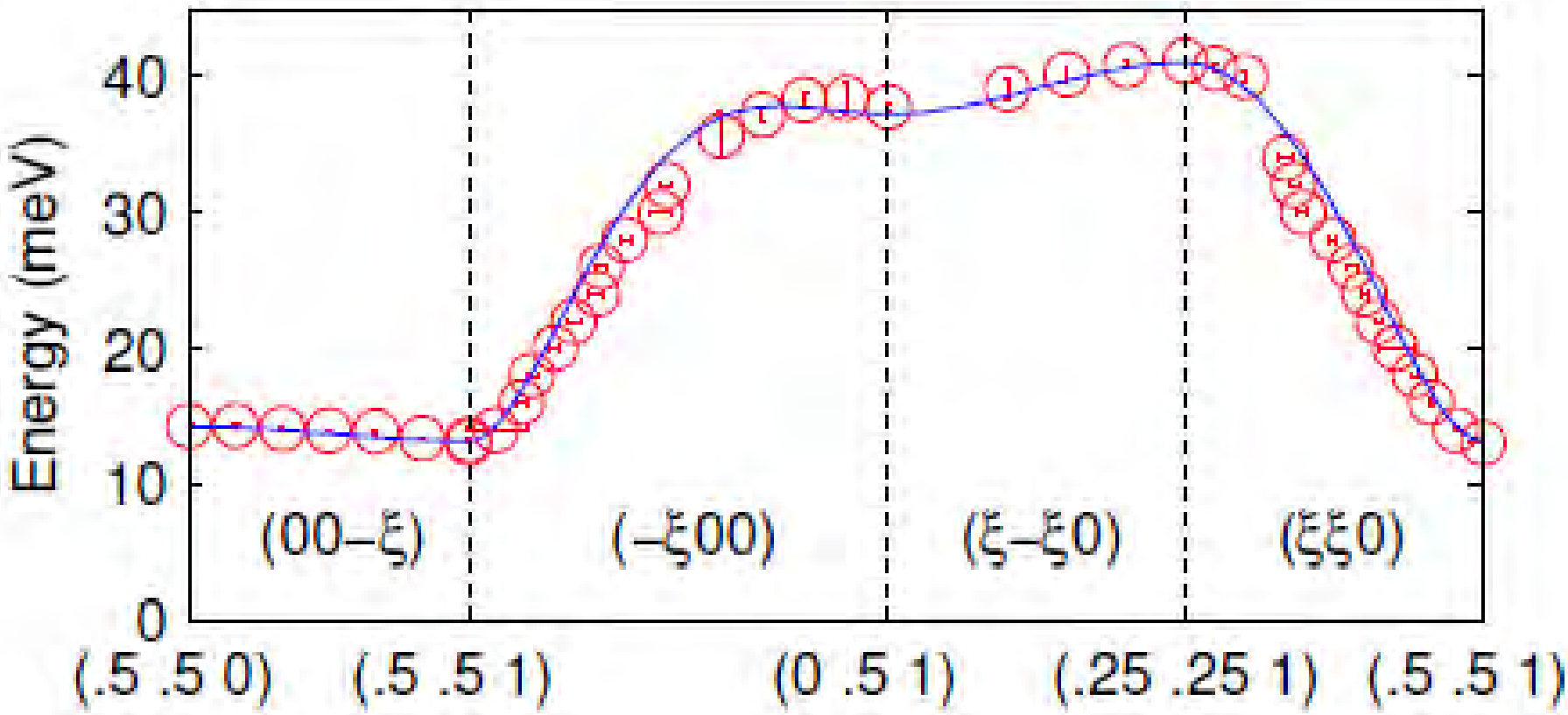

Kunkemöller, et al Phys. Rev. Lett. 115, 247201, 2015

4 Magnetic Characterisation: Magnetic Resonance

Ferromagnetic Resonance (FMR)

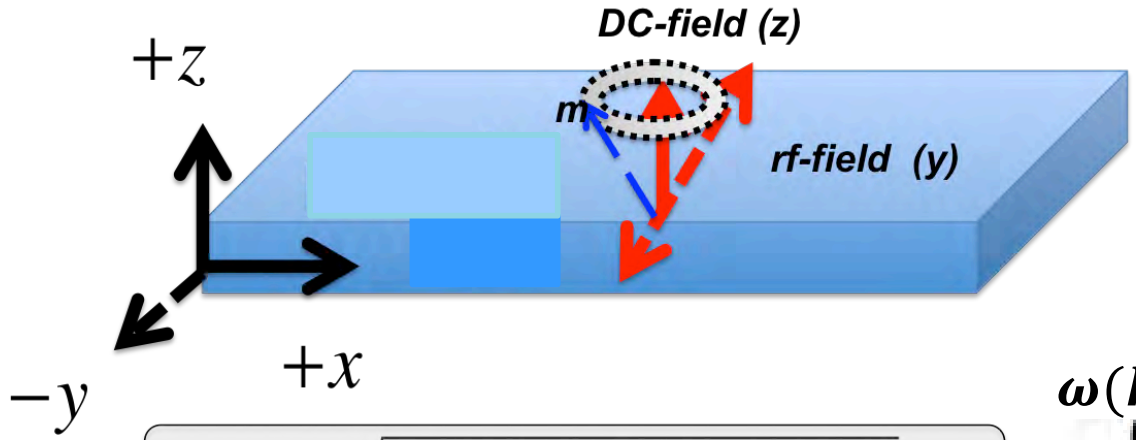

$$\omega_{Kittel} = \sqrt{(\omega_K + \omega_0)(\omega_K + \omega_0 + \omega_D)}$$

$$\omega_0 = \gamma H_{ext} \qquad \omega_K = \gamma H_K \qquad \omega_D = \gamma H_{demag.} = 0$$

Applied field — Anisotropy field — Demagnetising field

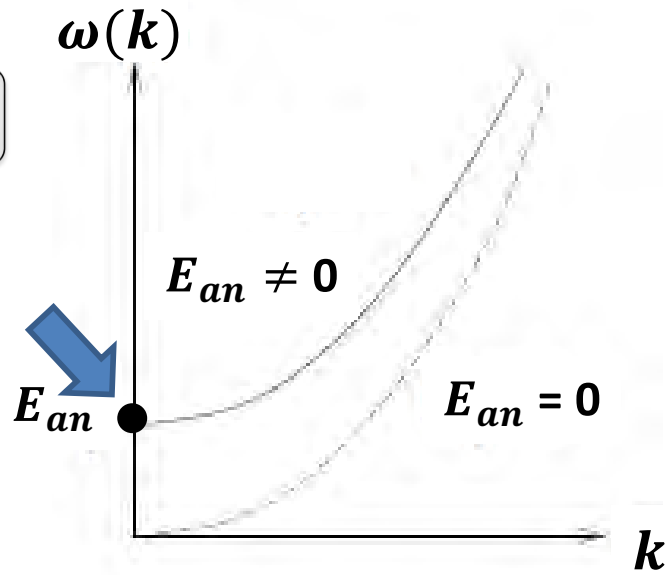

$H_{ext} \longrightarrow 0$ Excited modes are magnons with k ~ 0

Resonant frequencies ~ 1 -10 GHz. Natural speed of dynamics

Ferromagnetic Resonance (FMR): Anisotropy Energies

Zero applied field resonance due to anisotropy.

E_{an}~ 15μeV

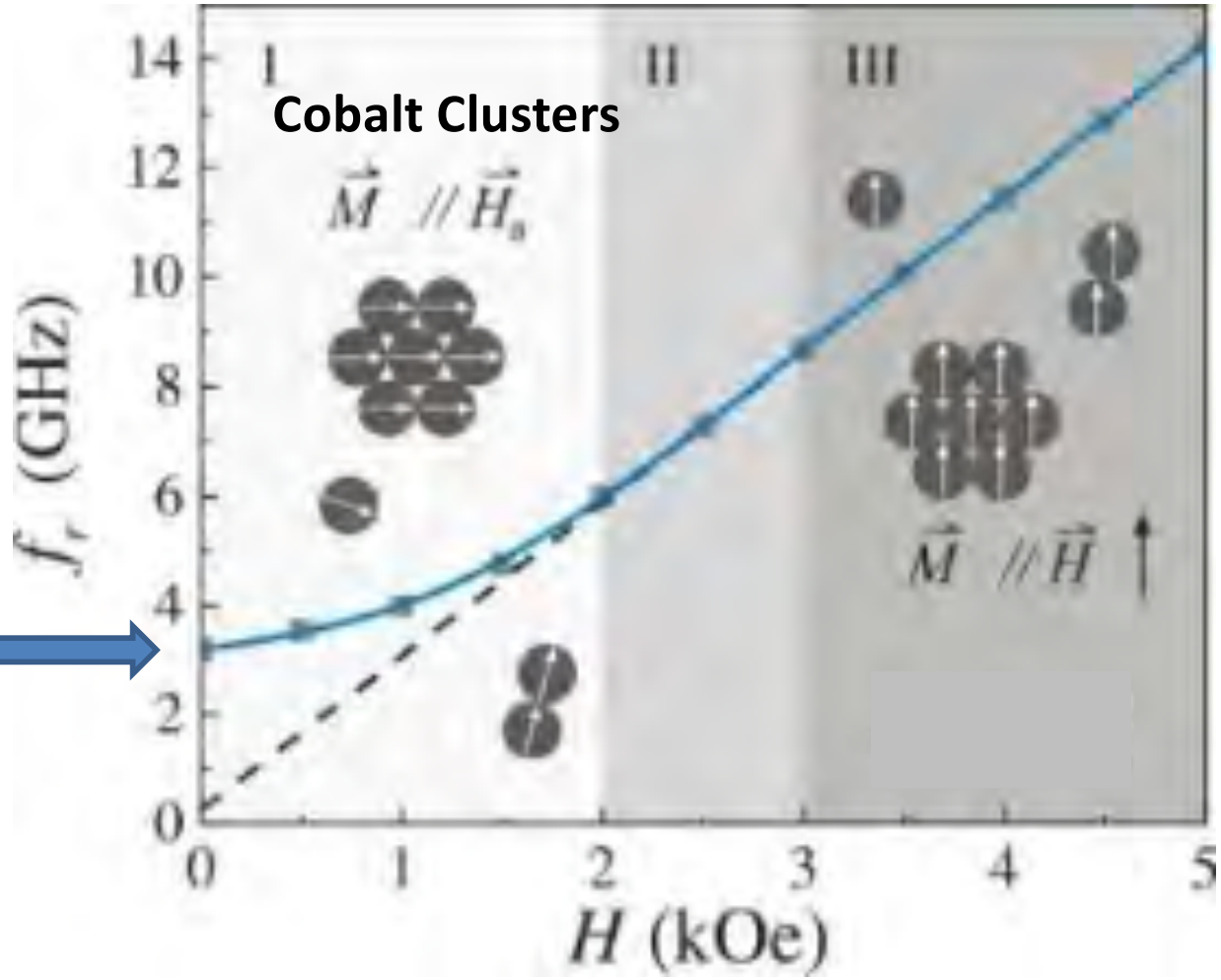

Ferromagnetic Resonance: Anisotropy

Angular dependence of ferromagnetic resonance frequency with a constant magnitude Applied magnetic field rotated in-plane.

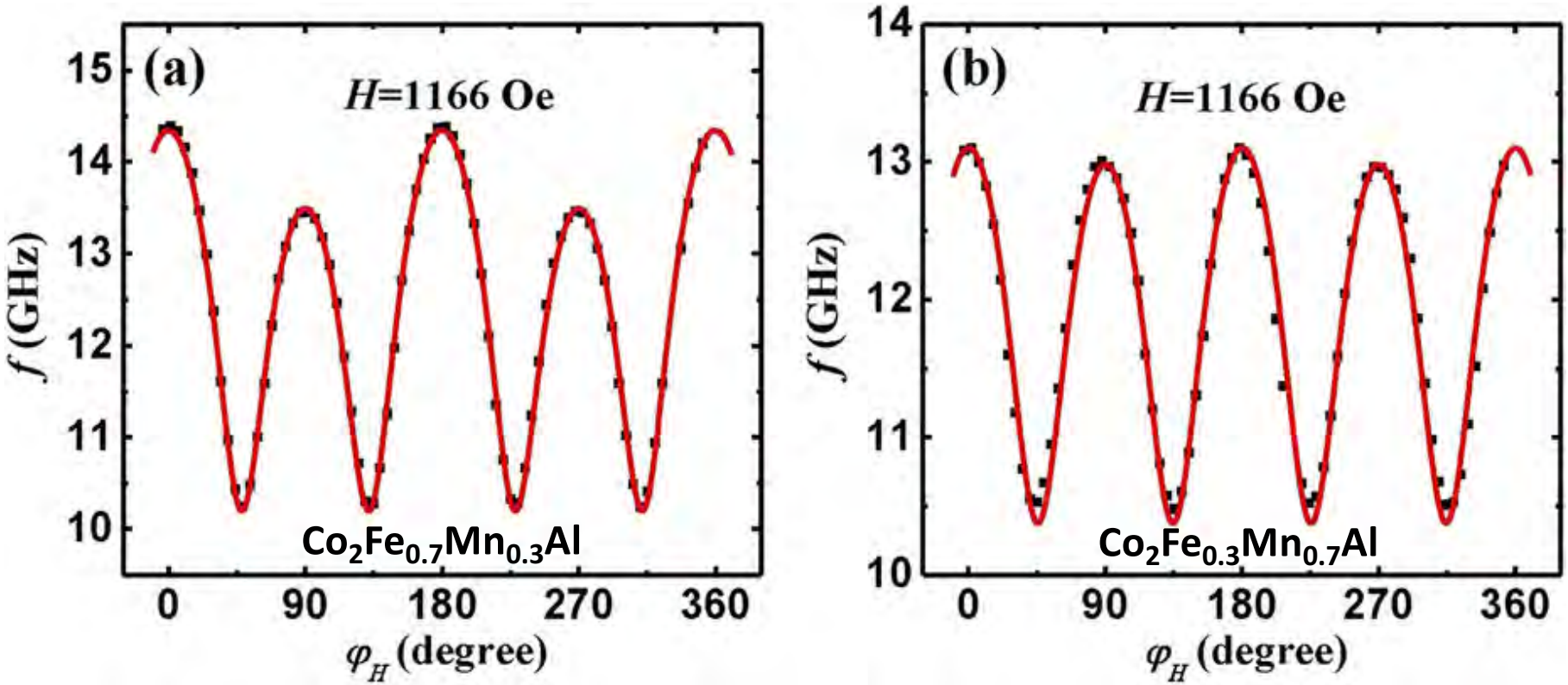

Tao et al Sci. Rep. 6, 18614 (2016)

Antiferromagnetic Resonance (AFMR)

$H_{ext} \longrightarrow 0$ Excited modes are magnons with k ~ 0

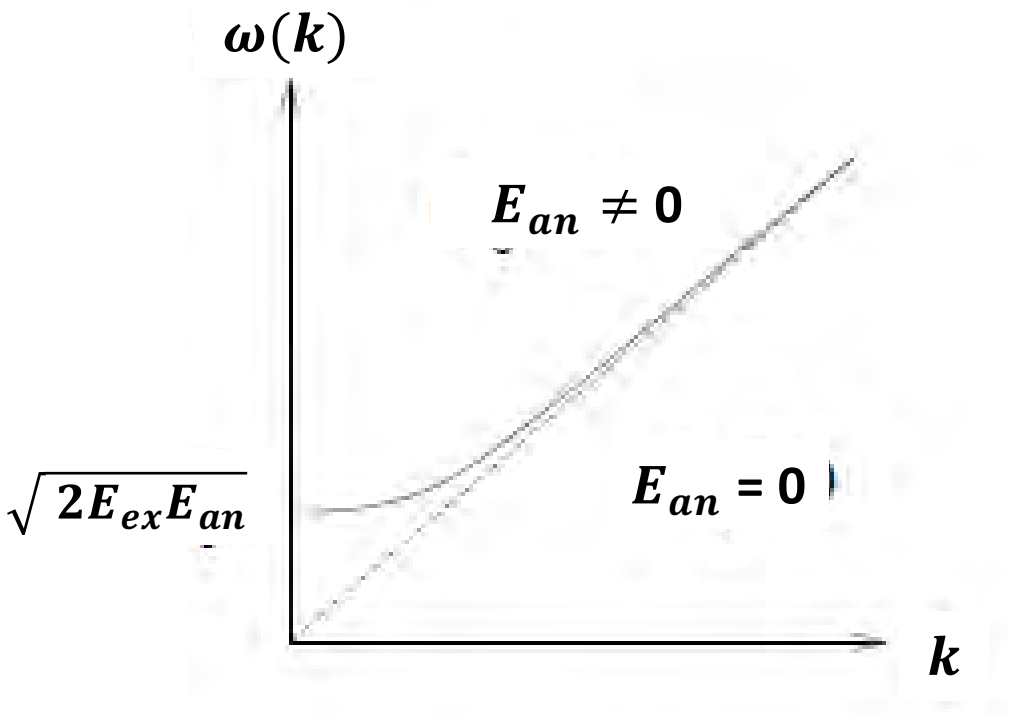

260 GHz

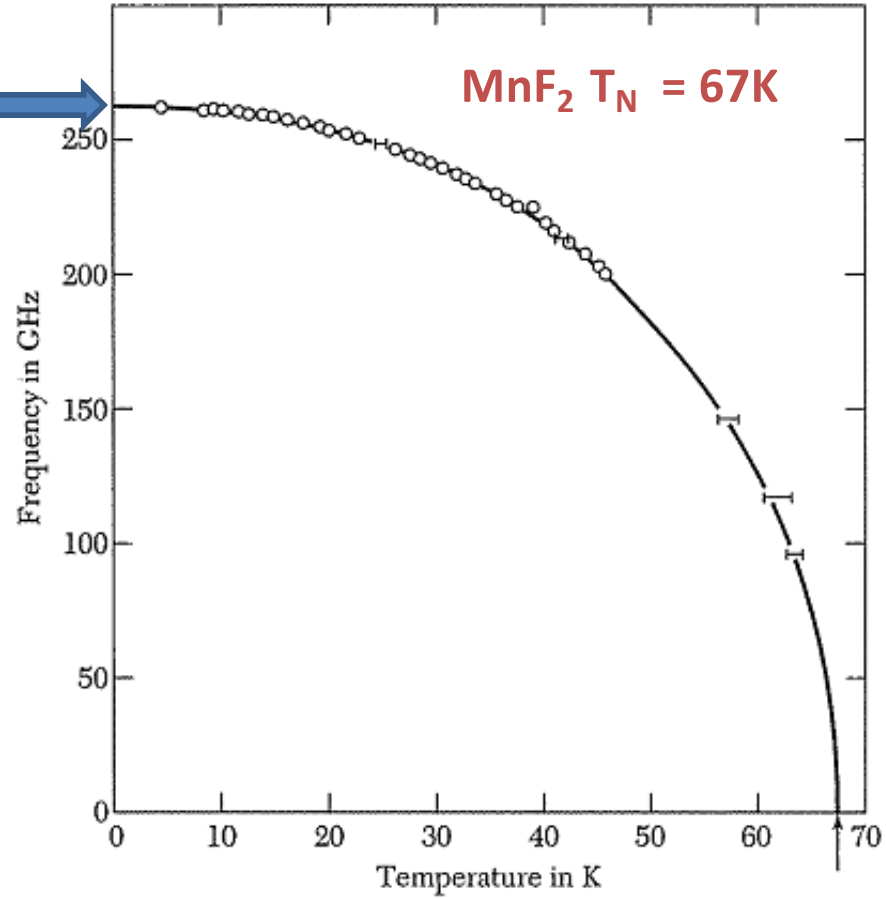

Resonant frequencies ~ 100 -1000 GHz. Natural speed of dymamics

Antiferromagnetic Resonance

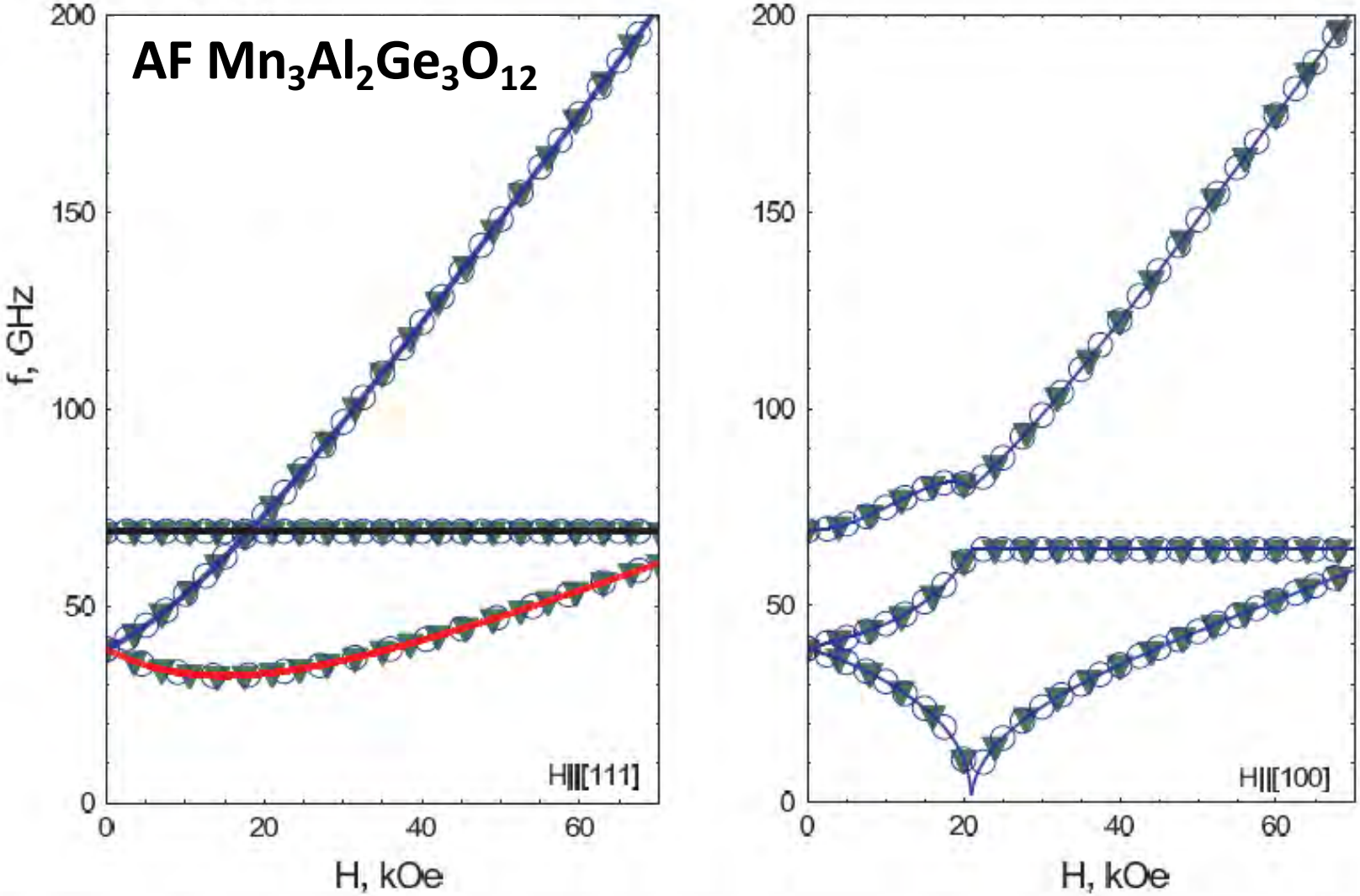

More than one type of Mn site : both "acoustic" and "optical" magnons

L.A. Prozorova, V.I. Marchenko, Yu.V. Krasnyak, JETP Letters, 41, 637 (1985)

3.4 Magnetic Characterisation: Remanence

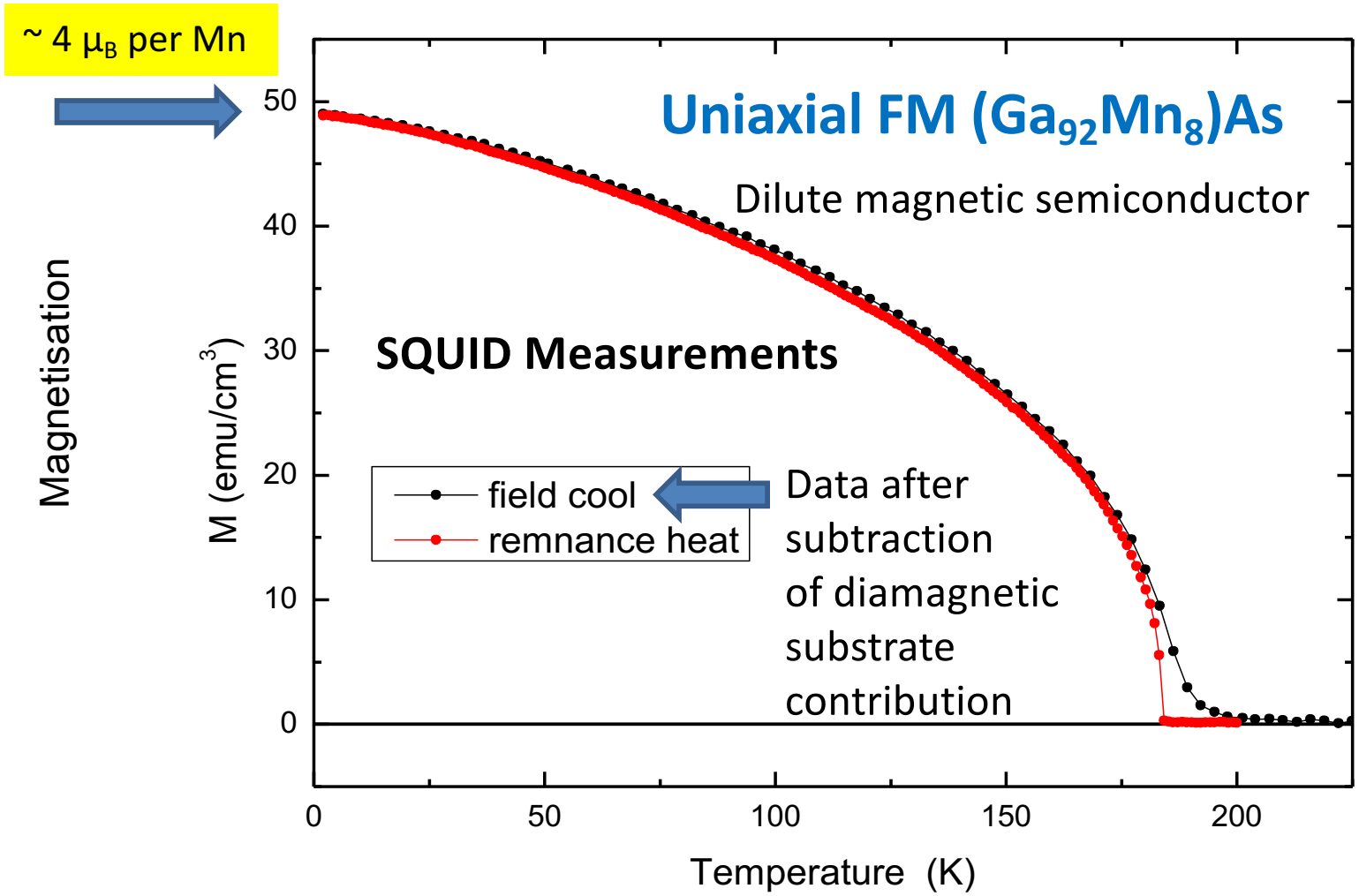

Measuring Remanence. Cool in field (in 300mT). Warm in zero field

Magnetisation: AF CuMnAs

1 emu cm^{-3} is about 0.01 Bohr magnetons per Mn

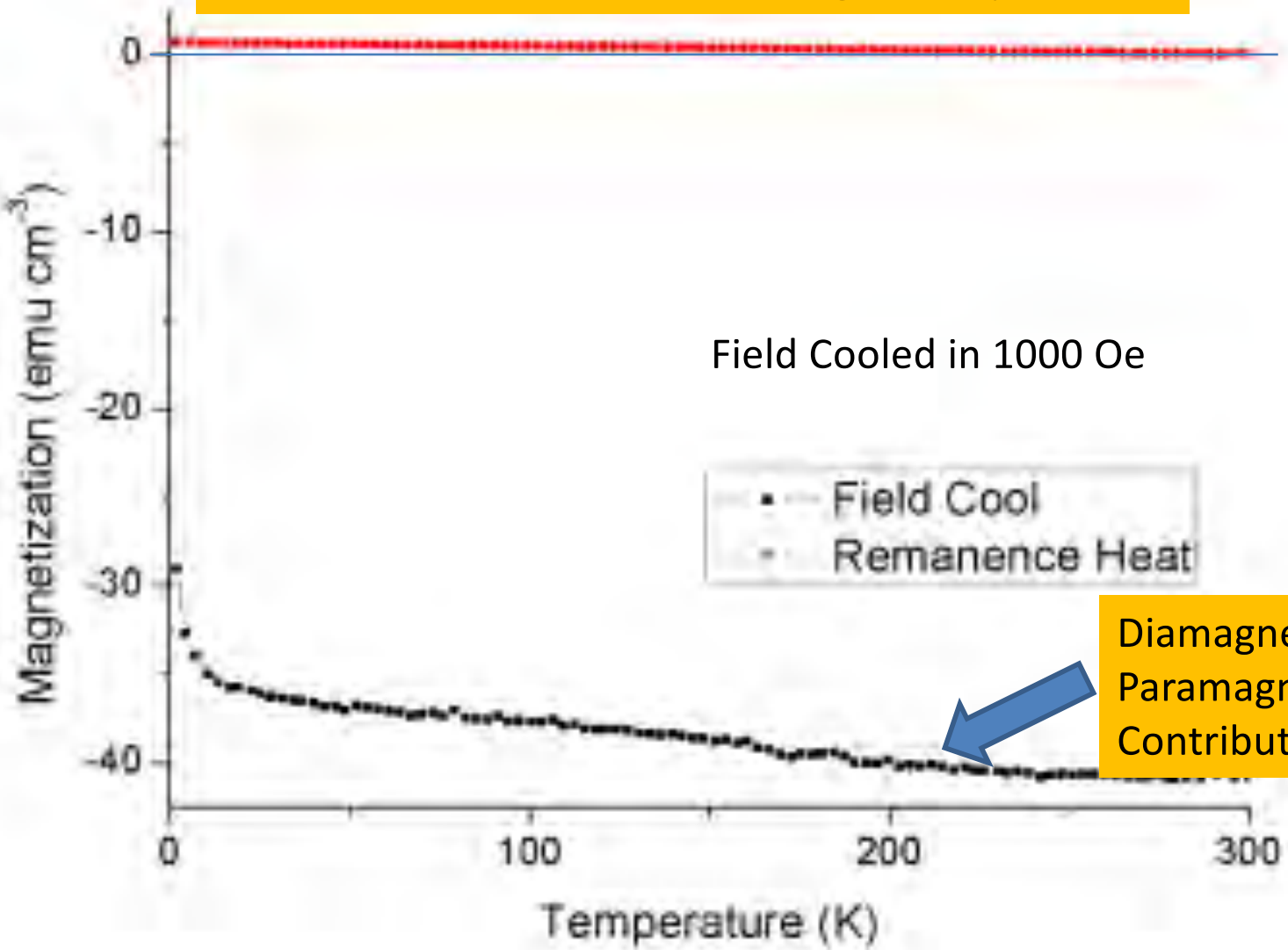

Diamagnetic + Paramagnetic Contributions

Magnetisation: AF CuMnAs

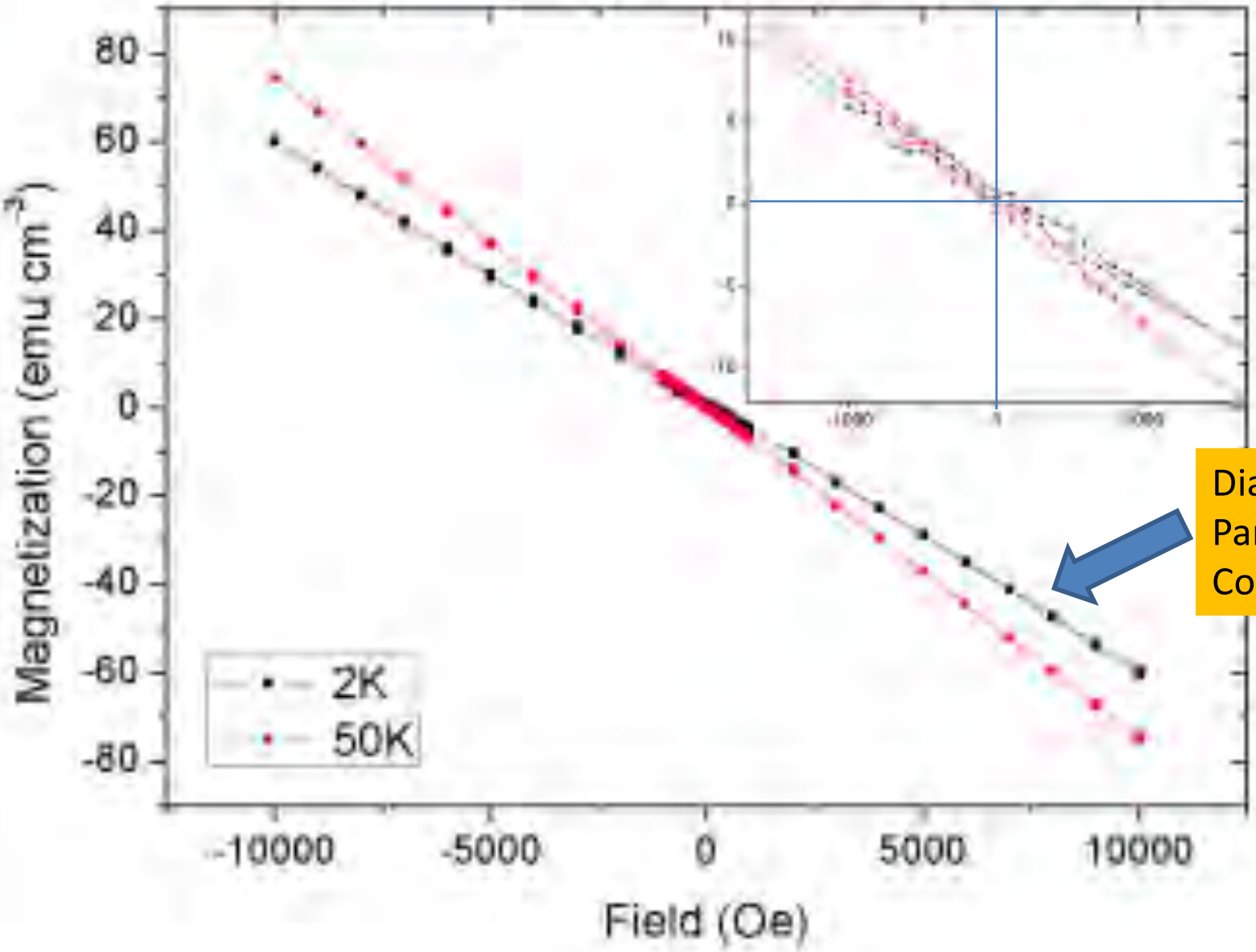

Diamagnetic + Paramagnetic Contributions

Susceptibility

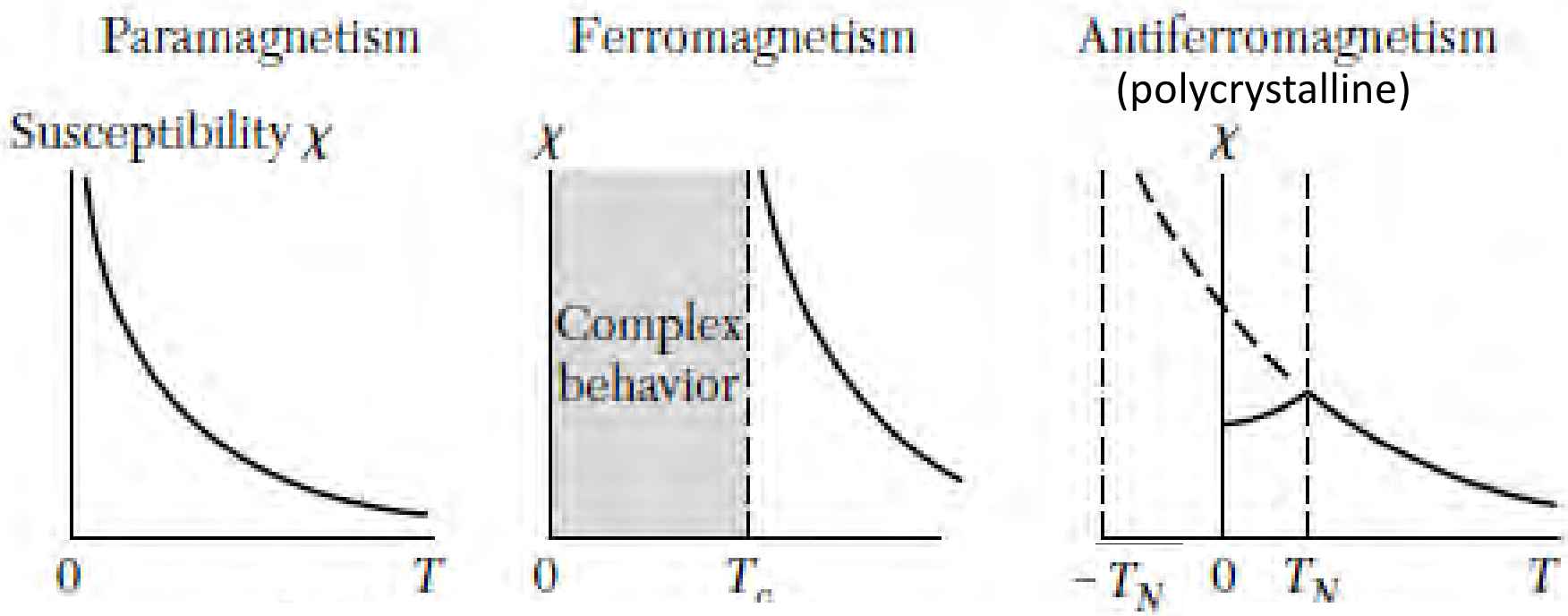

$$\chi = \frac{C}{T}$$

Curie Law

$$T > T_C$$

$$\chi = \frac{C}{T - T_C}$$

Curie - Weiss

$$T > T_N$$

$$\chi = \frac{C}{T + T_N}$$

From Kittle

Antiferromagnetic Susceptibility

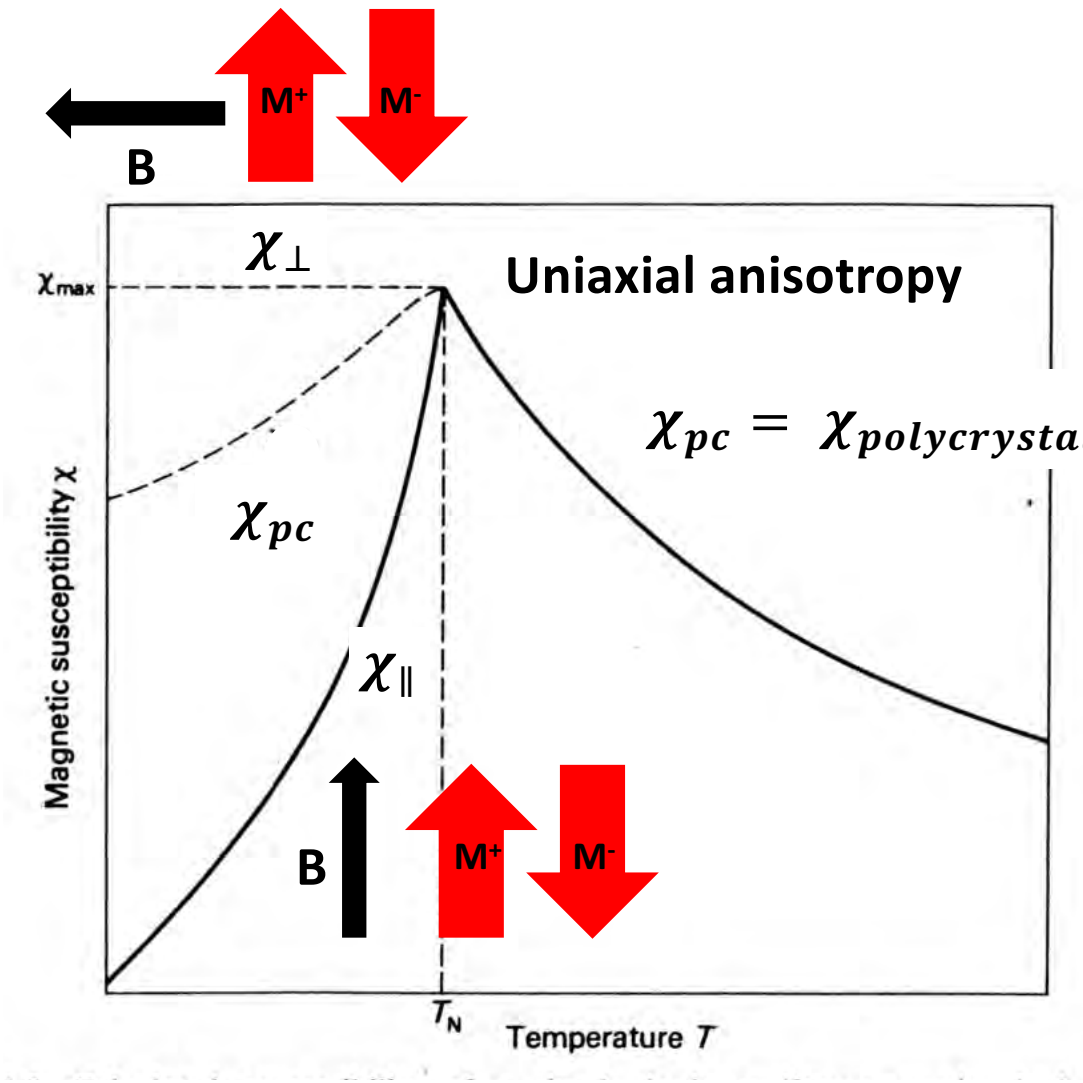

$$\chi_{pc} = \chi_{polycrystalline} = \frac{2}{3}\chi_\perp + \frac{1}{3}\chi_\parallel$$

Peak susceptibility gives Neel Temperature

Antiferromagnetic Susceptibility

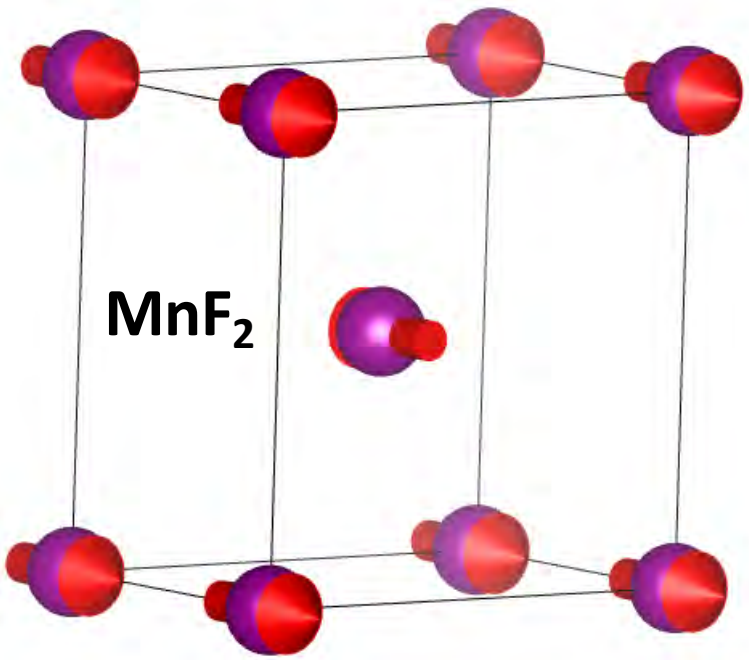

Positions of Mn atoms

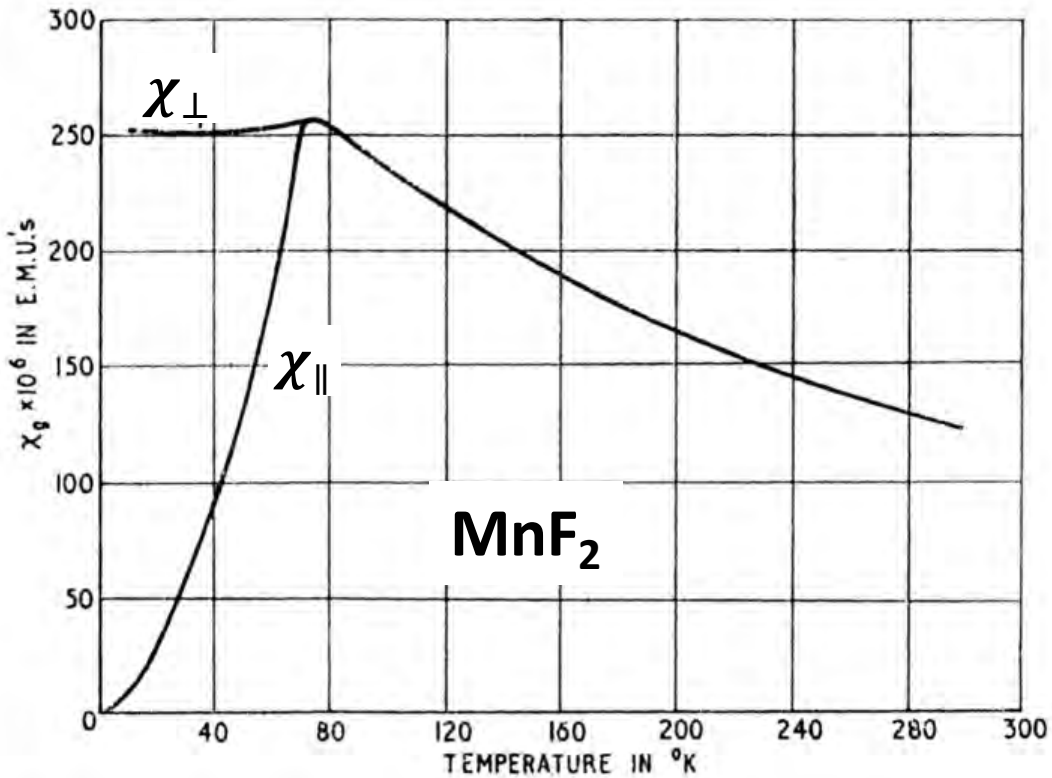

Stop / Jump ?

Magnetic Behaviour in "Large" Fields

Stoner–Wohlfarth model : single domain uniaxial ferromagnet

$$\epsilon = -K_u cos^2\phi - \mu_0 HMcos(\phi + \theta)$$

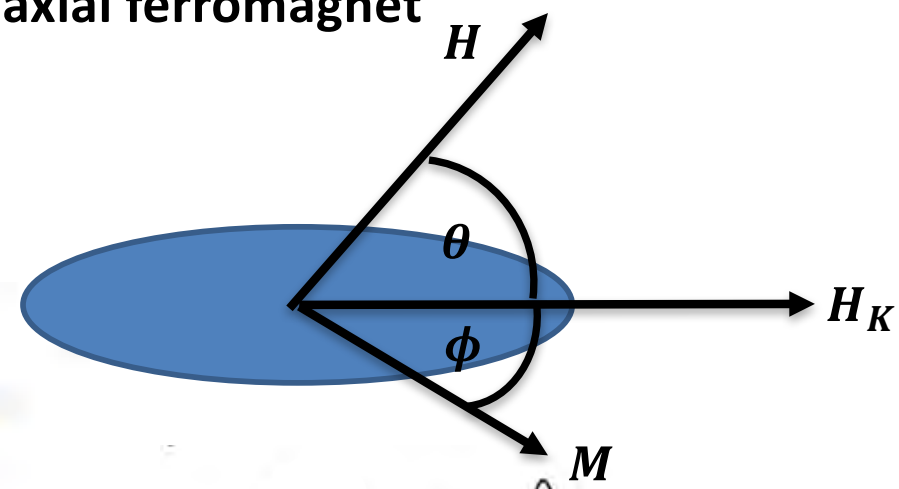

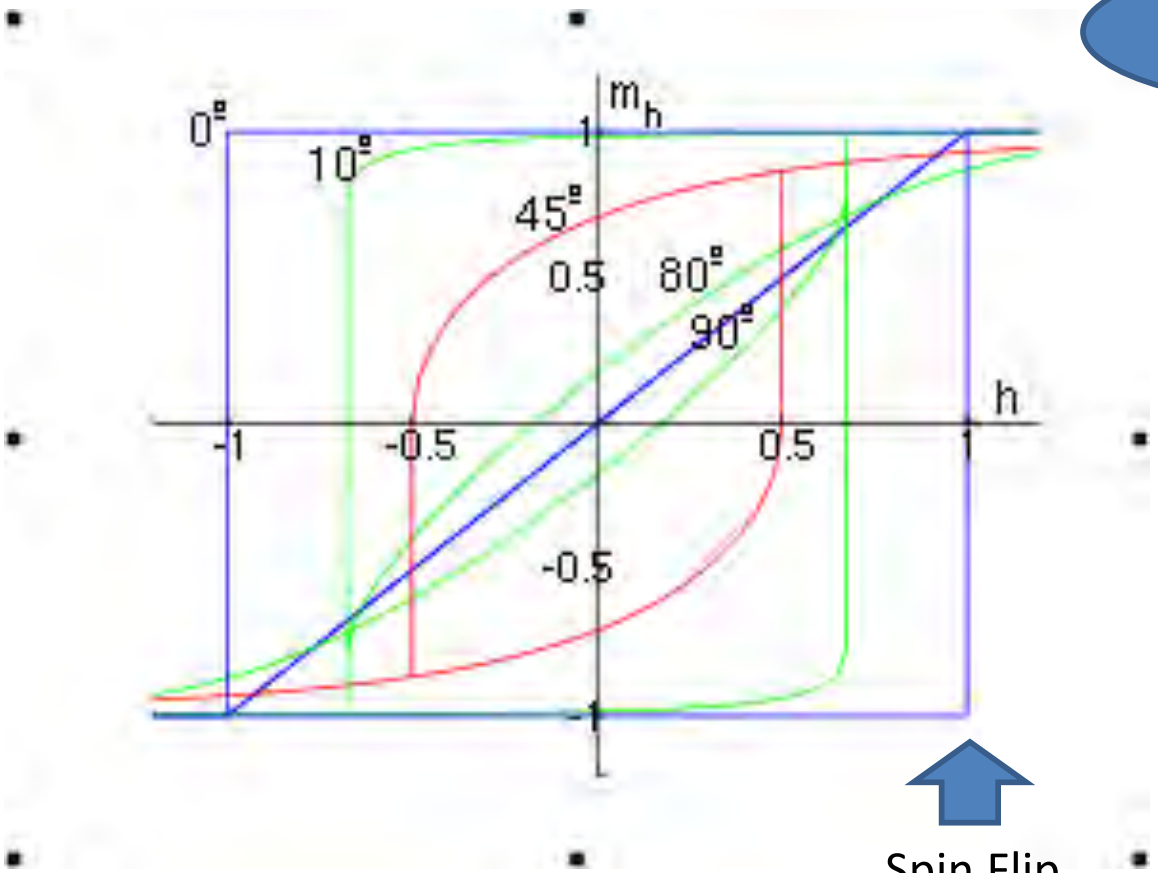

Spin Flip

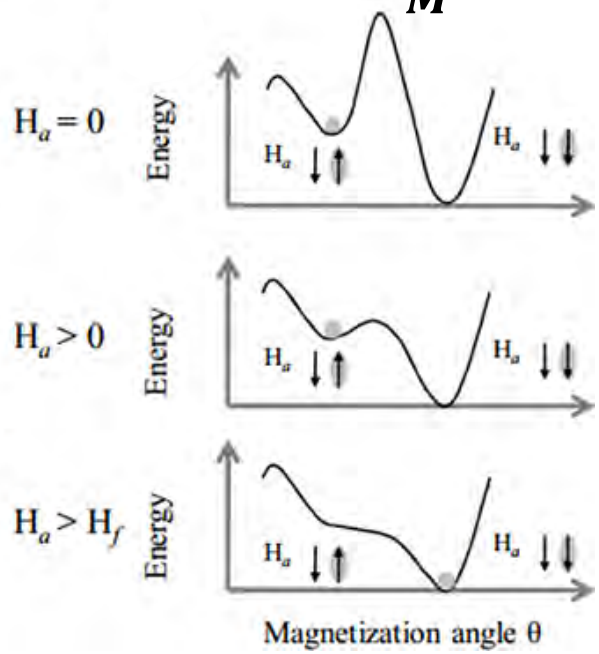

Magnetic Behaviour in “Large” Fields

FM Perpendicularly barium ferrite thin film

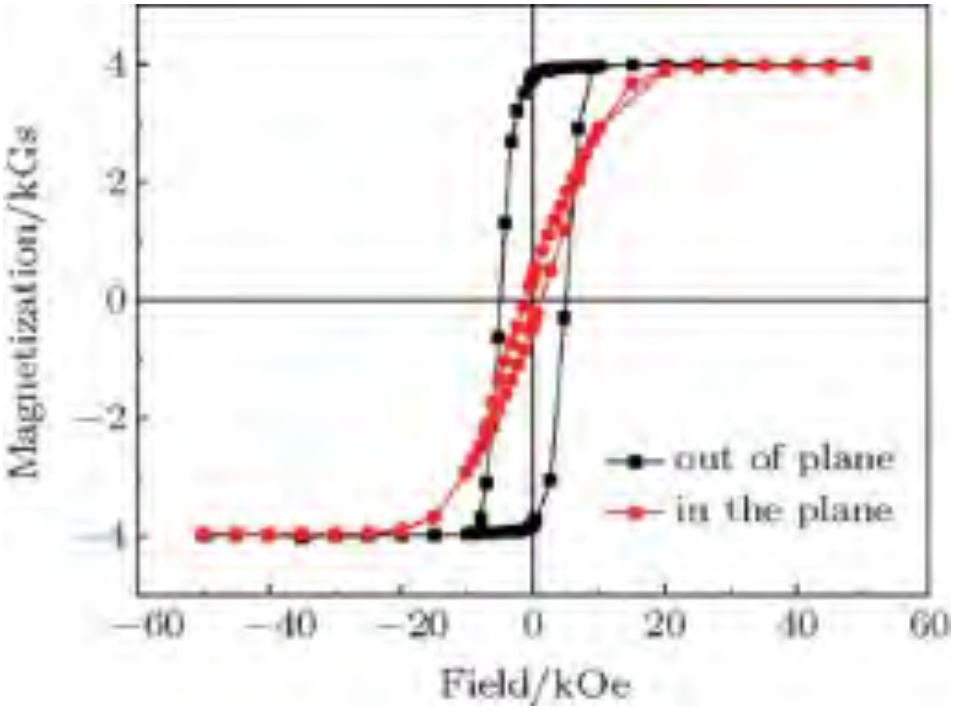

Da-Ming et al Chinese Physics B, 2016, 25(6): 068403

FM (Ga,Mn)($As_{70}P_{30}$)

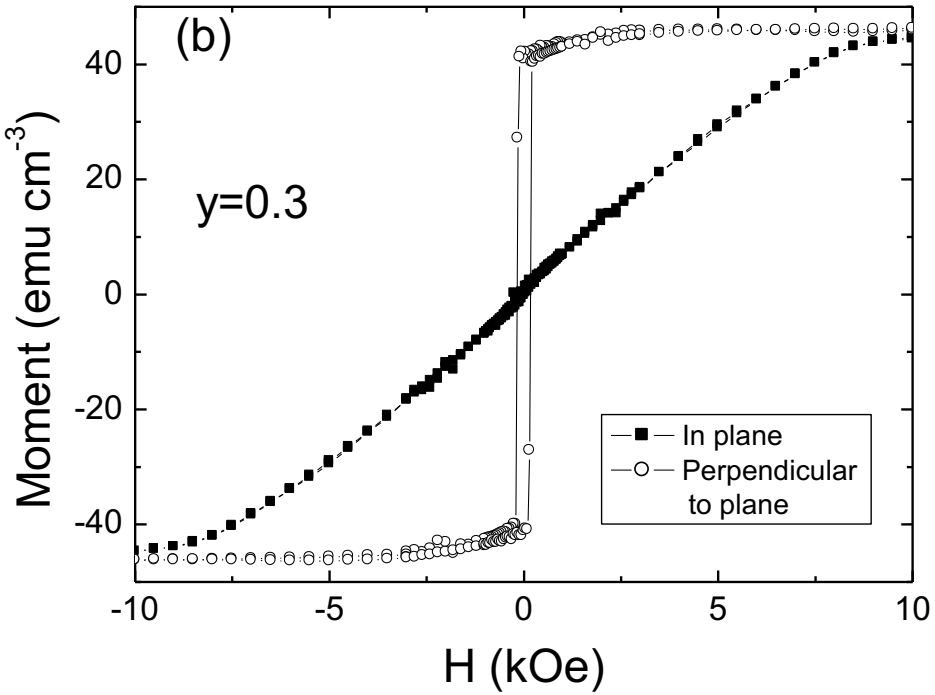

Normally don’t see ideal behaviour because of domain formation

FM: Strain-induced Anisotropy

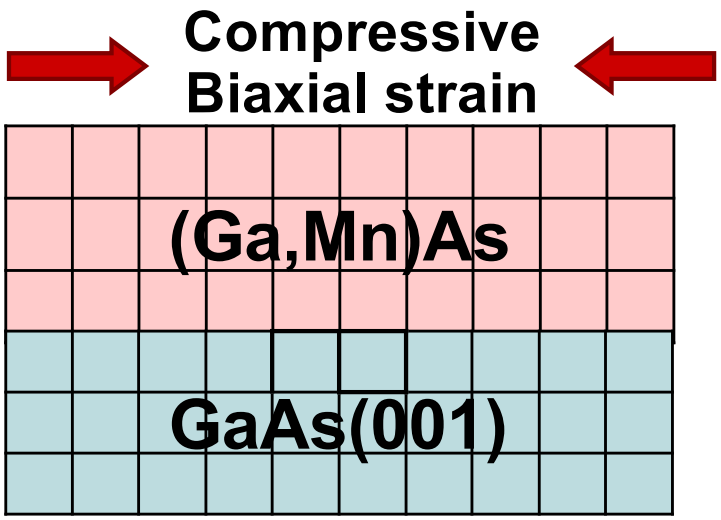

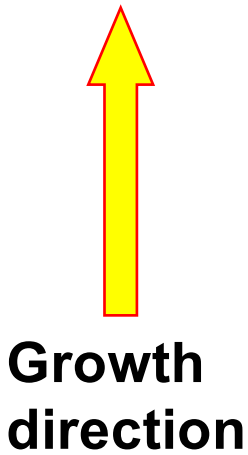

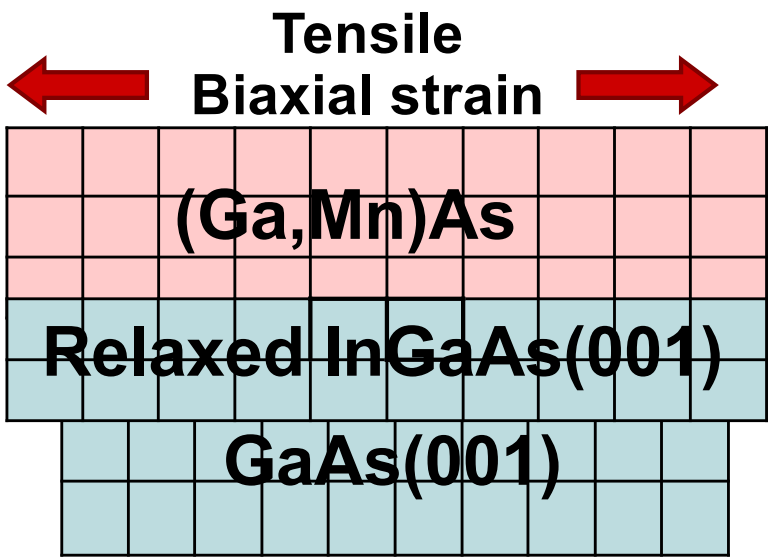

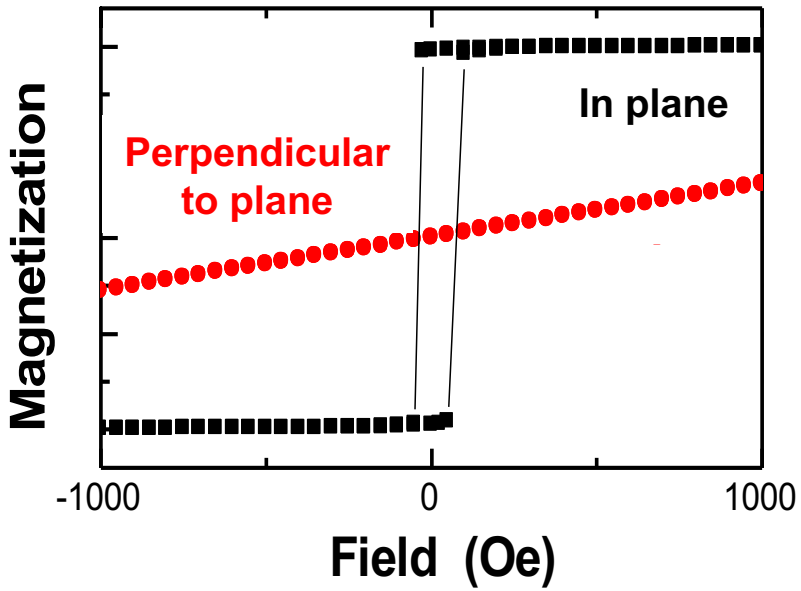

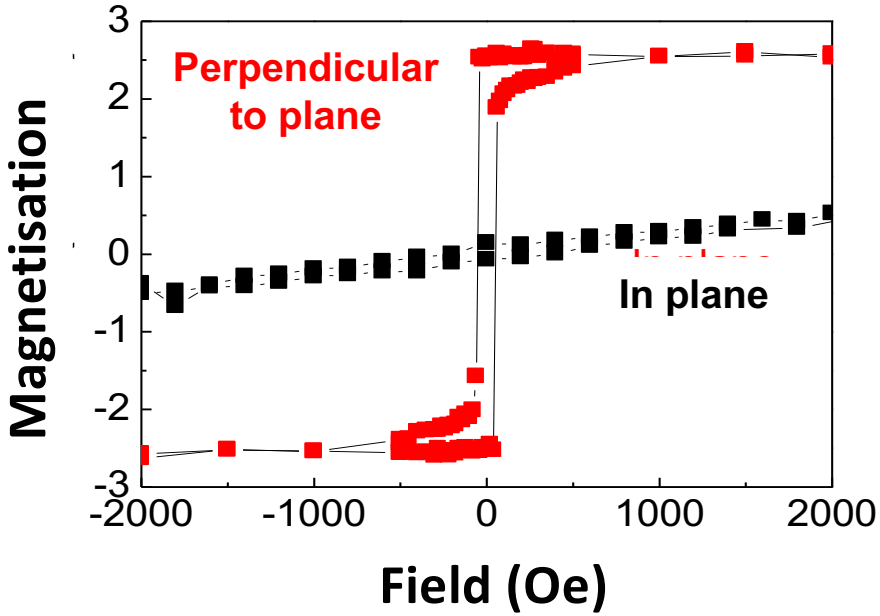

Dominant magneto-crystalline anisotropy in-plane for compressive strain and or out-of-plane for tensile strain strain

End Part One

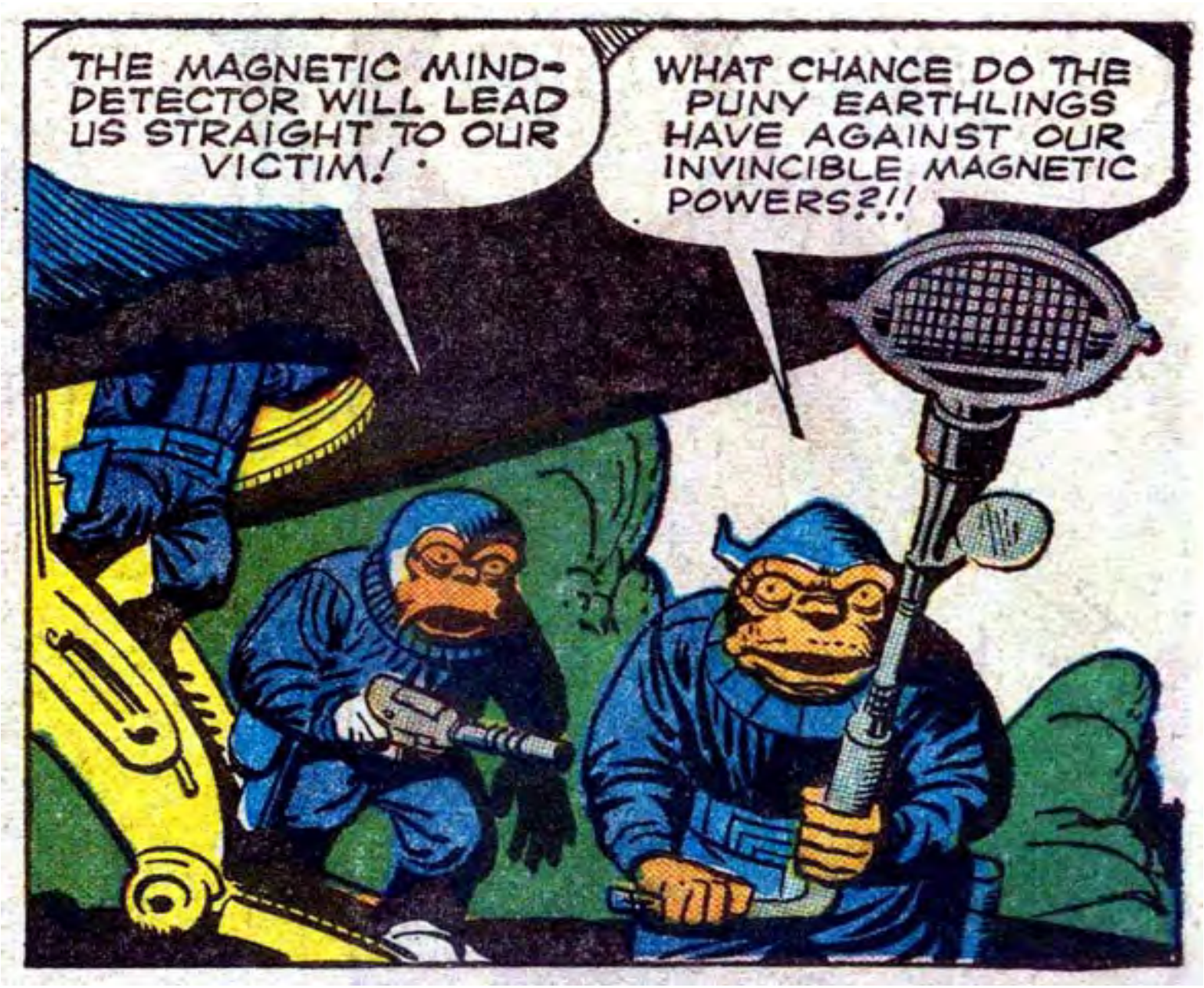

The importance of avoiding stray fields

Welcome back

Magnetic Behaviour in "Large" Fields

Stoner–Wohlfarth model : single domain uniaxial ferromagnet

$$\epsilon = -K_u cos^2\phi - \mu_0 HMcos(\phi + \theta)$$

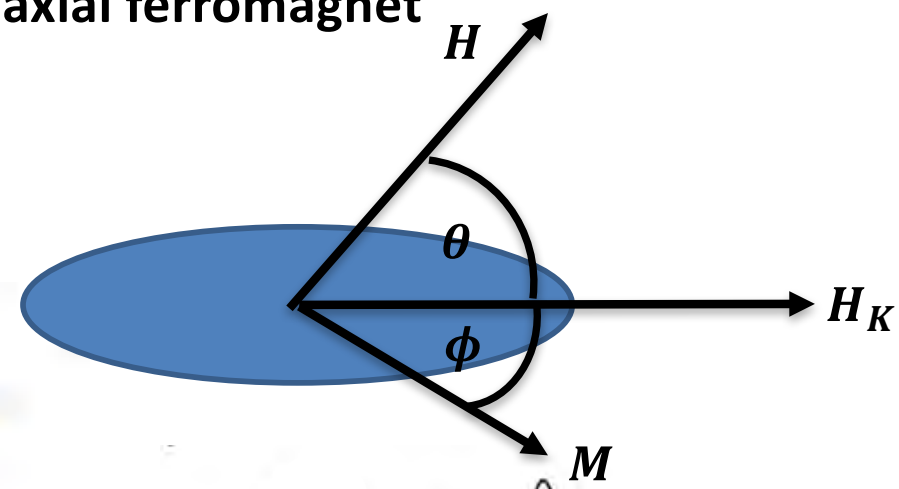

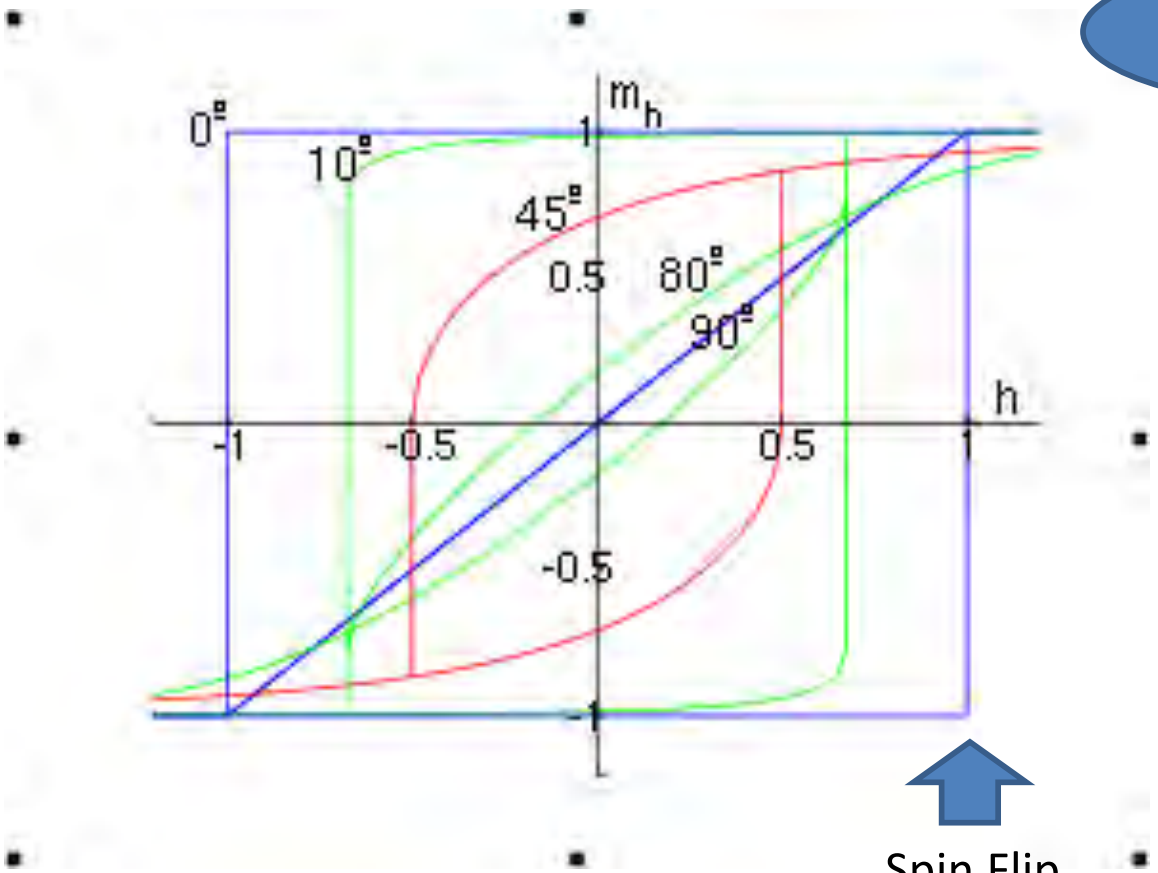

Spin Flip

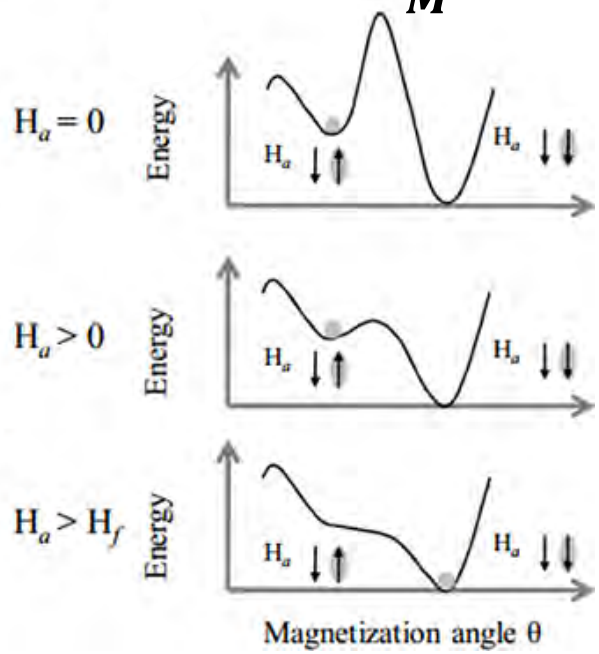

Magnetic Behaviour in "Large" Fields

Stoner–Wohlfarth model : single domain uniaxial ferromagnet

$$\epsilon = -K_u cos^2\phi - \mu_0 HMcos(\phi + \theta)$$

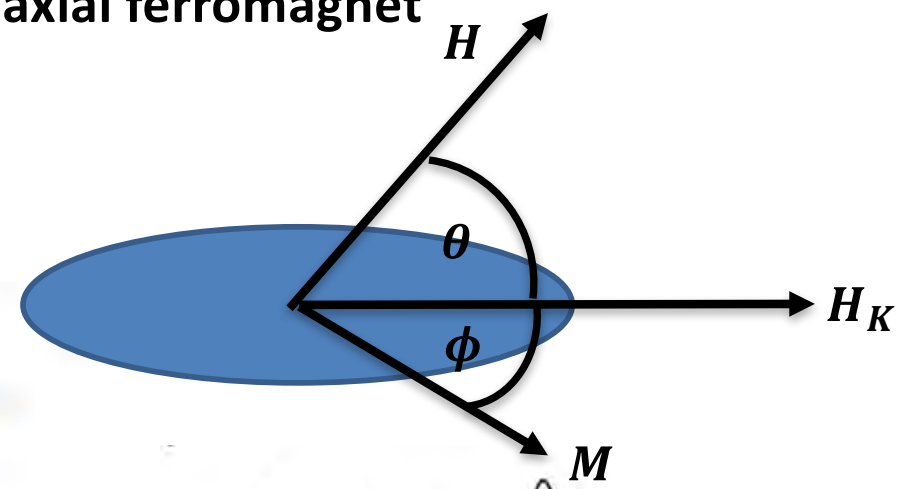

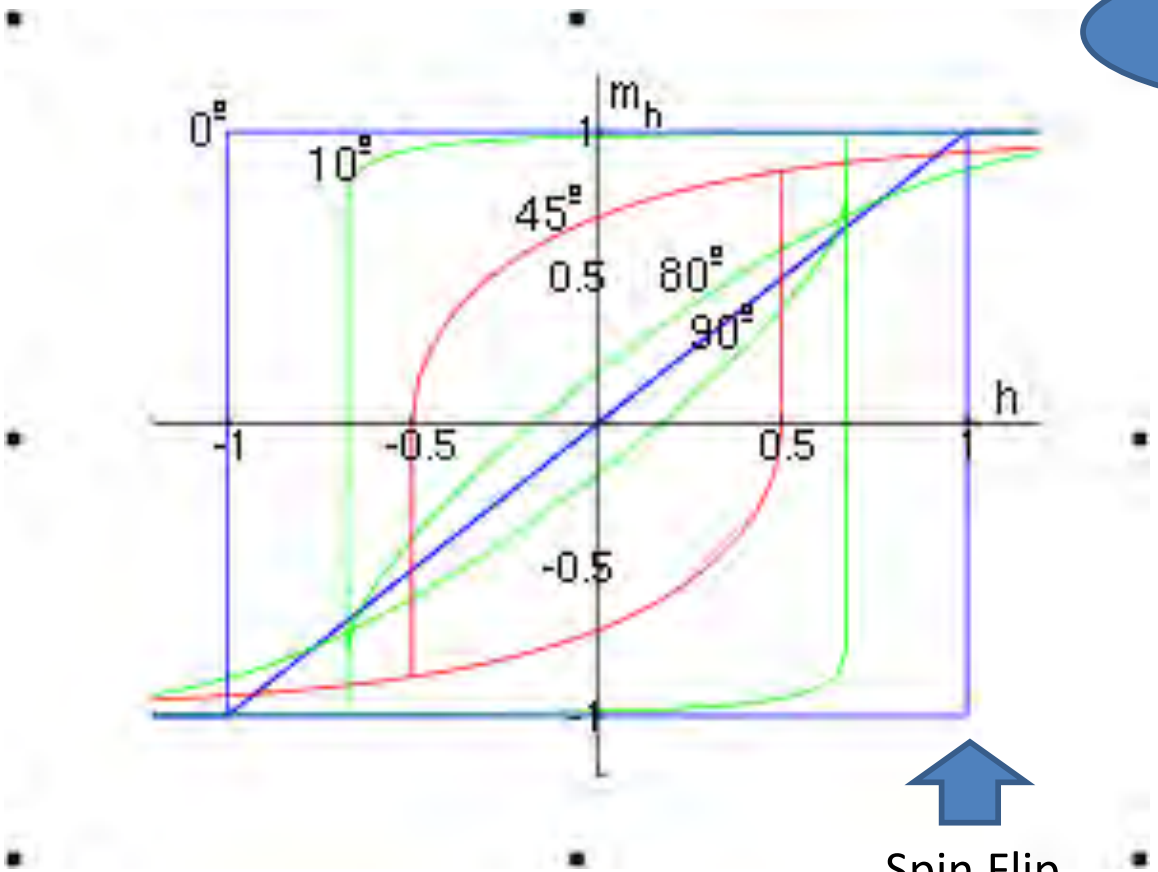

Spin Flip

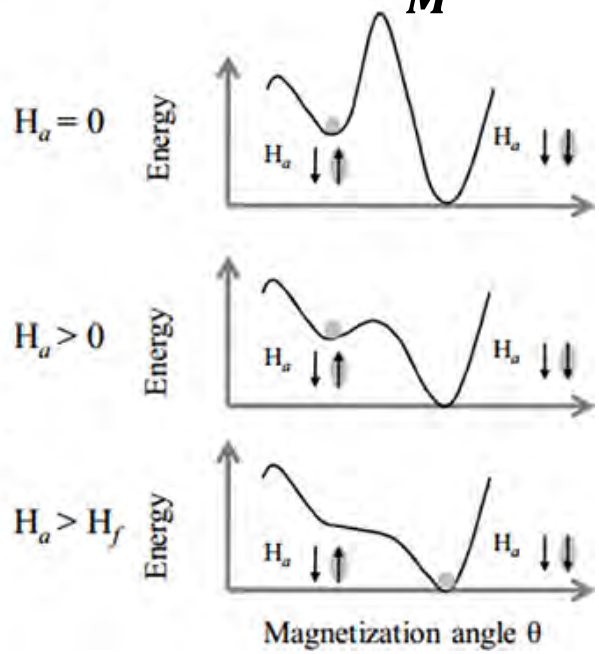

Magnetic Behaviour in “Large” Fields

FM Perpendicularly barium ferrite thin film

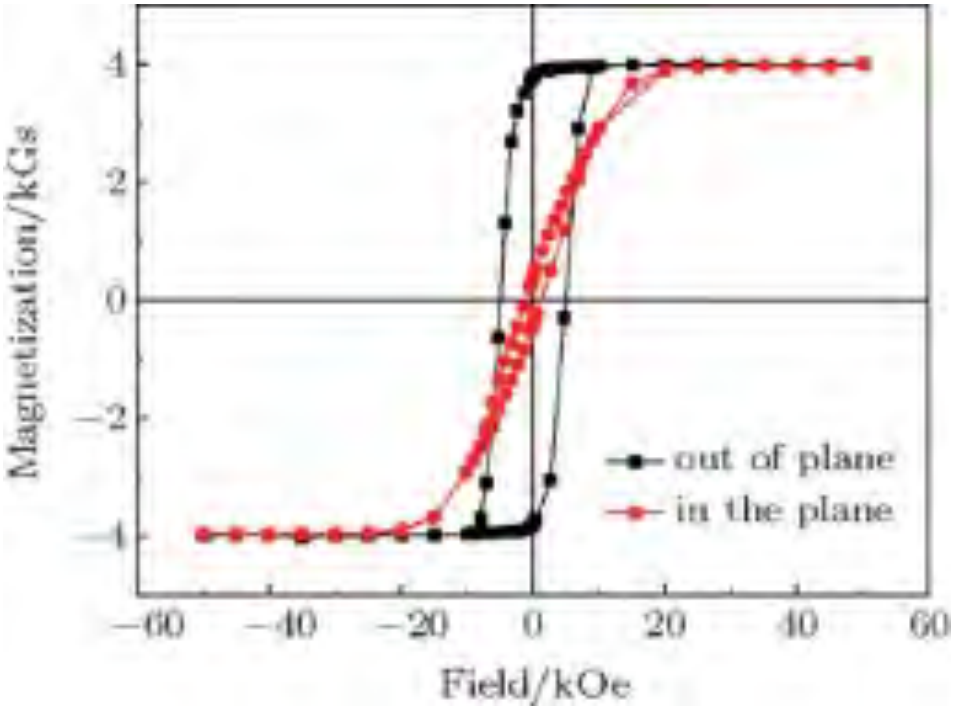

Da-Ming et al Chinese Physics B, 2016, 25(6): 068403

FM (Ga,Mn)($As_{70}P_{30}$)

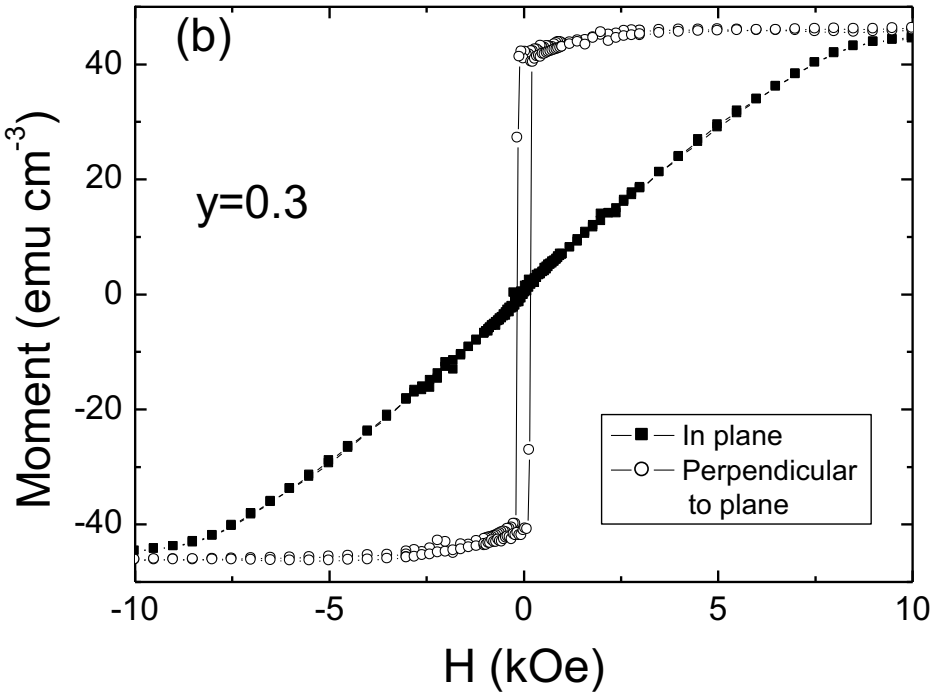

Normally don’t see ideal behaviour because of domain formation

FM: Strain-induced Anisotropy

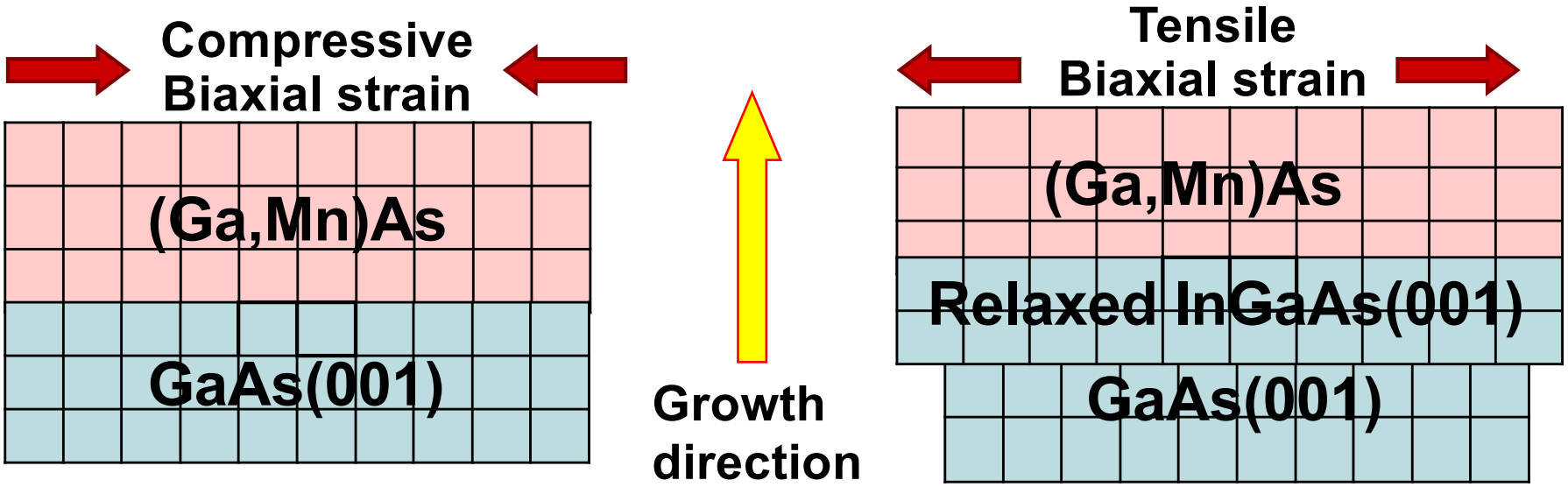

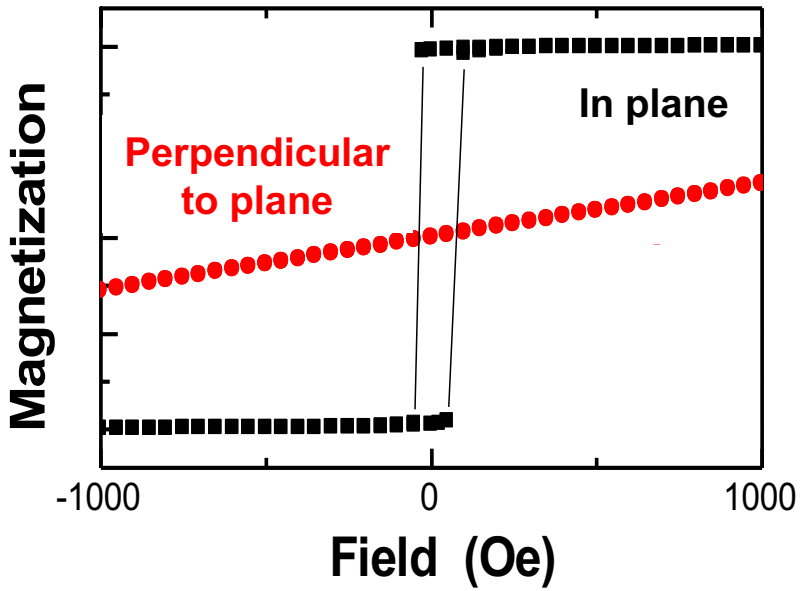

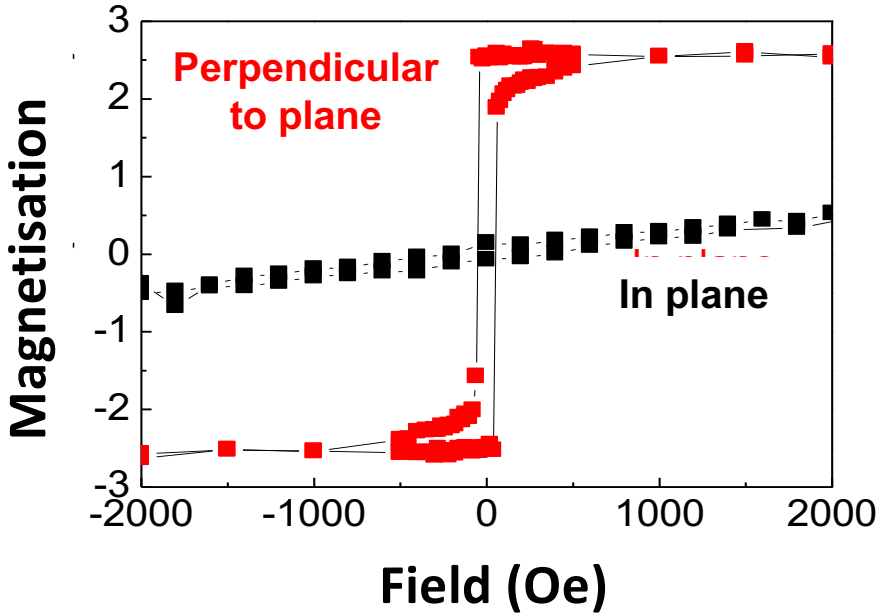

Dominant magneto-crystalline anisotropy in-plane for compressive strain and or out-of-plane for tensile strain strain

Antiferromagnets: Spin Flop Transitions

Single domain uniaxial antiferromagnet H perpendicular to easy axis

$$\epsilon = J_{ex,inter} M^2 cos(2\phi) + K_u cos^2\phi - \mu_0 H M cos(\phi)$$

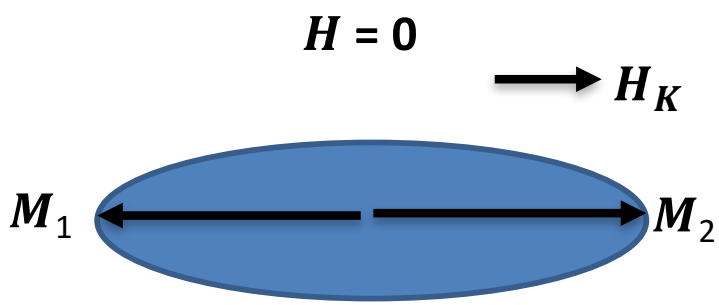

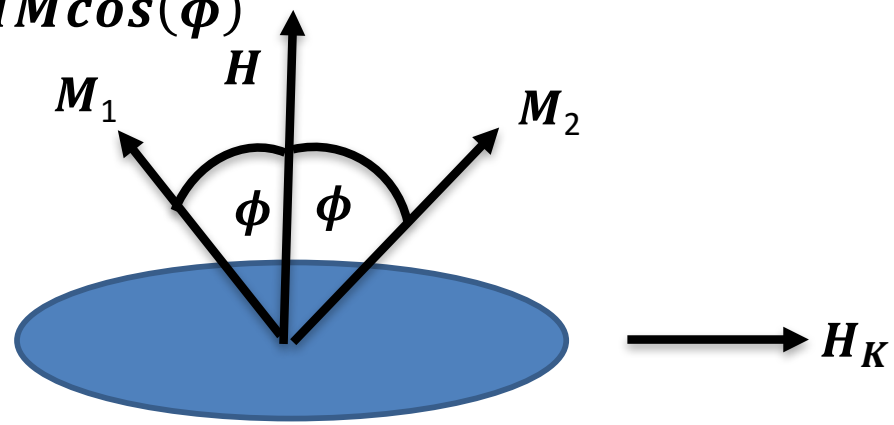

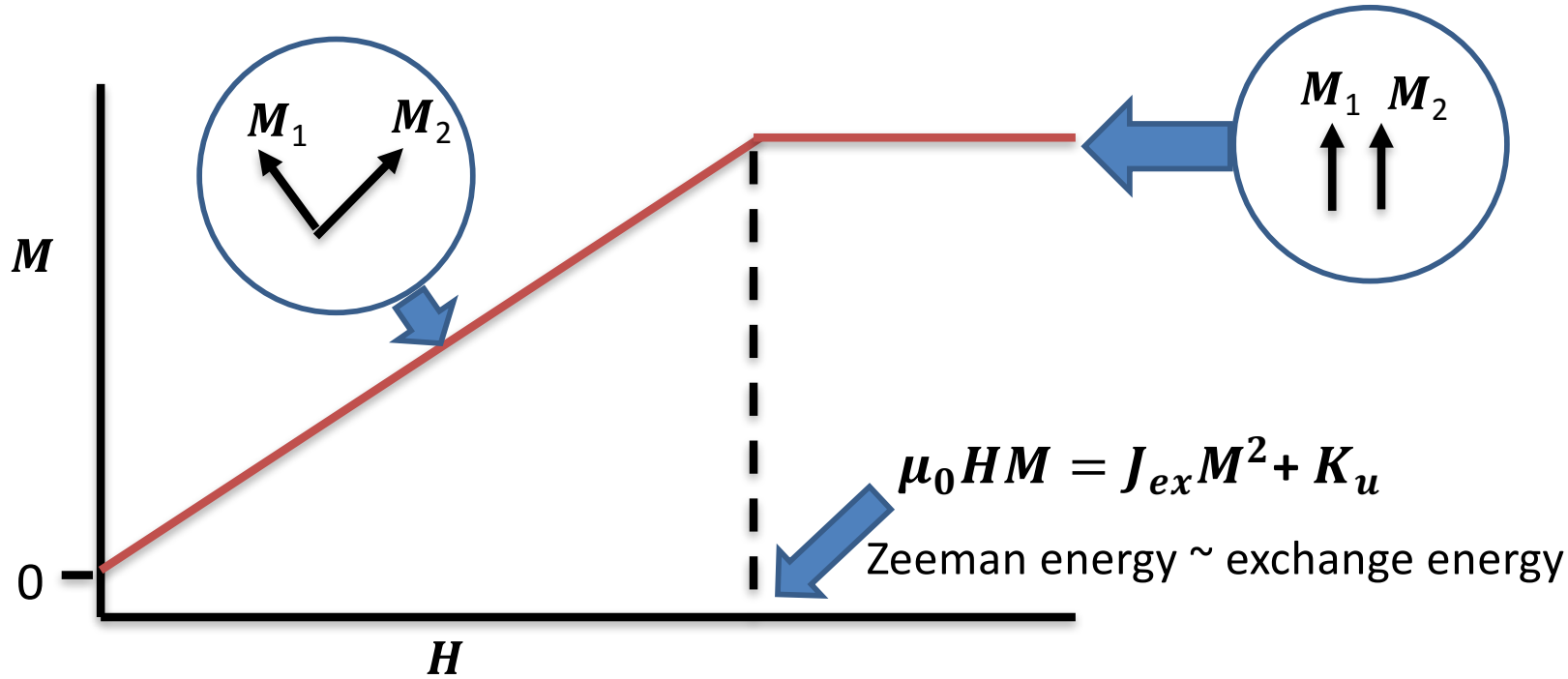

$$\mu_0 H M = J_{ex} M^2 + K_u$$

Zeeman energy ~ exchange energy

Antiferromagnets: Spin Flop Transitions

Single domain uniaxial antiferromagnet. H parallel to easy axis.

$$\epsilon = J_{ex,inter} M^2 cos(2\phi) - K_u cos^2\phi - \mu_0 HM cos(\phi)$$

Small K_u

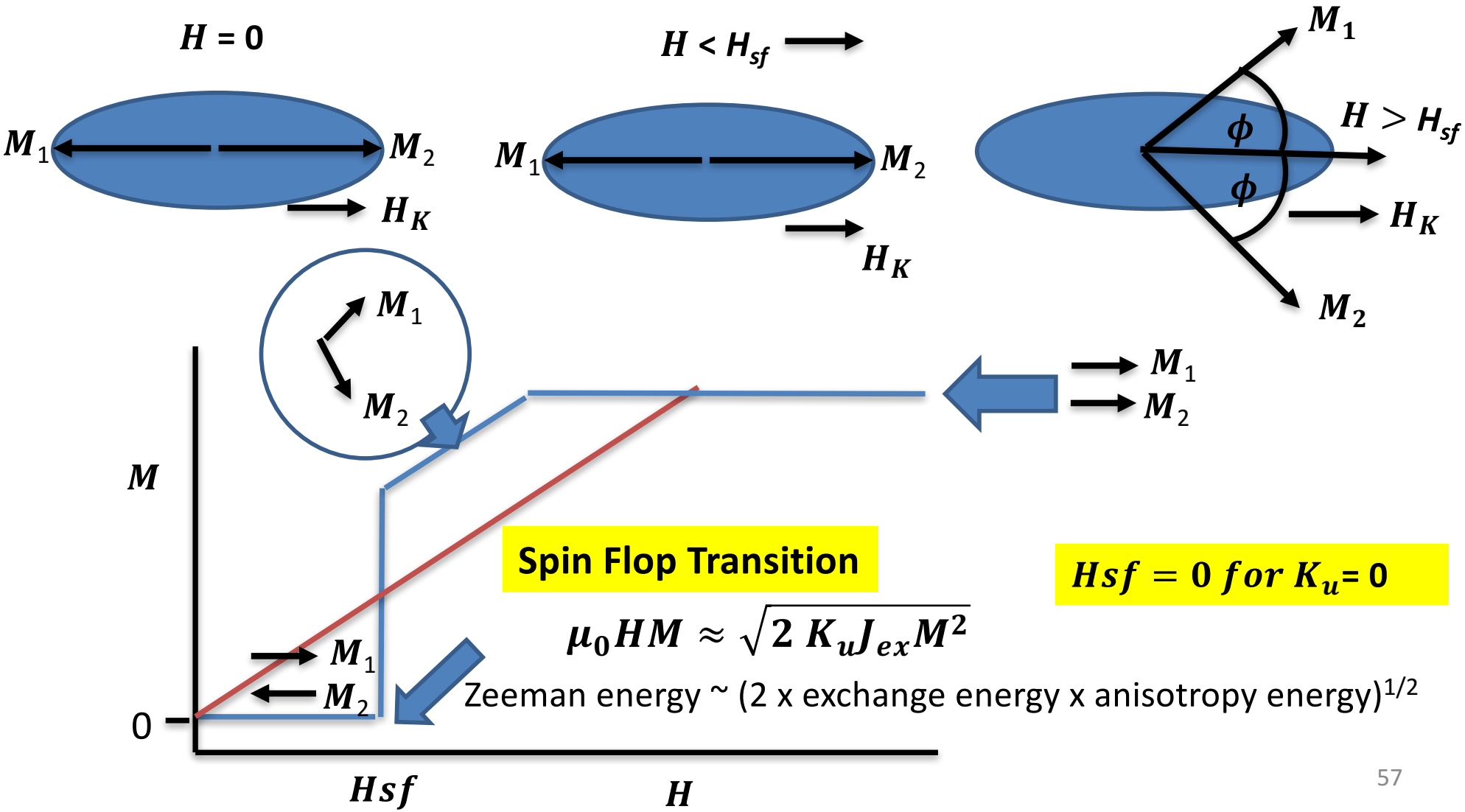

Spin Flop Transition

$$Hsf = 0 \; for \; K_u = 0$$

$$\mu_0 HM \approx \sqrt{2\, K_u J_{ex} M^2}$$

Zeeman energy ~ (2 x exchange energy x anisotropy energy)$^{1/2}$

Antiferromagnets: Spin Flip Transitions

Single domain uniaxial antiferromagnet. H parallel to easy axis.

$$\epsilon = J_{ex,inter} M^2 cos(2\phi) - K_u cos^2\phi - \mu_0 H M cos(\phi)$$

Large K_u

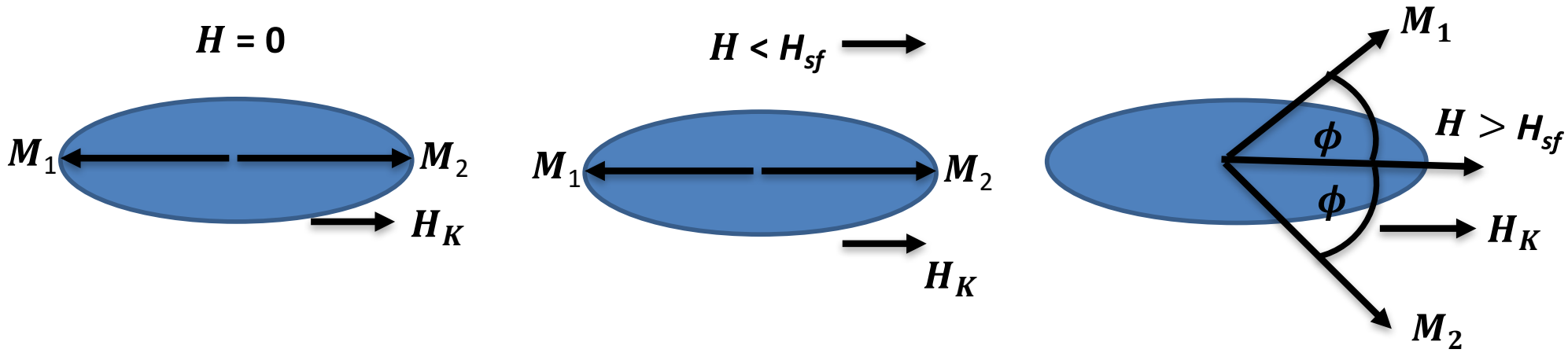

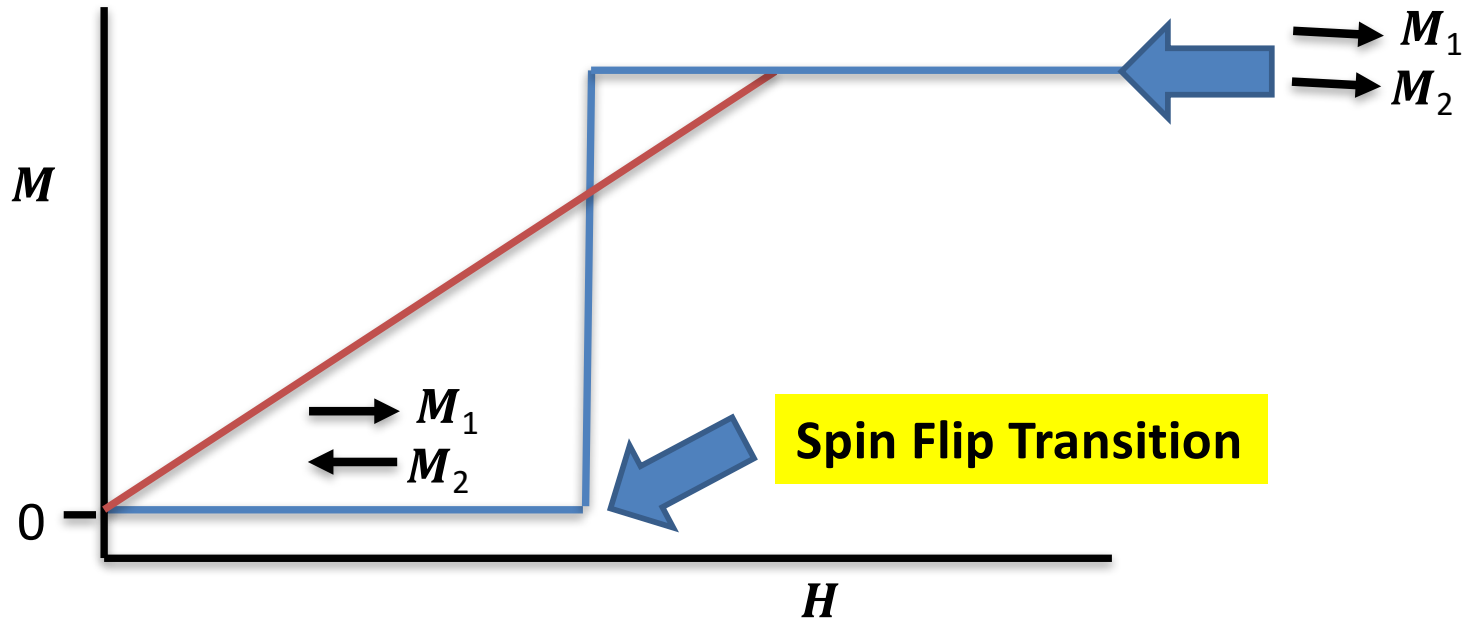

Antiferromagnets: Spin Flop Transitions

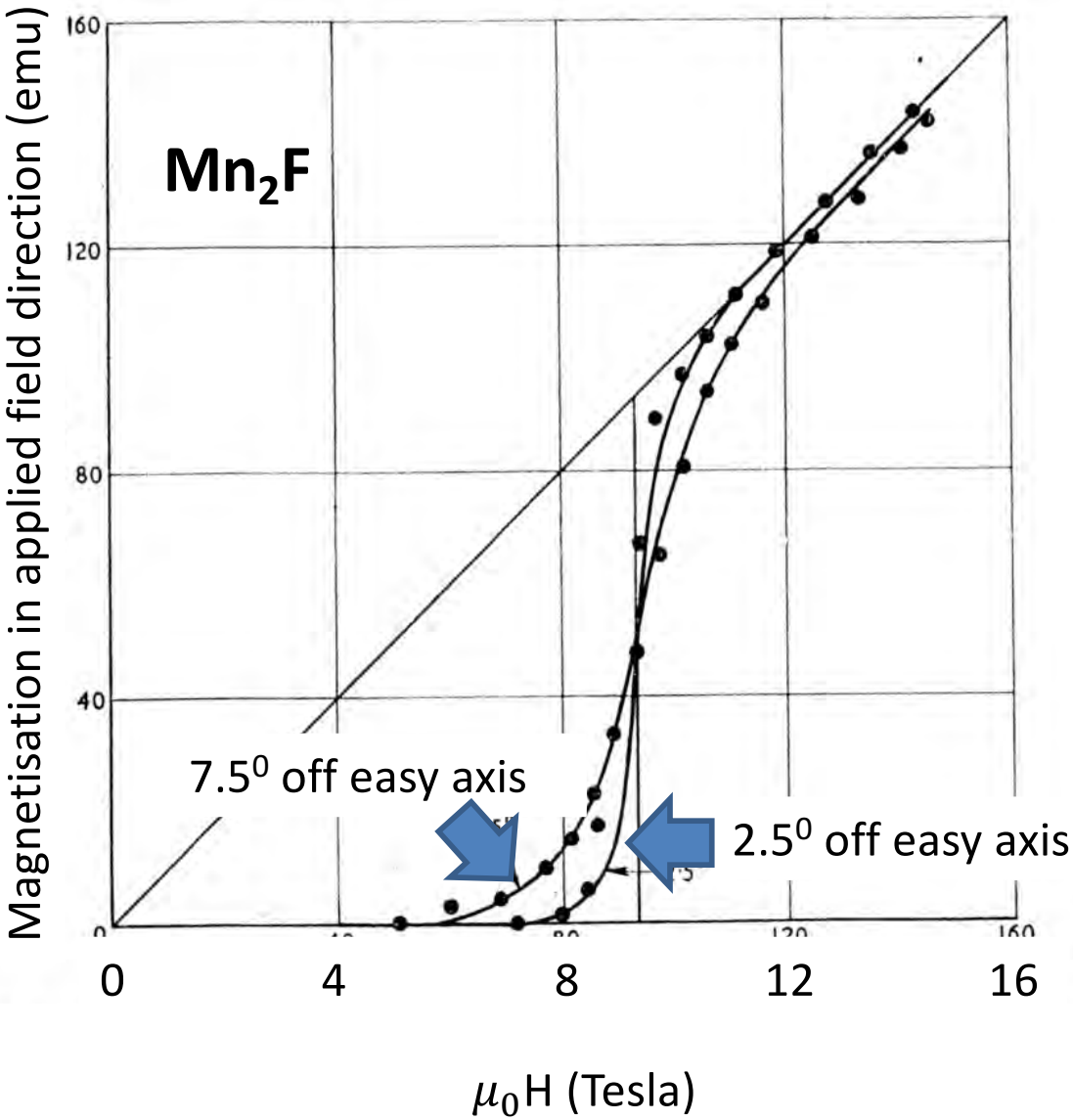

Spin Flop Transition seen in AFMR

If Exchange energy >> Anisotropy energy and T << T_N

$$H_{app} \perp c - axis \quad \hbar\omega = g\mu_B(B_{sf}^2 + B_{app}^2)^{1/2}$$

$$H_{app} \parallel c - axis \text{ and } B_{app} < B_{sf} \quad \hbar\omega = g\mu_B(B_{sf} \pm B_{app}) \qquad B_{sf} = spin\ flop\ field$$

$$H_{app} \parallel c - axis \text{ and } B_{app} > B_{sf} \quad \hbar\omega = g\mu_B(B_{sf}^2 - B_{app}^2)^{1/2}$$

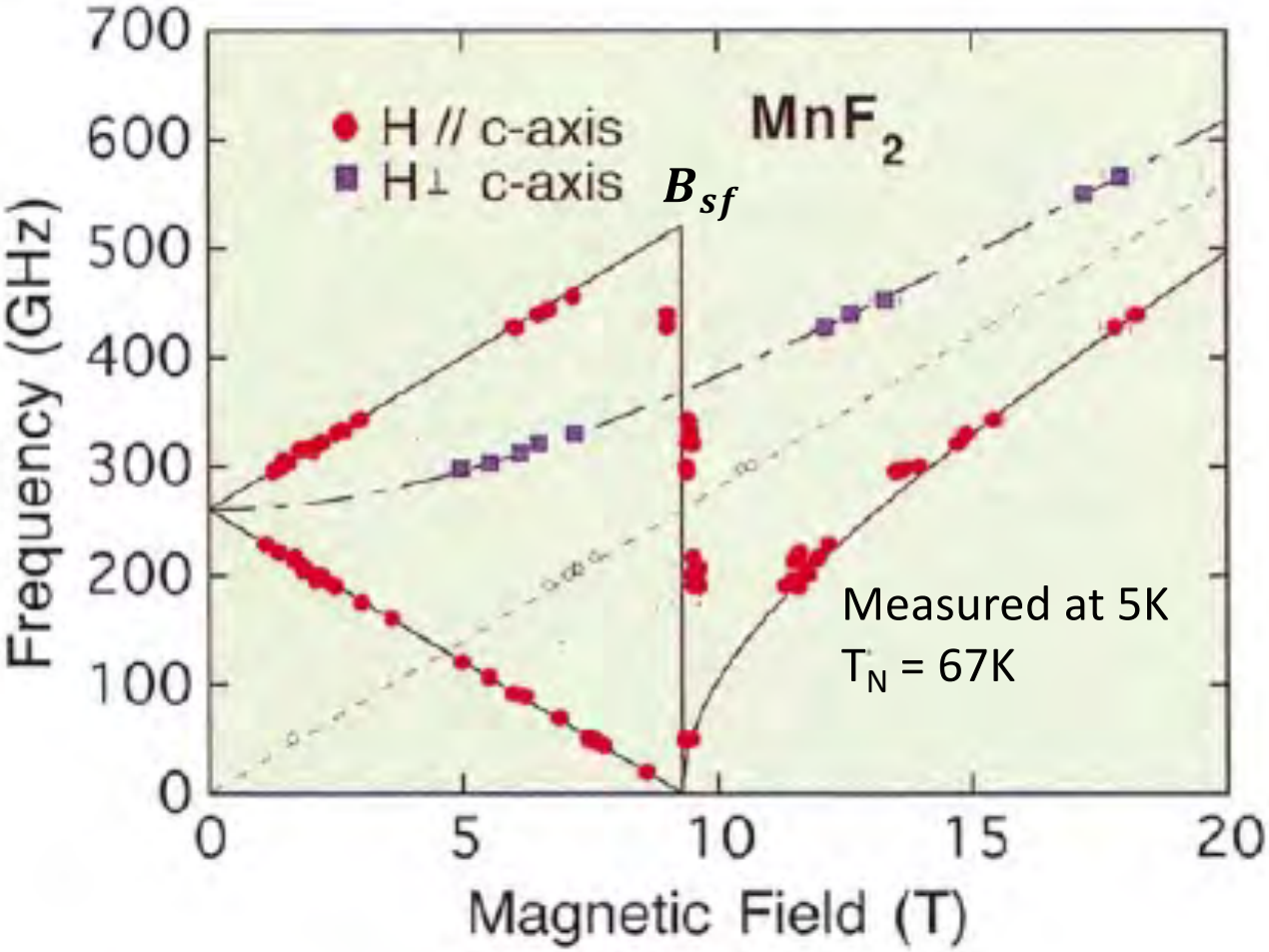

Hagiwara, et al : J. Phys. C**8**, 7349 (1996). *Nagamiya et al Adv. Phys.* ***4****, 1 (1955). Foner Phys. Rev.* ***107****, 683 (1957).*

Torque Magnetometry: α-MnTe

Can give symmetry and strength of anisotropy

NiAs-structure Six fold symmetry

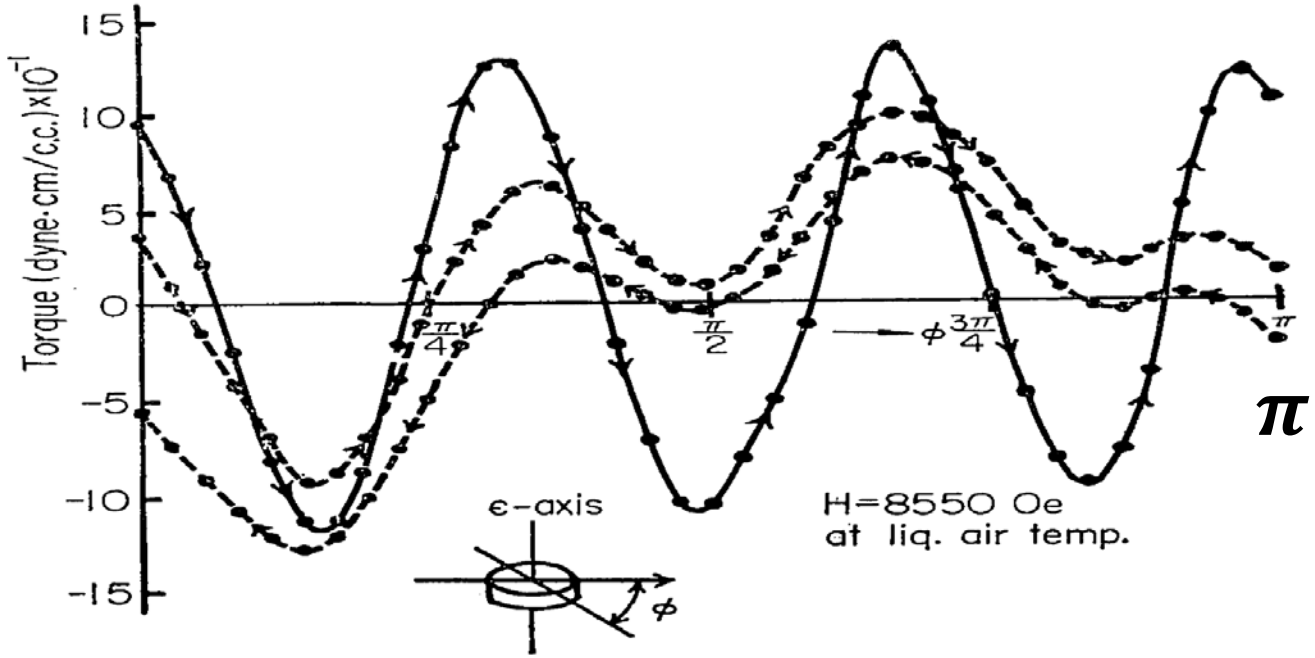

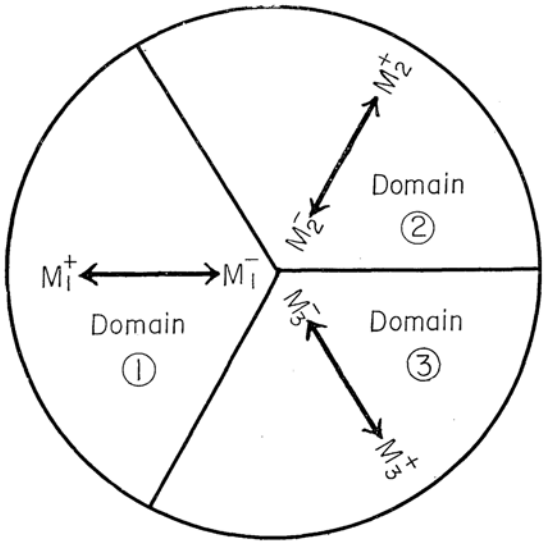

Fig. 6. The three-domain structure in the *c*-planes. The arrows in each domain indicate a pair of the antiferromagnetic spins, the common axis of spin pairs make angle of $2\pi/3$ with each other.

1 cm diameter single crystal disk.
Field rotated in c-plane
Solid line first measurements.
Others after sample deterioration

Komatsubara et al J Phys Soc Japan 18, 3 (1963)

Torque Magnetometry

monoclinic quasi-one-dimensional S = 1/2 Heisenberg antiferromagnet $CuSb_2O_6$

Bulk Sample
Quite small magnetic fields

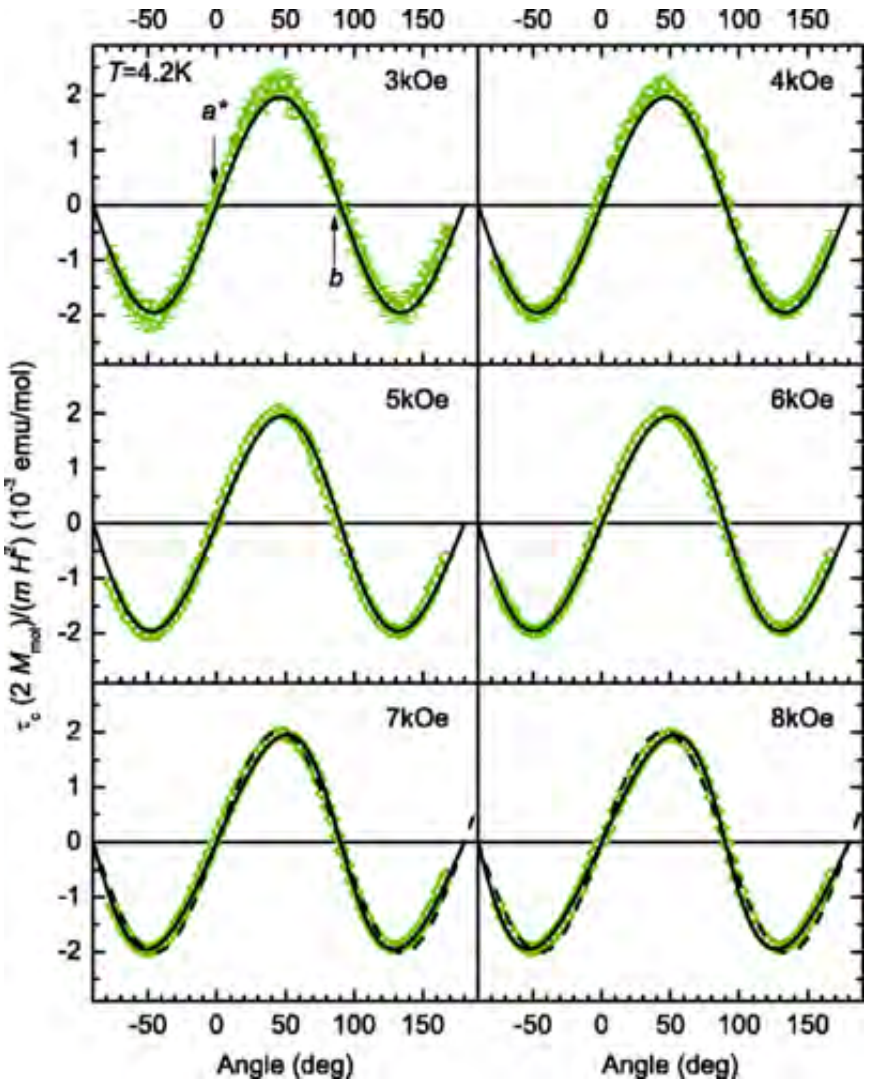

Herak et al Phys. Rev. B 91, 174436 (2015)

Zero Field NMR in Antiferromagnets

^{153}Eu and ^{69,71}Ga Zero-Field NMR Study of Antiferromagnetic State in $EuGa_4$

Mamoru Yogi[1]*, Saori Nakamura[1], Nonoka Higa[1], Haruo Niki[1], Yusuke Hirose[2], Yoshichika Ōnuki[2], and Hisatomo Harima[3]

In ordered AF state the magnetic field is the same at each equivalent nuclear site → NMR signals for zero applied field.

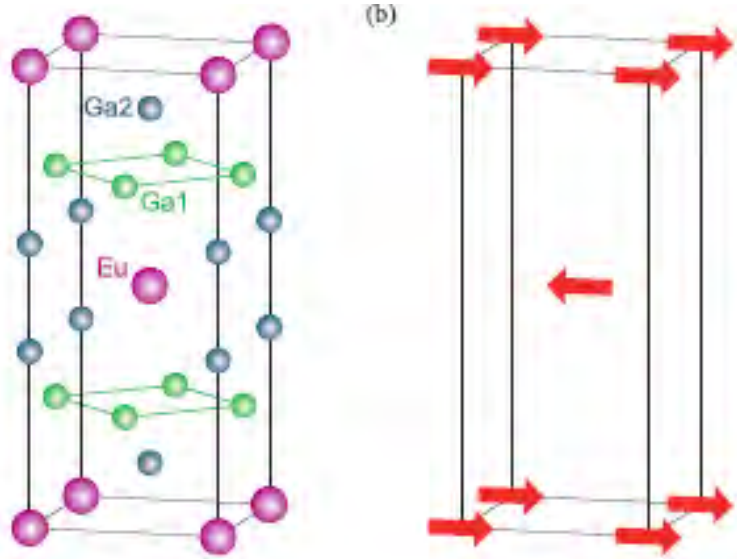

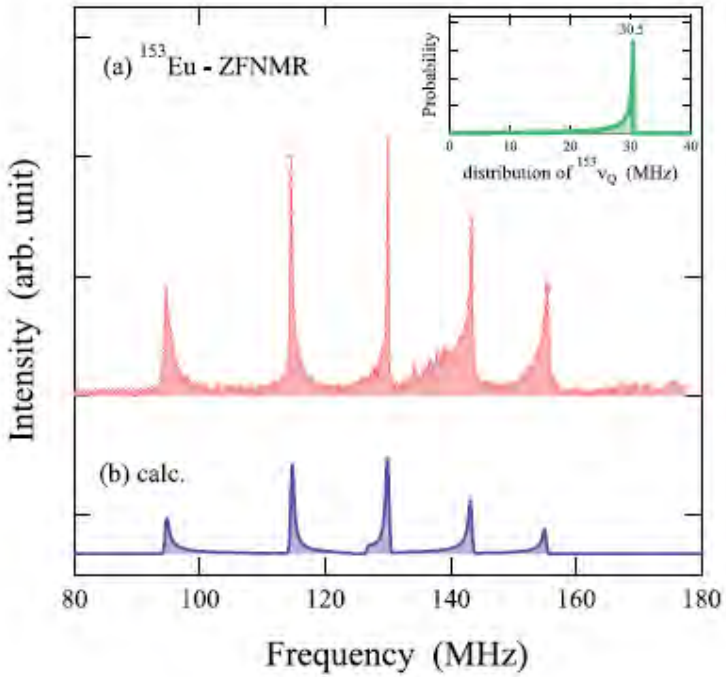

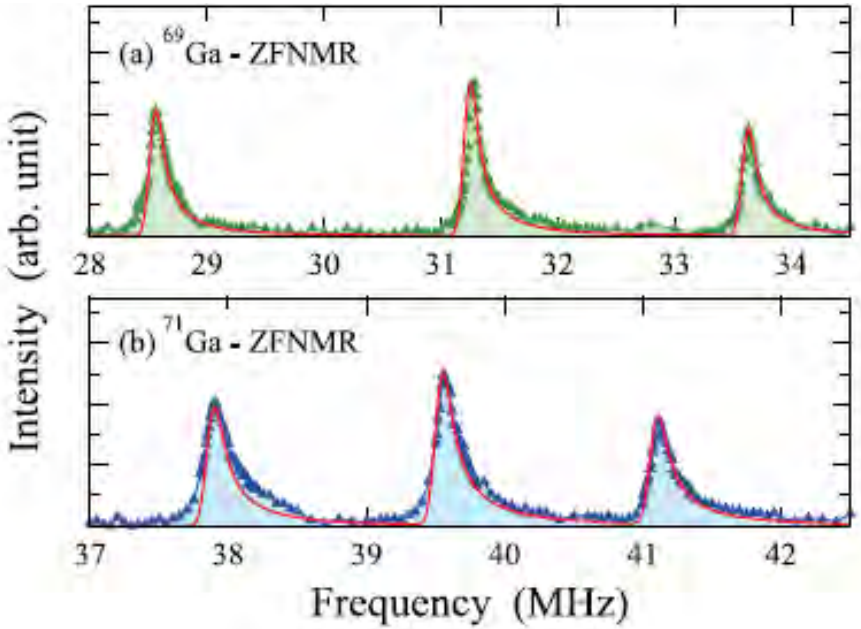

Yogi et al J. Phys. Soc. Jpn. 82, 103701 (2013)

Antiferromagnetism : ZFNMR

^{153}Eu and ^{69,71}Ga Zero-Field NMR Study of Antiferromagnetic State in $EuGa_4$

Mamoru Yogi[1]*, Saori Nakamura[1], Nonoka Higa[1], Haruo Niki[1], Yusuke Hirose[2], Yoshichika Ōnuki[2], and Hisatomo Harima[3]

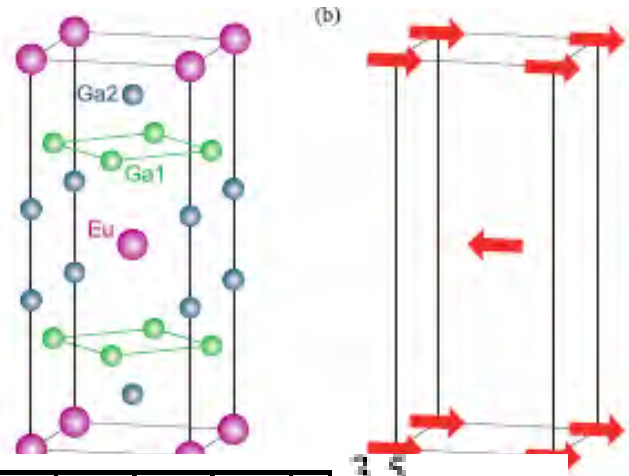

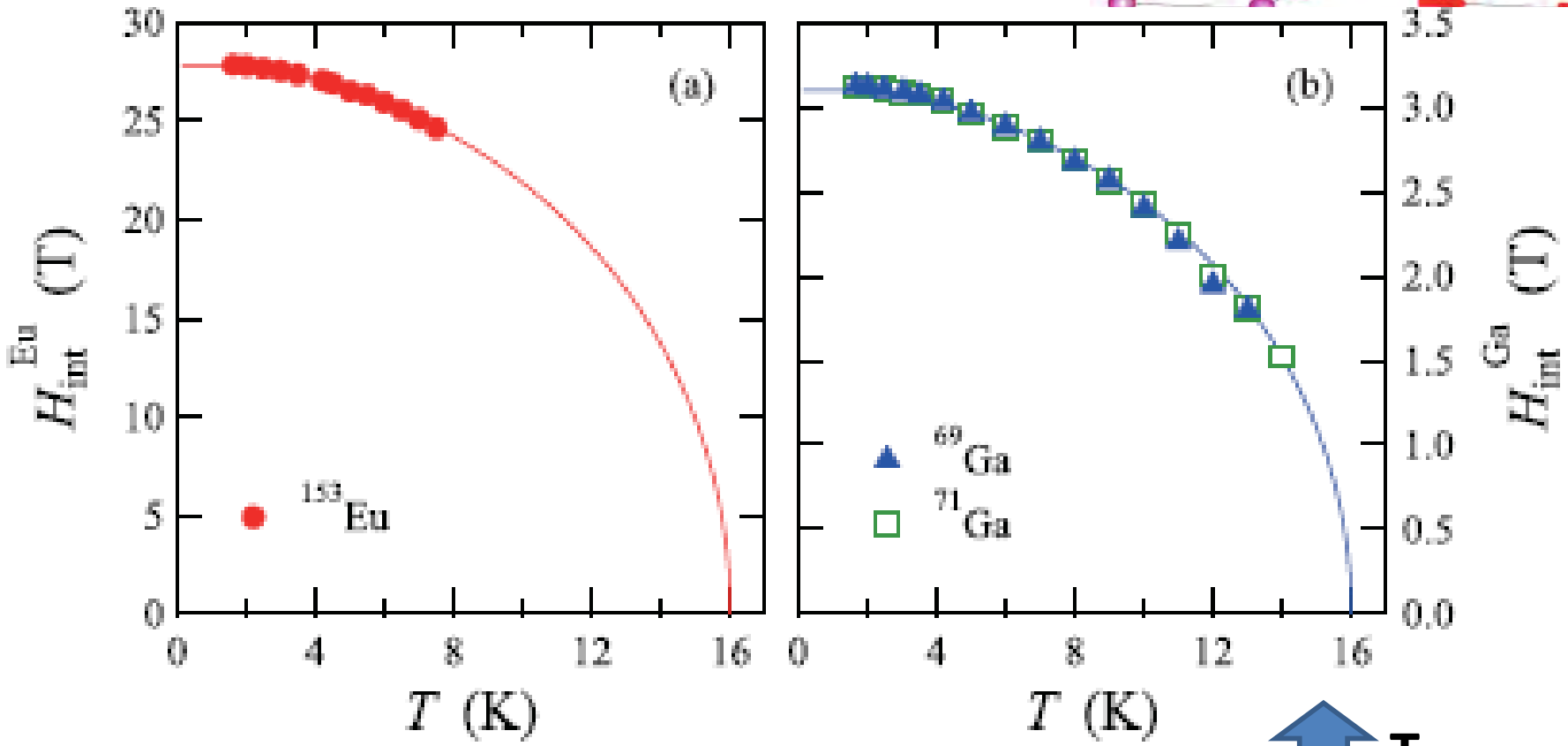

T_N

But need to find resonances!

Yogi et al J. Phys. Soc. Jpn. 82, 103701 (2013)

Antiferromagnetism : ZFNMR

Polycrystalline Mn_2Au

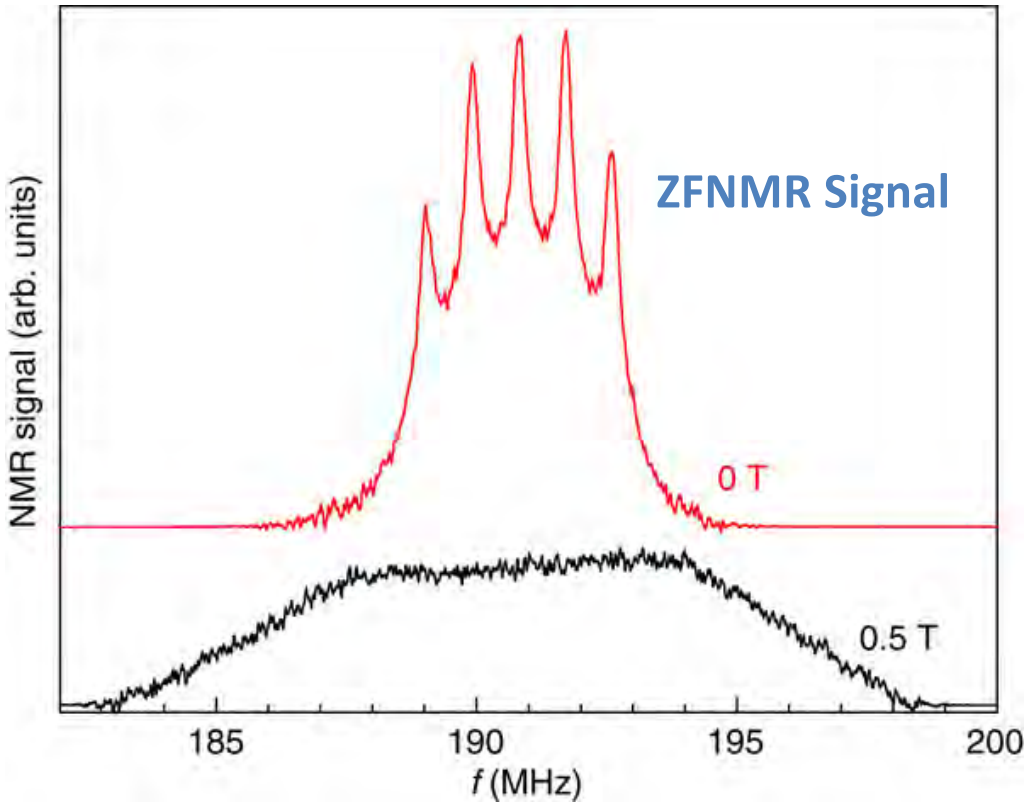

Applying a magnetic field of $\mu_0 H_{app}$=0.5 T changes the five-peak ZFNMR spectrum into an unresolved broad spectrum extending.

In the applied field equivalent sites in the constituent grains experience different fields because of the distribution of angles between internal and applied fields. The total field experienced by ^{55}Mn nuclei takes all values between $H_{hyp}+H_{app}$ and $-H_{hyp}+H_{app}$.

Barthem et al Nature Communications 4:2892 · December 2013

4.1 Critical behaviour: Specific Heat

Second order phase transition. Specific heat diverges at critical

Antiferromagnet Garnet
$NaCa_2Co_2V_3O_{12}$

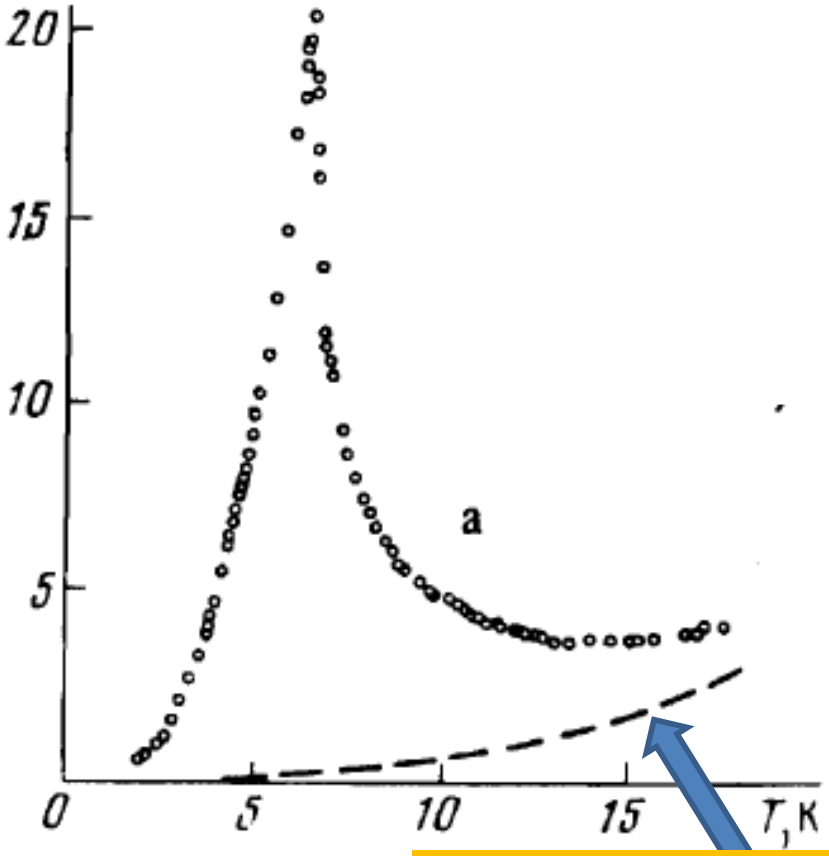

Lattice specific heat

Increasing applied field
0 to 4.5 Tesla reduces T_N

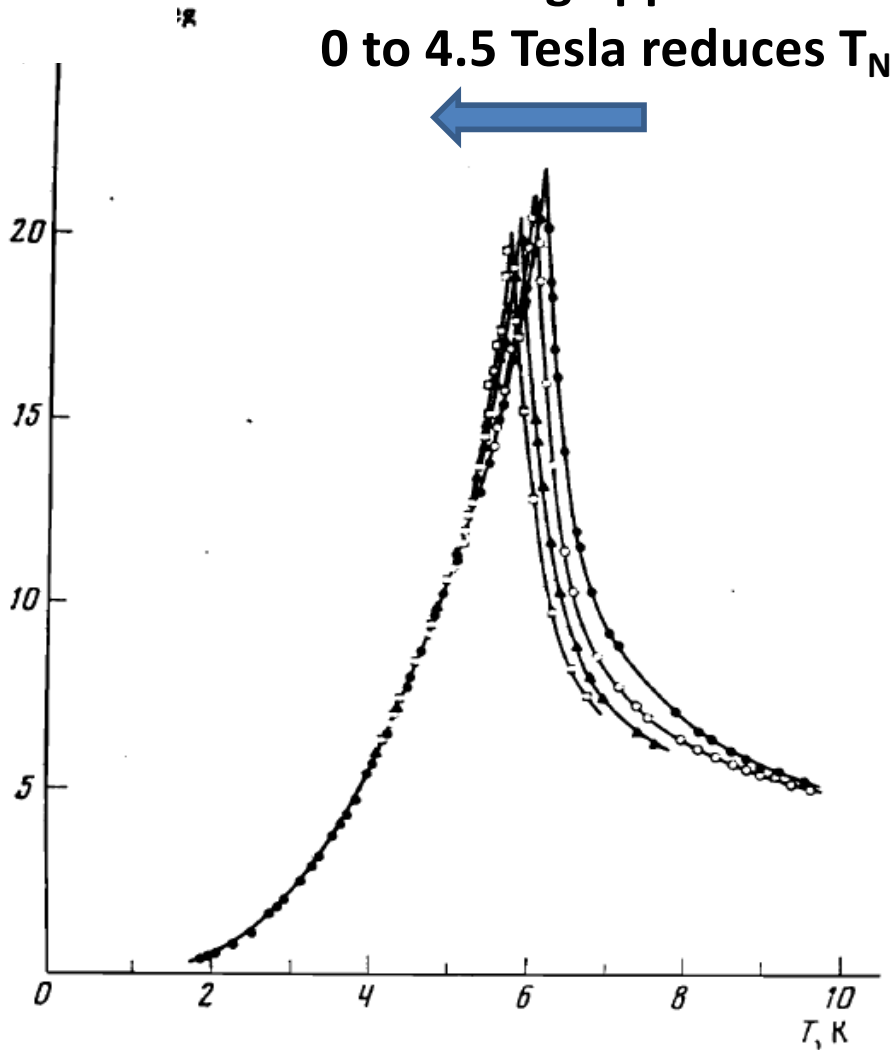

Mamsurova et al Zh. Eksp. Teor. Fiz. 69, 666, (1975)

Antiferromagnets : Specific Heat

Measurement much more difficult at higher temperatures

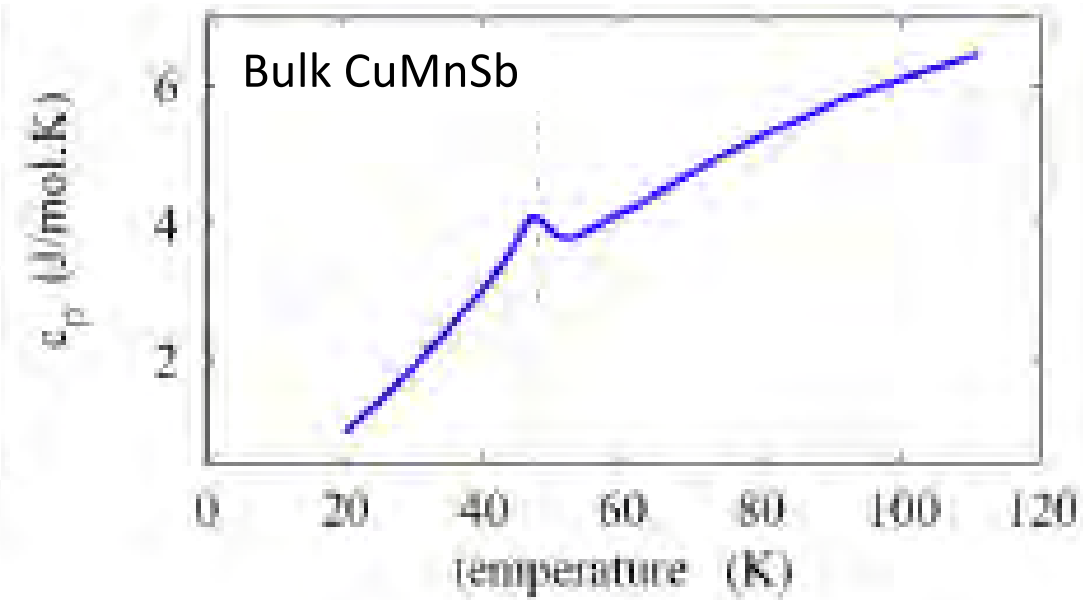

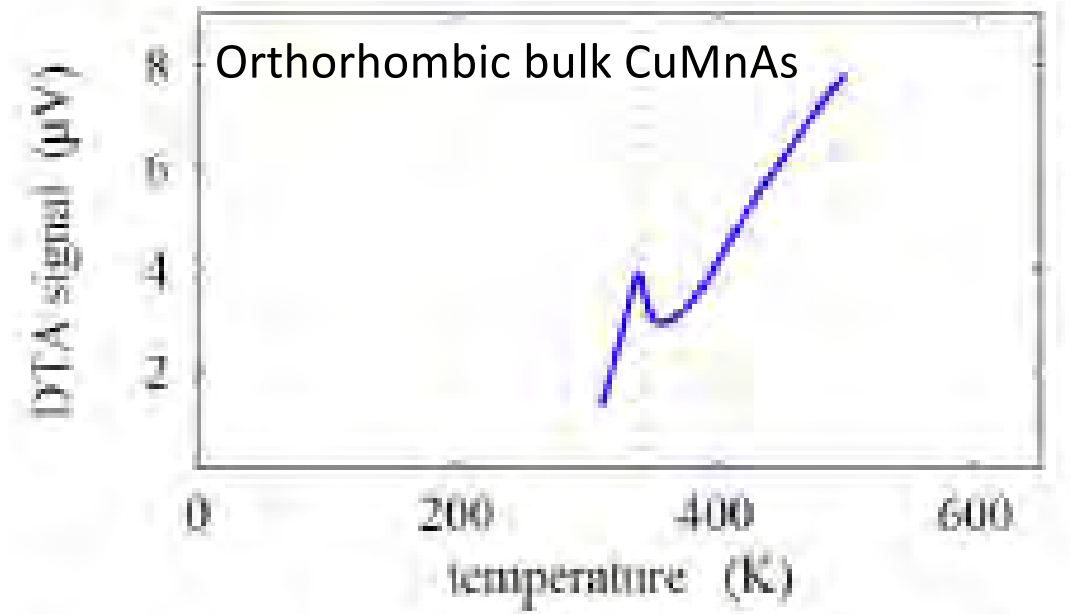

Maca et al J. Mag. Mag. Mater. 1606, 324, 8, (2012)

4.2 Critical Behaviour: Resistivity

For dense moment magnetic semiconductors the moment density >> carrier density. Only long wavelength spin fluctuations scatter carriers effectively [1] and the mobility has a peak at T_C / T_N with the same form as the susceptibility [2].

FM semiconductor EuO T_N = 73K

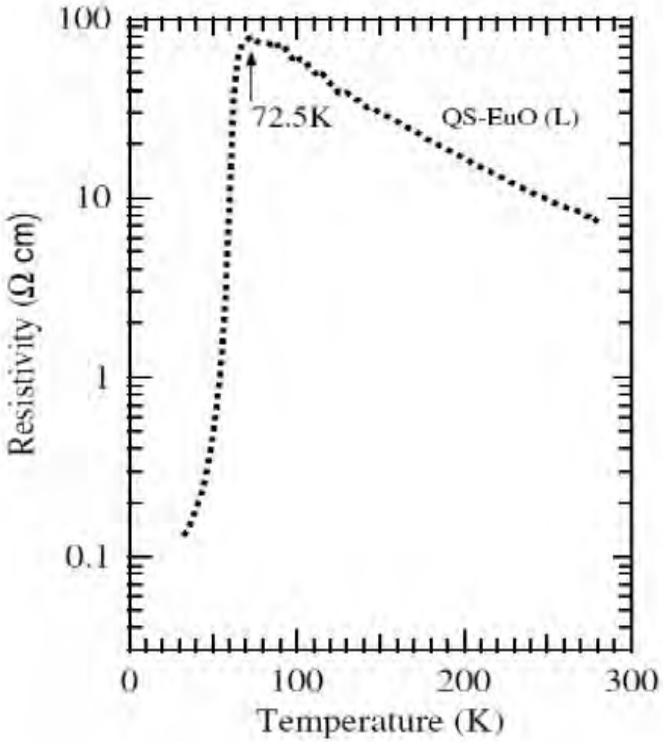

AF semiconductor MnTe T_N =310K

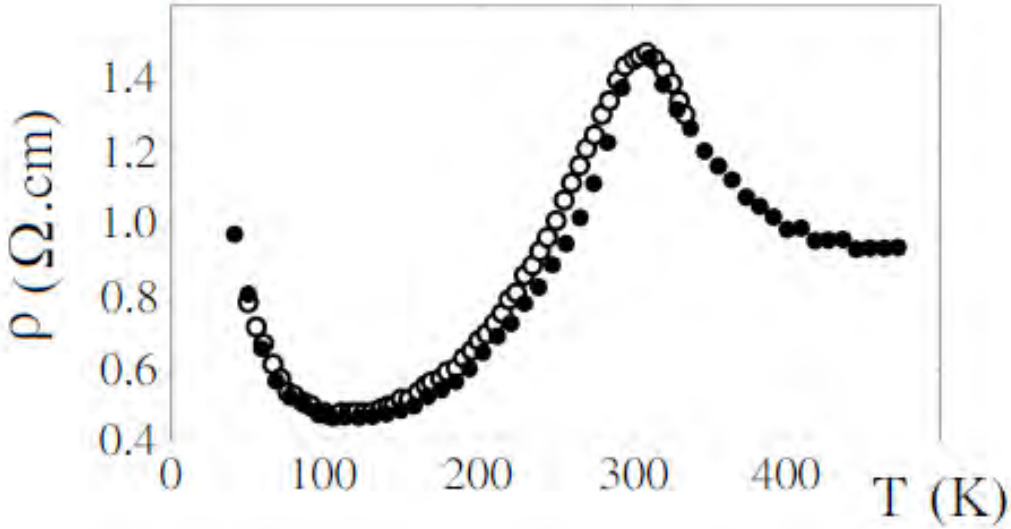

Y. Magnin and H. T. Diep Cond - Mat

Carrier density << moment density
See clear peak in resistivity at ~ T_N

*[1] de Gennes and Friedel, J. Phys. Chem. Solids **4**, 71 (1958)*
*[2] Haas, Crit. Rev. Solid State Sci. **1**, 47 (1970)*

4.2 Critical Behaviour: Resistivity

In ferromagnetic metals [1} and dilute ferromagnetic semiconductors [2] carrier density ~moment density. Critical fluctuations produce a peak in $d\rho_{xx}/dT$ at T_C with same form as specific heat [3].

FM Metal $SrRu0_3$

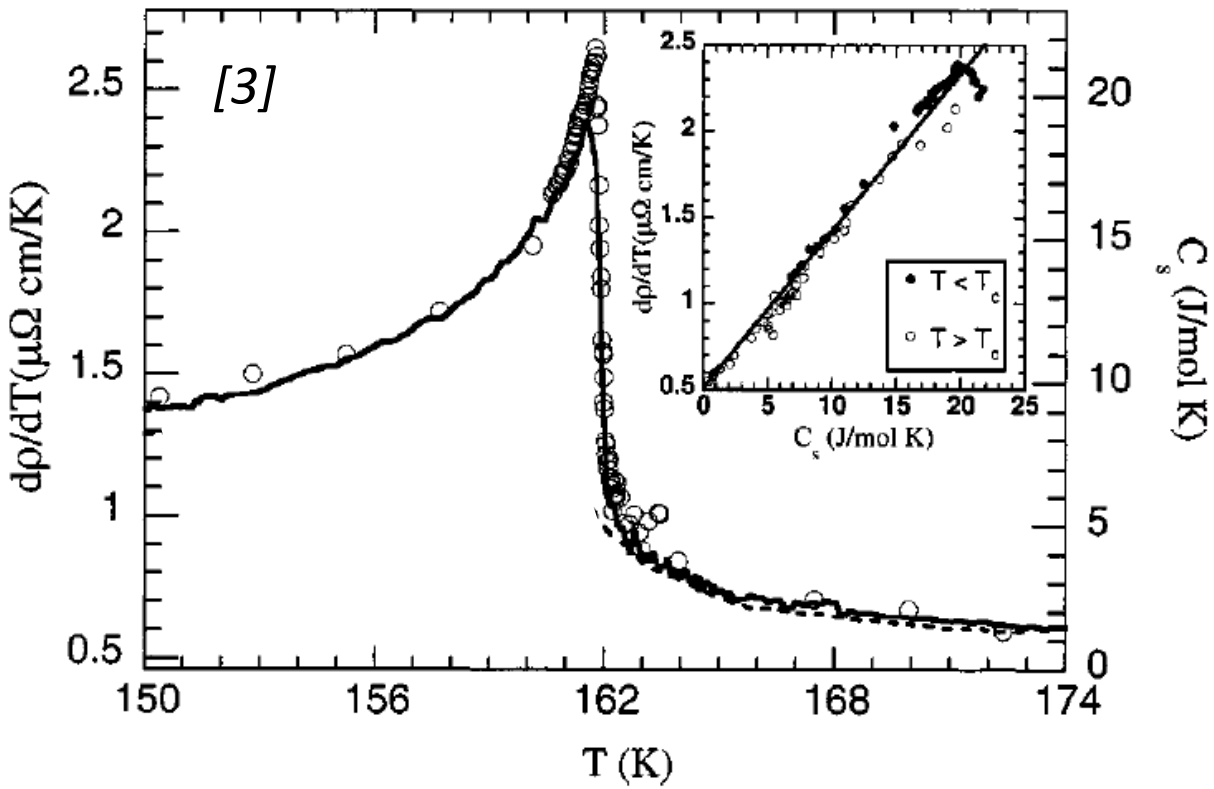

Dilute FM semiconductor

$(Ga_{88}Mn_{12})As$

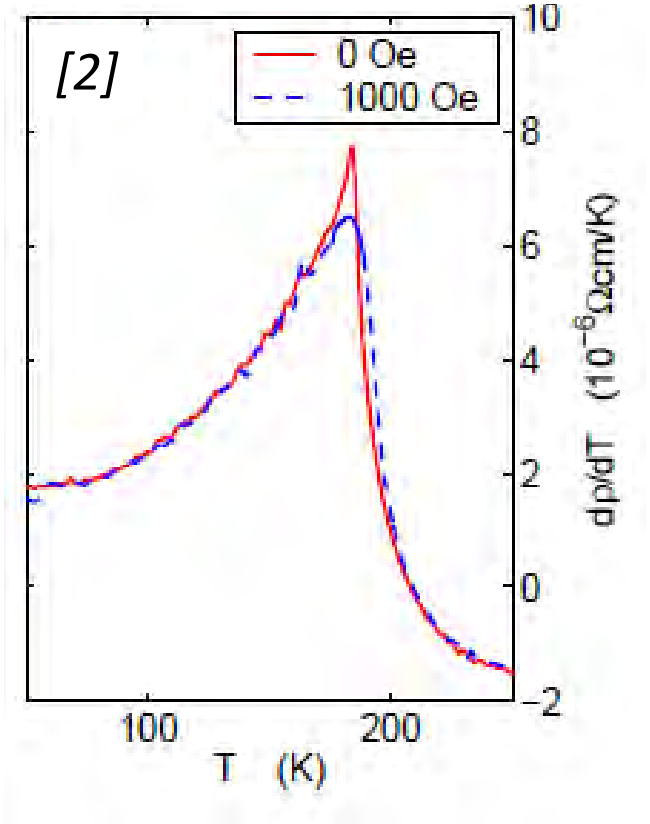

[1] Craig et al Phys. Rev. Lett. ***19****, 1334 (1967); Shacklette , et al , Phys. Rev. B* ***9****, 3789 (1974)*
[2] Novák, et al Phys. Rev. Lett. ***101****, 077201 (2008) [3] Kim, et al Phys. Rev. B* ***67****, 100406(R) (2003)*

Critical Behaviour: Resistivity

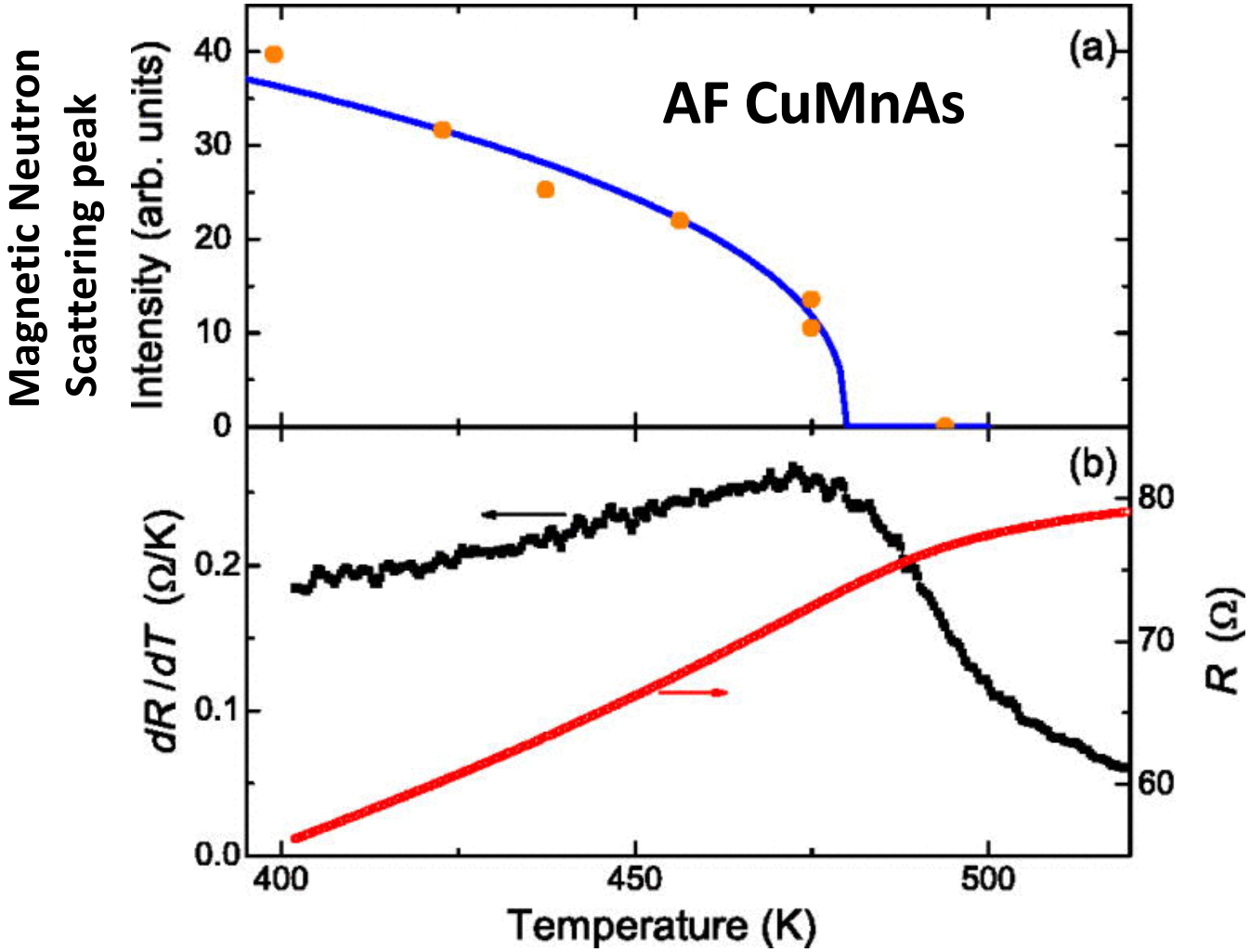

CuMnAs AF semimetal (?)
Carrier density ~ moment density
See clear peak in dR/dT at ~ T_N

Hills et al JAP 2015

AF CuMnAs with FM MnAs inclusions

CuMnAs grown with excess Mn producing
~15% by volume FM MnAs in CuMnAs matrix

MFM

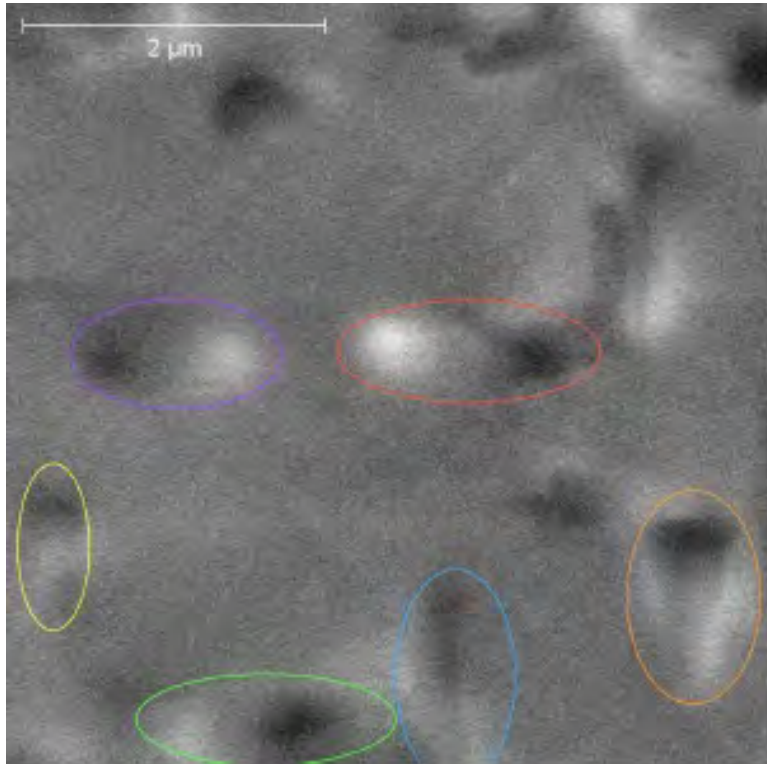

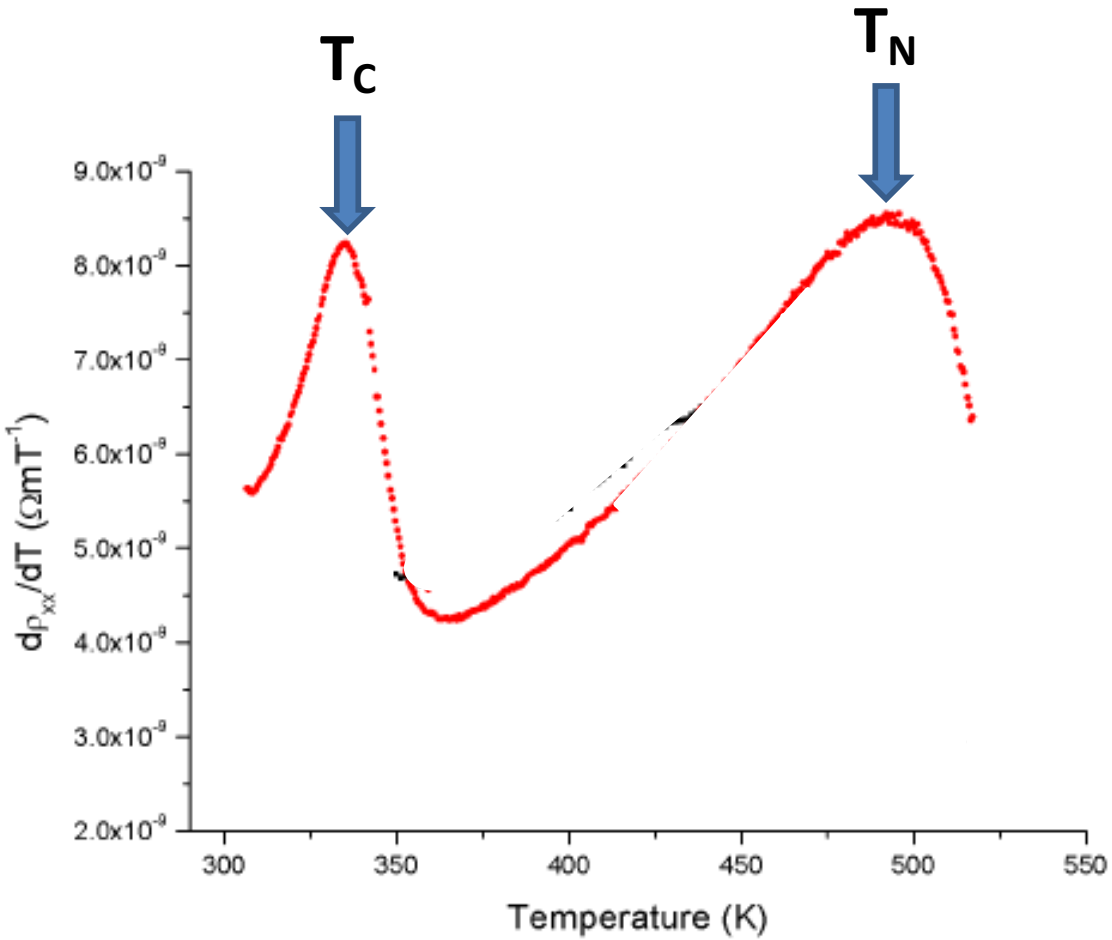

4.3 Critical Exponents

Close to a second order phase transition power law relationships between thermodynamic variables exist.

Ferromagnet **M** is order parameter

$M \propto t^{\beta}$ where t = (1-T/T_C) for T < T_C

$\chi \propto (-t)^{-\gamma}$ for T > T_C

$C_V \propto |t|^{-\alpha}$

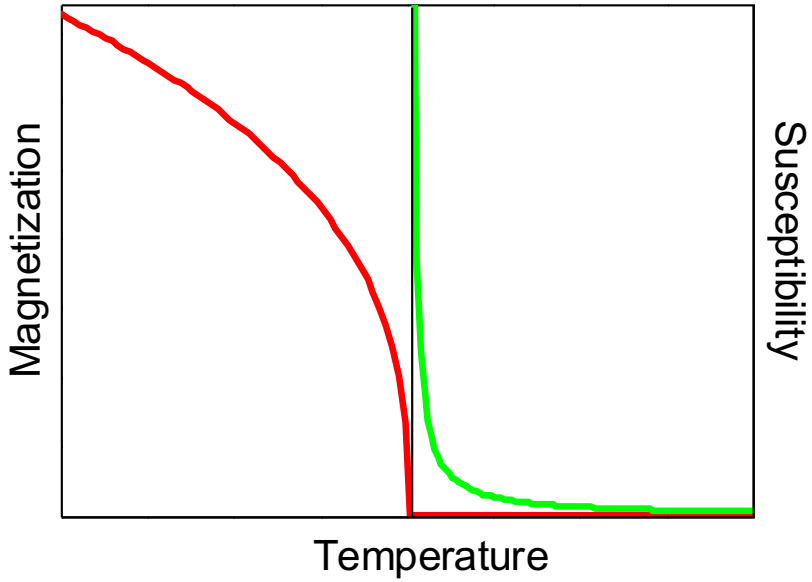

Antiferromagnet L = M_1 – M_2 is order parameter

$L \propto t^{\beta}$ where t = (1-T/T_N) for T < T_N

$C_V \propto |t|^{-|\alpha|}$

Only C_V is easy to measured accurately in an antiferromagnet.

Critical Exponents

The values of the exponents close to the critical temperature often depend only on the dimensionality and symmetry of the system and belong to a small number of universality classes.

	α	β	γ
Mean Field	0	0.5	1.0
Ising	0.11	0.326	1.237
3D Heisenberg	-0.134	0.369	1.396

Determining critical exponents can give information on dimensionality of moment system and range of exchange interactions.

FM (Ga,Mn)As	??	0.366 +/- 0.003	1.47 +/- 0.05

Three-dimensional Heisenberg critical behaviour in the highly disordered dilute ferromagnetic semiconductor (Ga,Mn)As *M. Wang, R. A. Marshall, K. W. Edmonds, A. W. Rushforth, R. P. Campion, and B. L. Gallagher* ***Physical Review B*** *93, 184417* ***(2016)***

Critical Exponents of Antiferromagnets

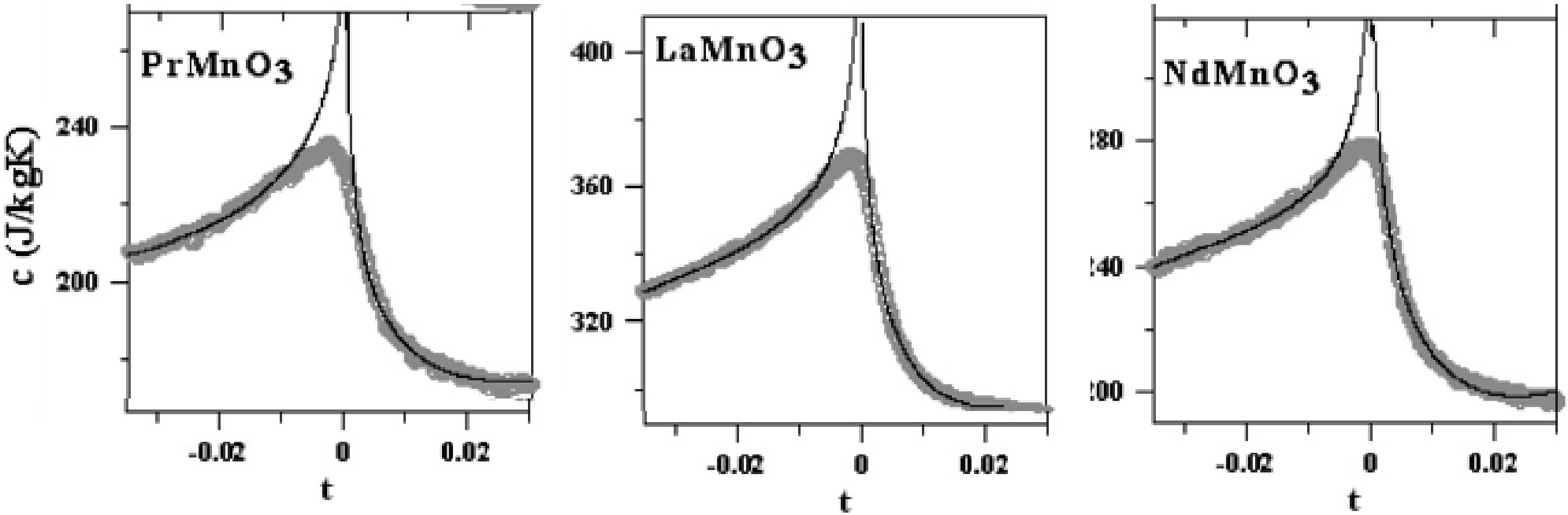

Fitting functions used to obtain critical exponent α

$$c = B + C(T - T_N) + A^+|T - T_N|^{-\alpha}(1 + E^+|T - T_N|^{0.5}) \qquad T > T_N$$

$$c = B + C(T - T_N) + A^-|T - T_N|^{-\alpha}(1 + E^-|T - T_N|^{0.5}) \qquad T < T_N$$

Eight free parameters plus choice of fitting temperature range

Conclude α = -0.11 +/- 0.01 3D Heisenberg value

A Oleaga[1], A Salazar[1], D Prabhakaran[2] and A T Boothroyd[2]

J. Phys.: Condens. Matter 17 (2005) 6729–6736

5. X-ray magnetic dichroism

Peter Wadley tomorrow

Lab x-ray source

- **fixed energy (*e.g.*, Cu Ka)**
- **unpolarized**

Synchrotron x-ray source

- **controllable energy (sub-eV → 100s of keV)**
- **high flux, high coherence**
- **controllable polarization (linear or circular)**
- **BUT limited availability**

X-ray Magnetic Circular Dichroism (XMCD)

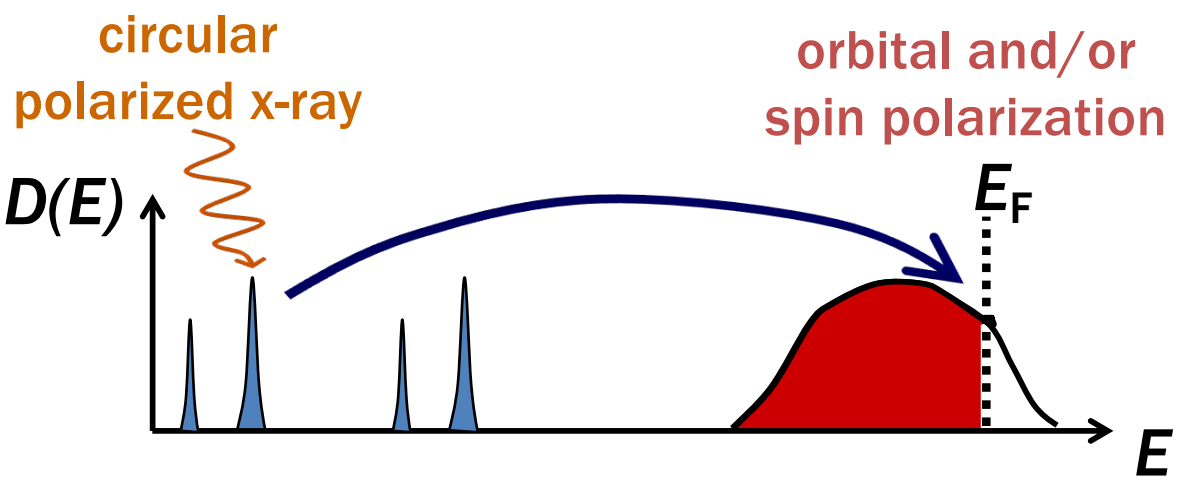

Magnetic Dichroism: Polarization Dependent Absorption

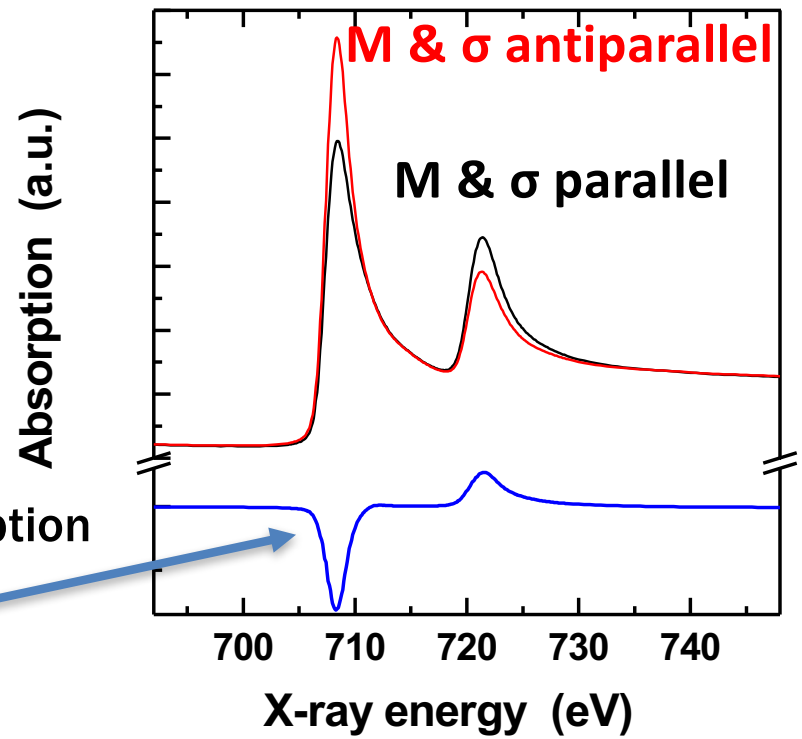

Difference = x-ray magnetic circular dichroism (XMCD)

- Probes unfilled local density of states around excited atom
- Combined chemical and magnetic probe
- Element-specific magnetometer
- Depth-dependent information
- Semi-quantitative (orbital and spin magnetic moments per atom)

X-ray Magnetic Circular Dichroism (XMCD)

FM (Ga,Mn)As

$2p \rightarrow 3d$ transitions

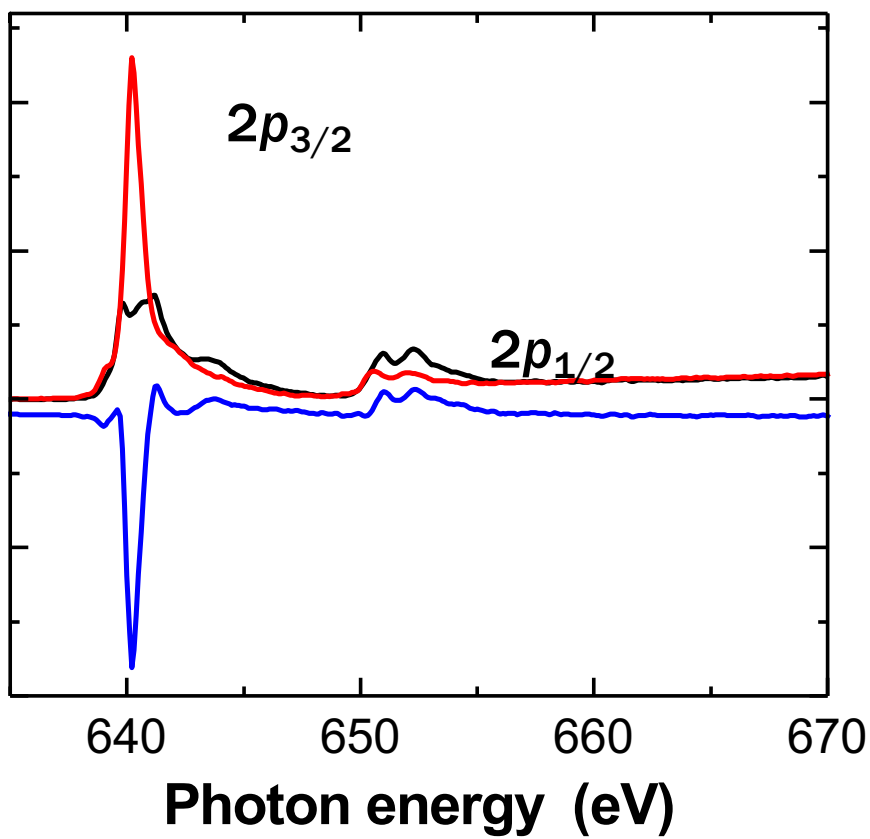

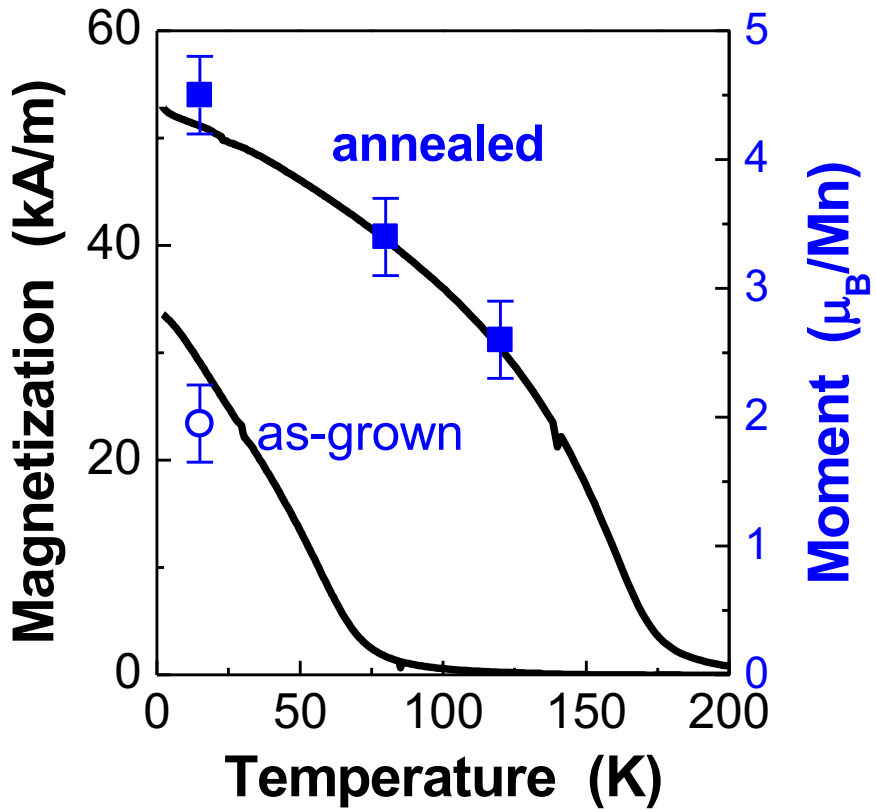

<u>Sum rules:</u> **integrated absorption** $\rightarrow$ **orbital and spin magnetic moments**

Sum rule reference: Paolo Carra, et al Phys. Rev. Lett. 70, 694 1993

X-ray Magnetic Circular Dichroism (XMCD)

X-ray magnetic circular dichroism (XMCD)

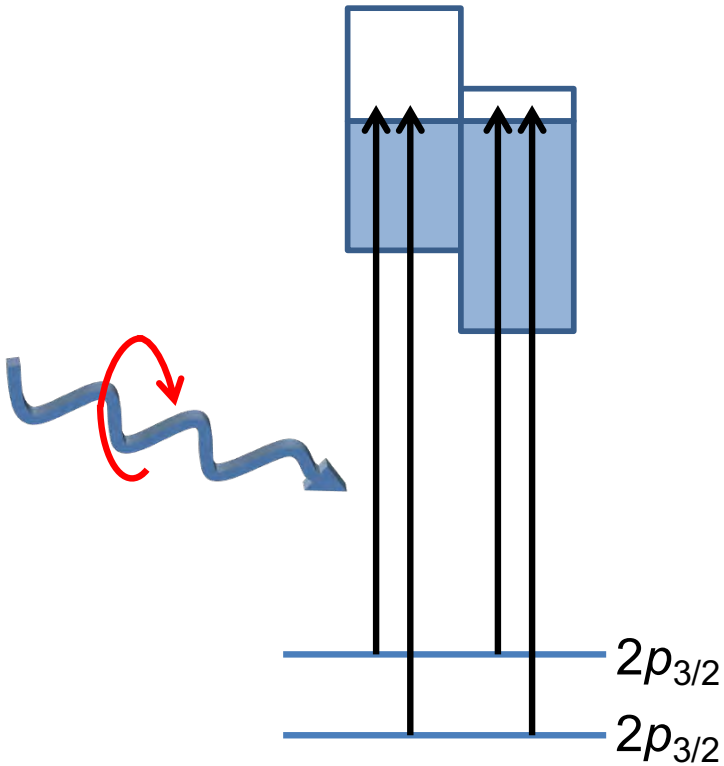

Sensitive to unpaired spin or orbital magnetic moments, *ie* **ferromagnetic order**

X-ray linear dichroism (XLD)

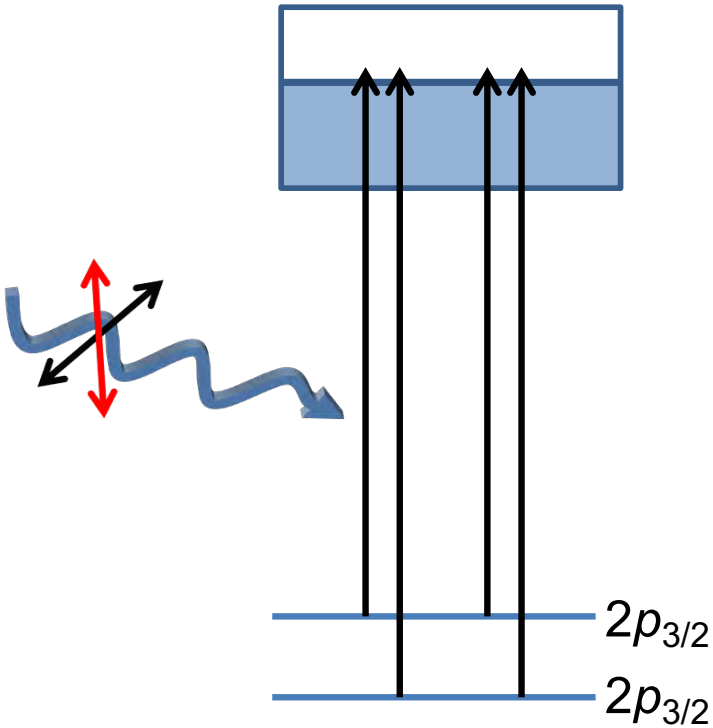

Sensitive to electric, magnetic or structural anisotropies, *including* **antiferromagnetic order**

XMLD AF CuMnAs

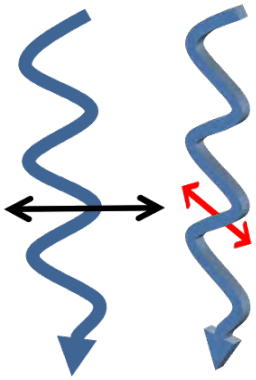

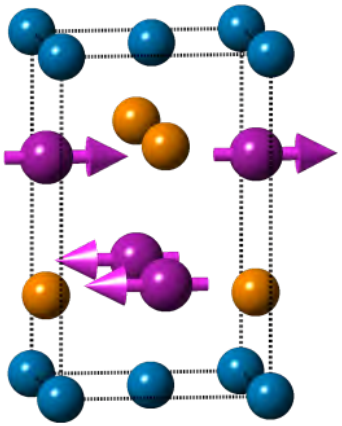

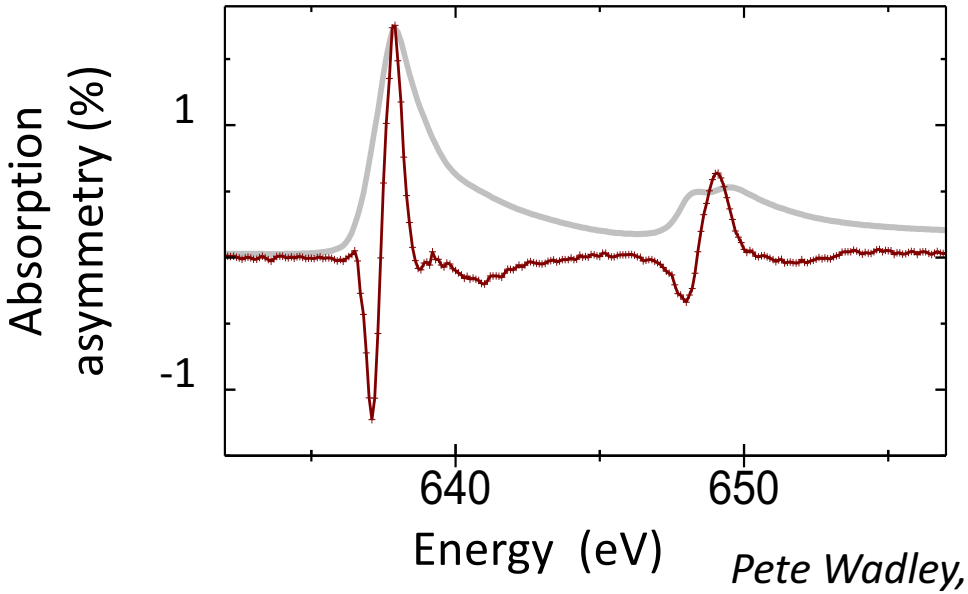

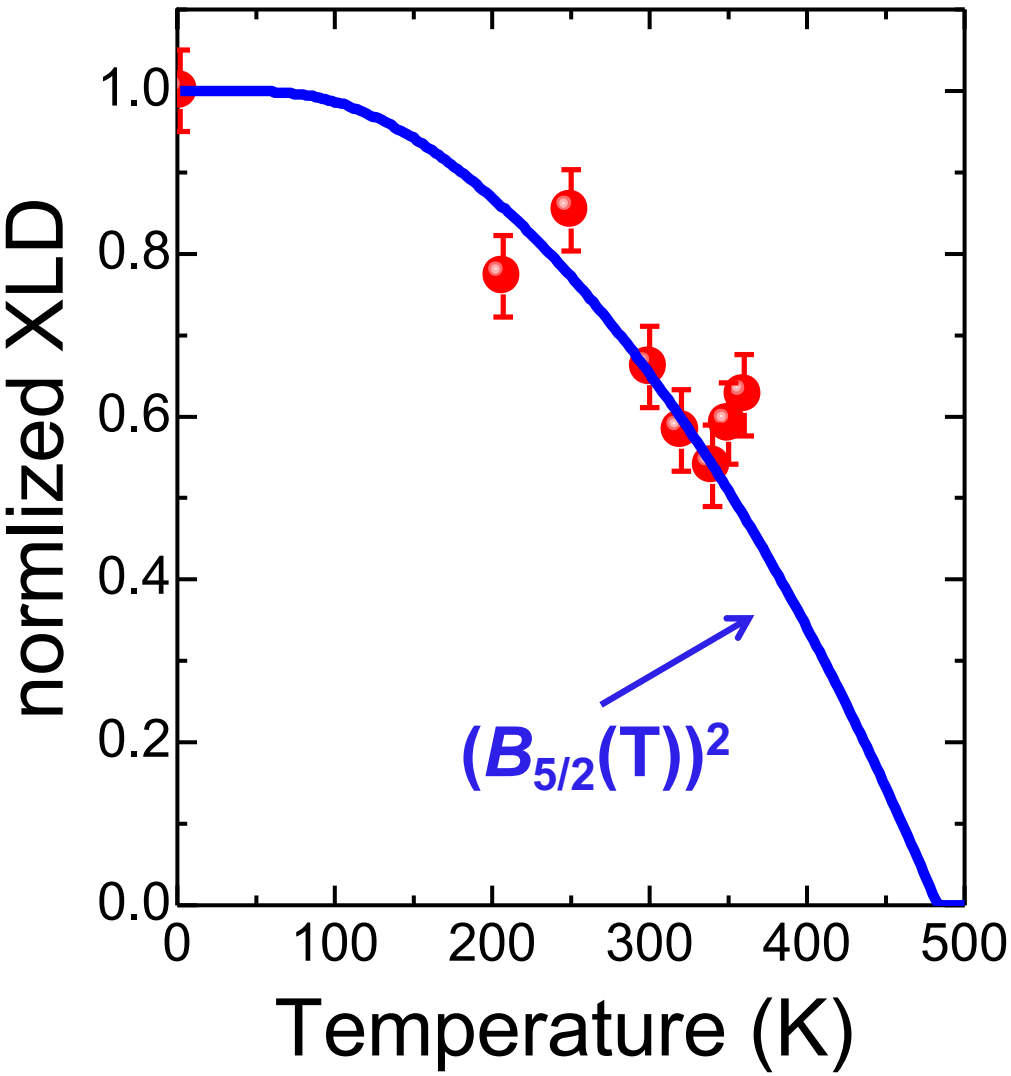

Pete Wadley, et al. SCIENTIFIC REPORTS 5, 17079 (2015)

XMLD ➡ thin CuMnAs layers uniaxial

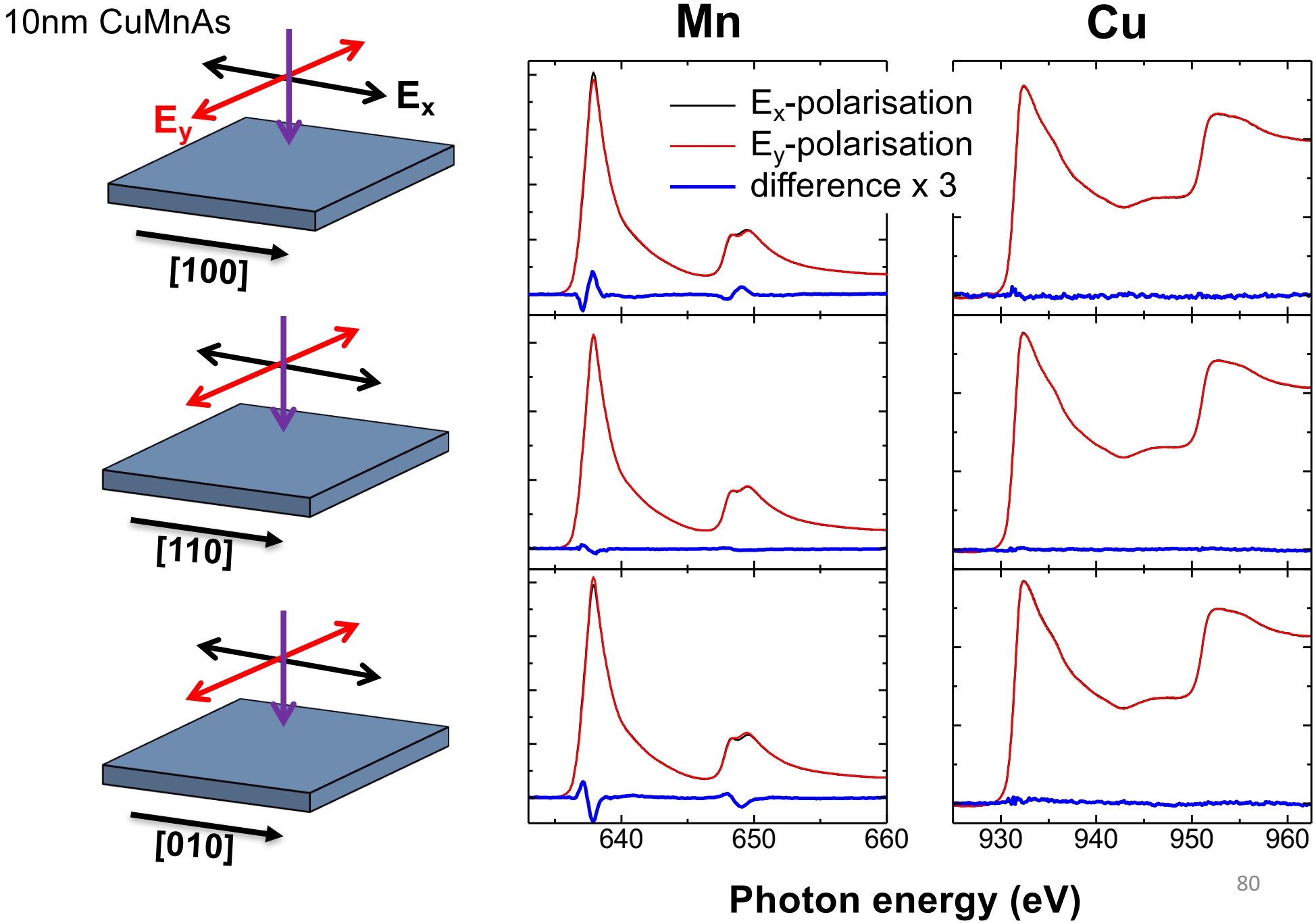

Spatial resolution

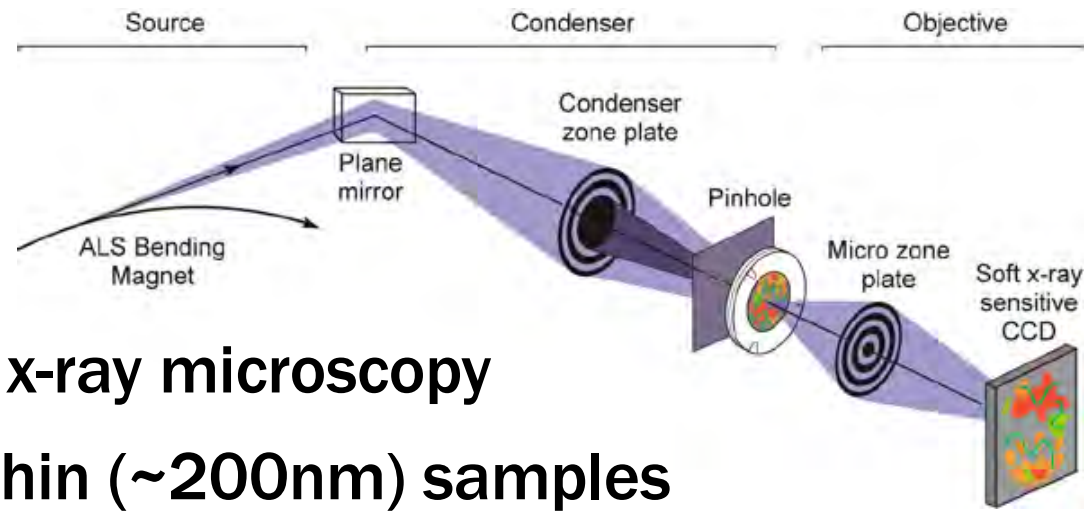

1. Scanning transmission x-ray microscopy

- powerful, but limited to thin (~200nm) samples

2. X-ray photoelectron emission microscopy (X-PEEM)

- collect and focus secondary electrons
- surface sensitive

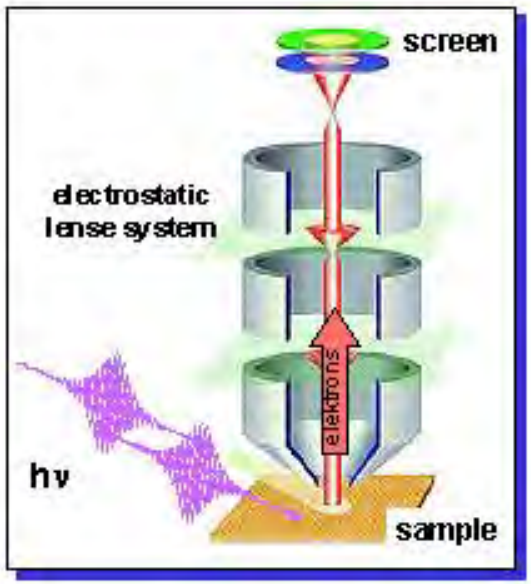

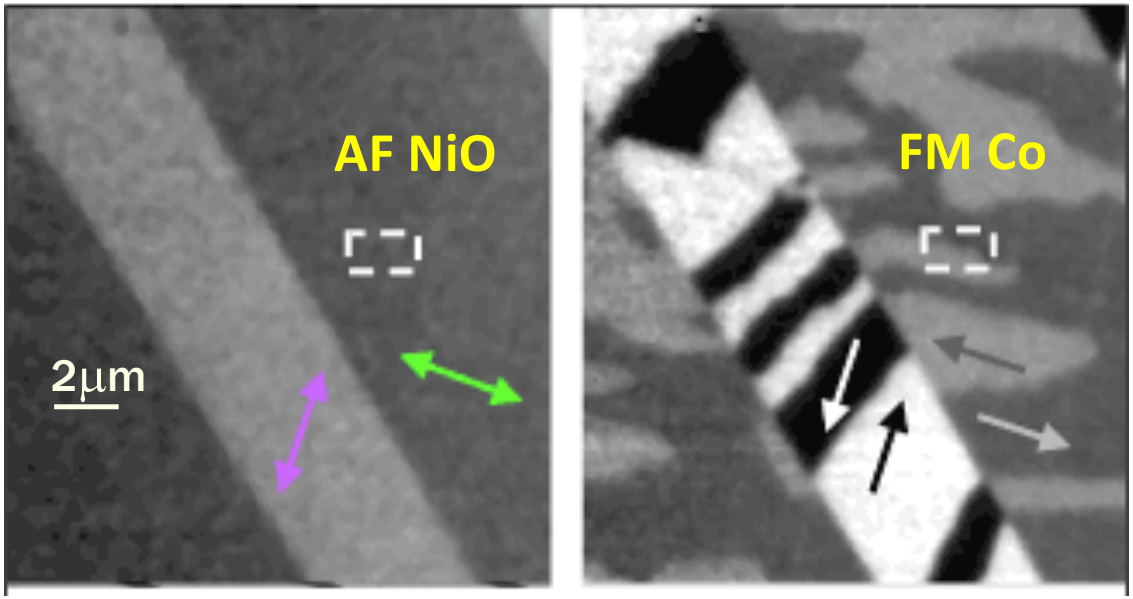

Imaging exchange coupling in AF NiO/ FM Co bilayers

Ohldag et al., PRL 86, 2878 (2001)

XMLD X-PEEM CuMnAs domains

40nm CuMnAs layer: uniaxial anisotropy with 180° domain walls

Peter Wadley tomorrow

40 μm field-of-view

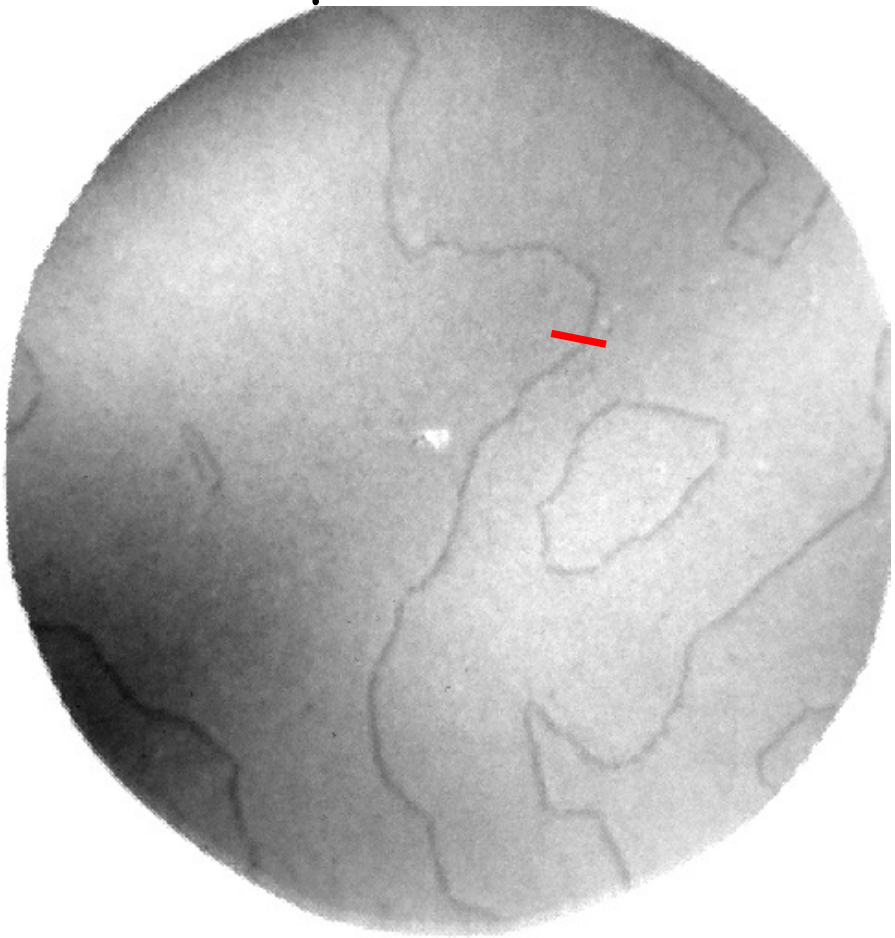

Uniaxial Domains

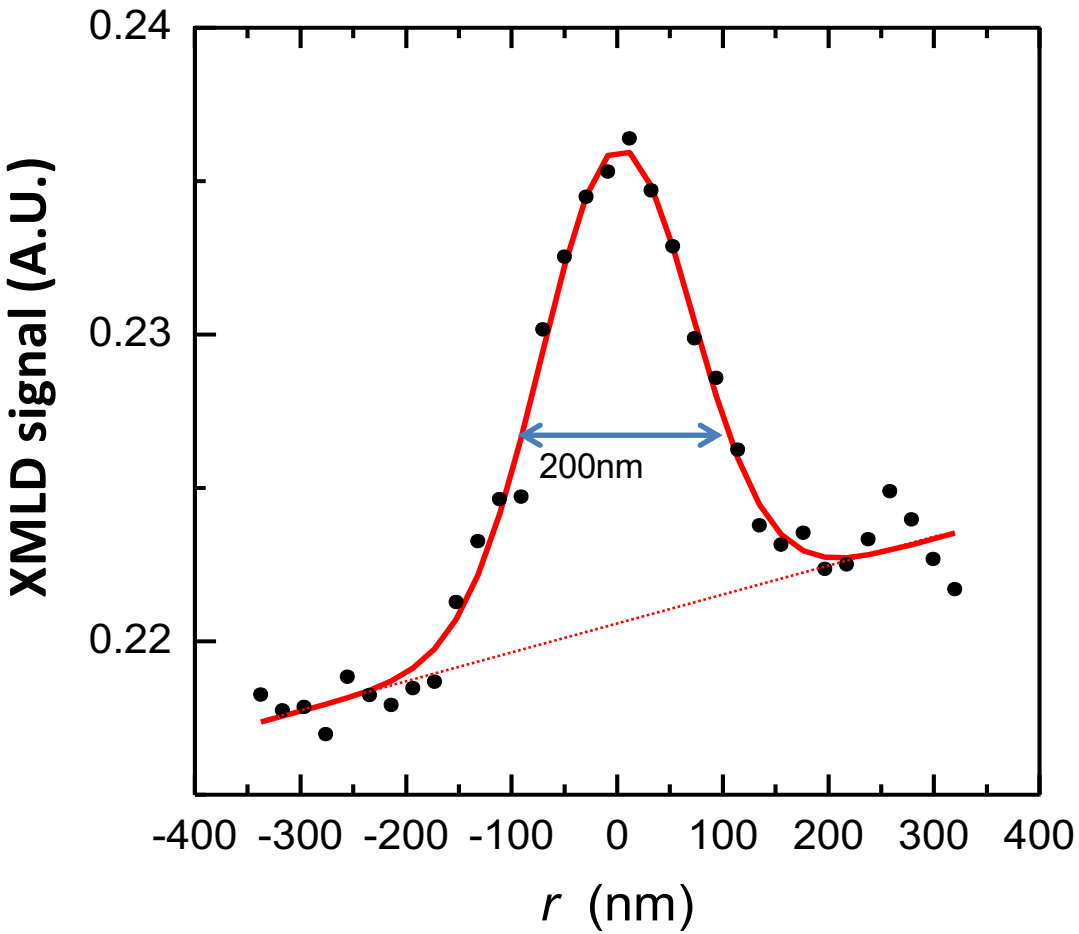

Domain Wall Profile

6 Spin-Polarised Scanning Tunnelling Microscopy (SP-STM)

Tunnelling current depends on local spin dependent densities of states

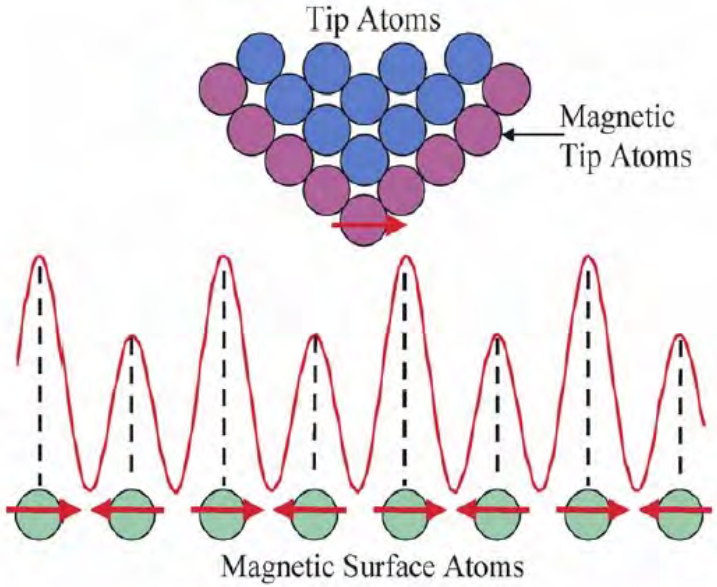

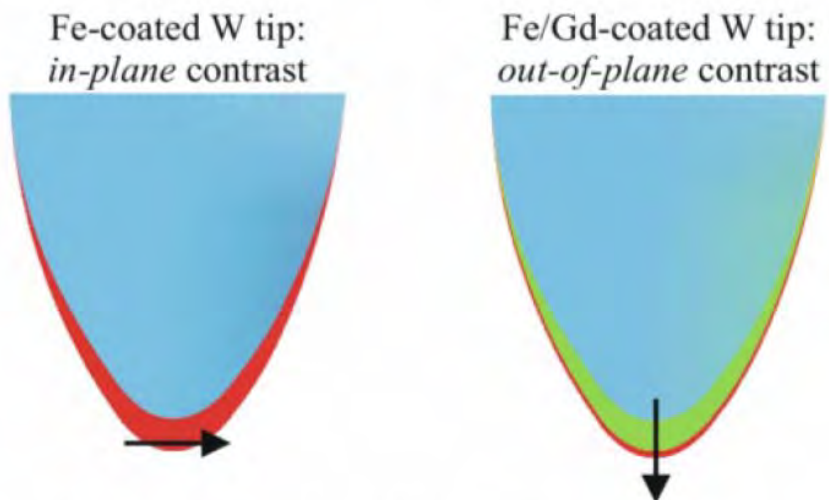

- Atomic resolution
- Sensitive to surface monolayer and few subsurface monolayers
- Need near perfect surfaces: no oxidation etc
- Usually produce sample within UHV STM system by deposition or cleavage.
- Surface properties may not reflect bulk properties: surface reconstructions, uncompensated moments etc.

SP-STM AF Mn_3N_2

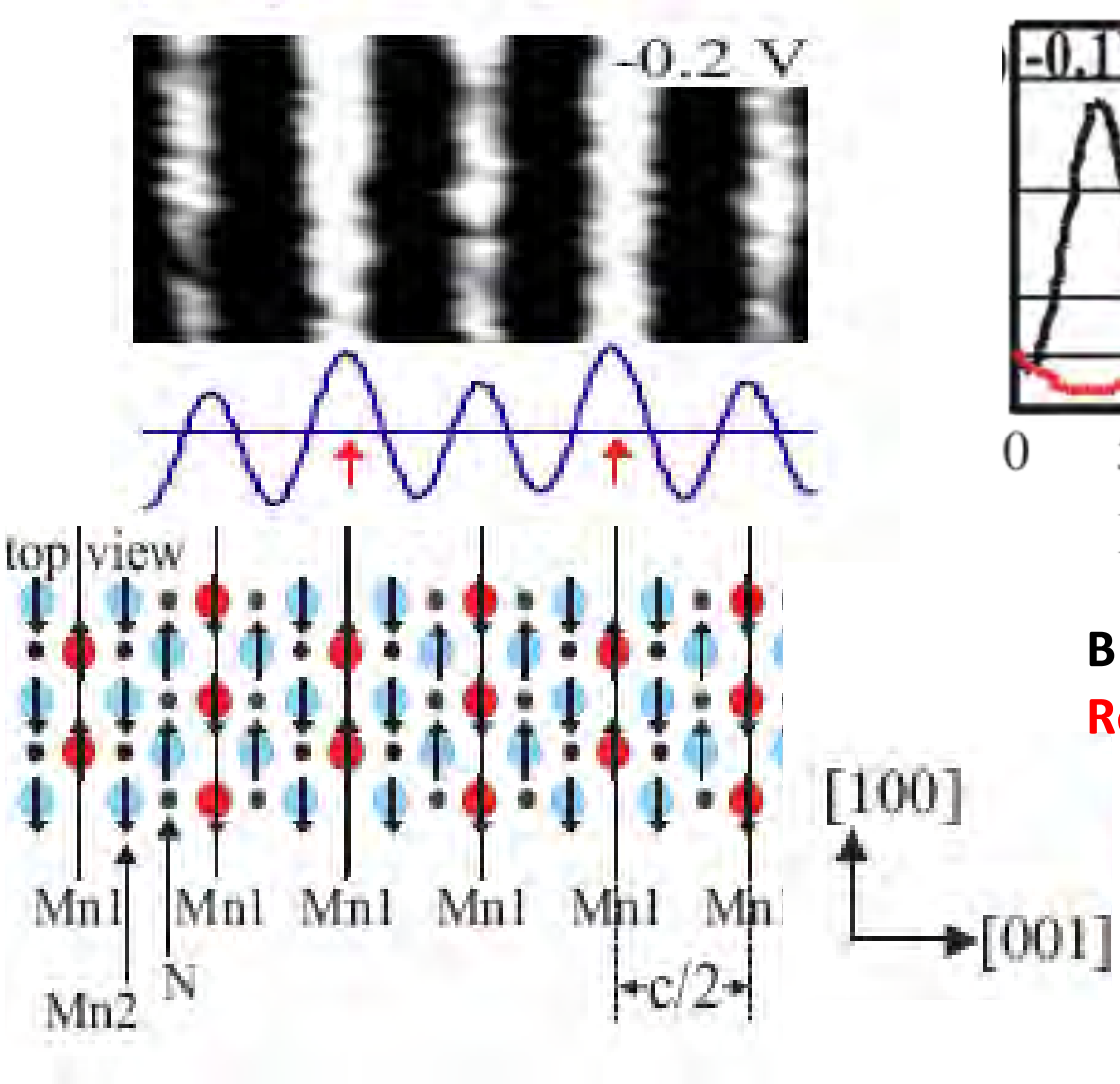

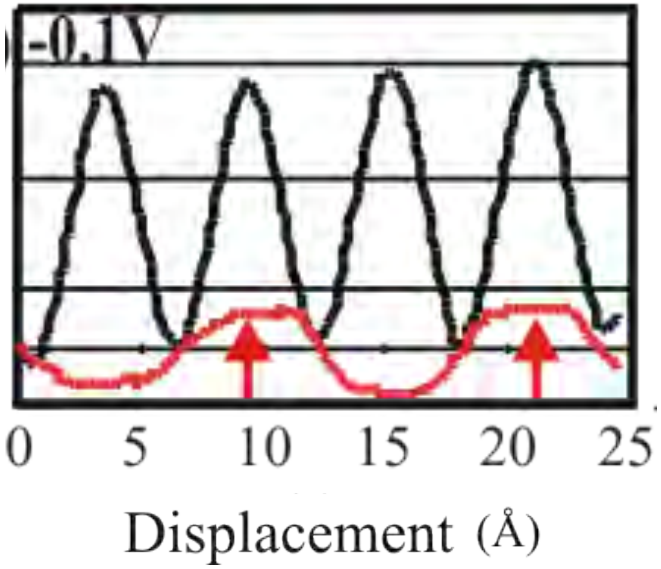

Black structural signal

Red magnetic signal

Yang et al https://arxiv.org/pdf/cond-mat/0510147.pdf

SP-STM AF Mn_3N_2

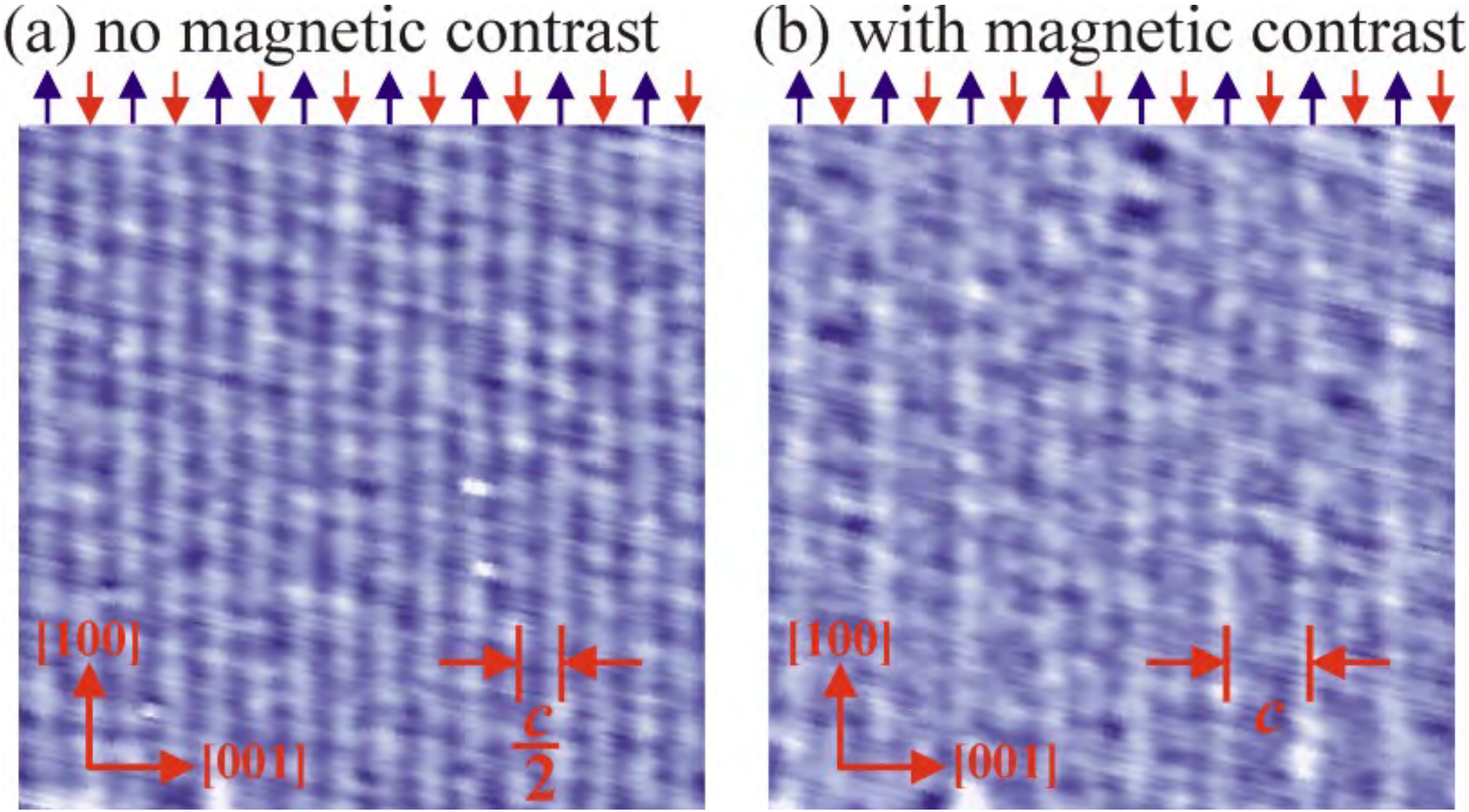

SP-STM: Atomic spin structure of an antiferromagnetic wall

Deposit Iron monolayer on (001) surface of Tungsten. Iron layer antiferromagnetic

Right: Simulated (grey) and measured (colour) SP-STM signals

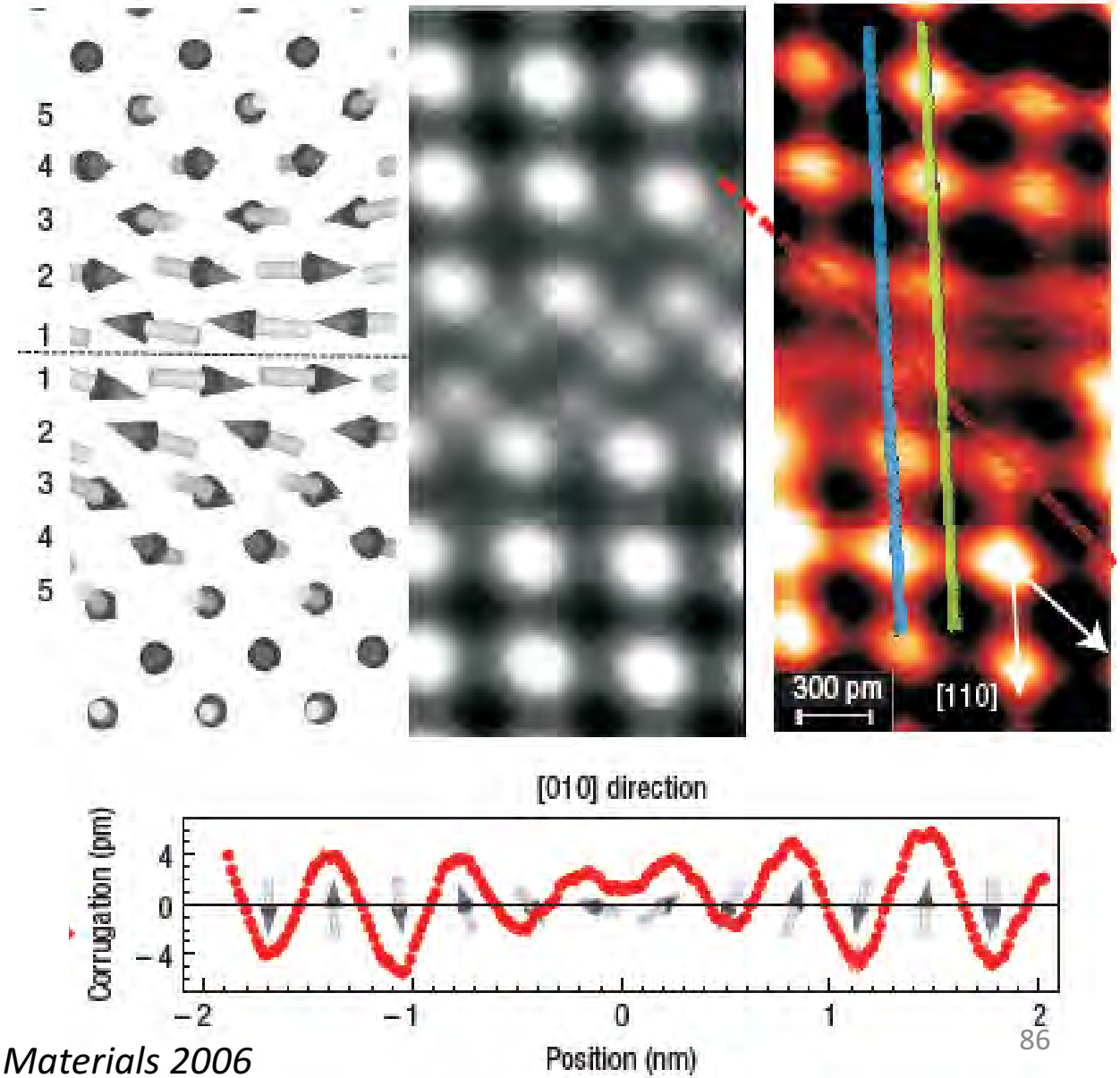

M. BODE, …Wiesendanger et al Nature Materials 2006

SP-STM AF Mn_3N_2

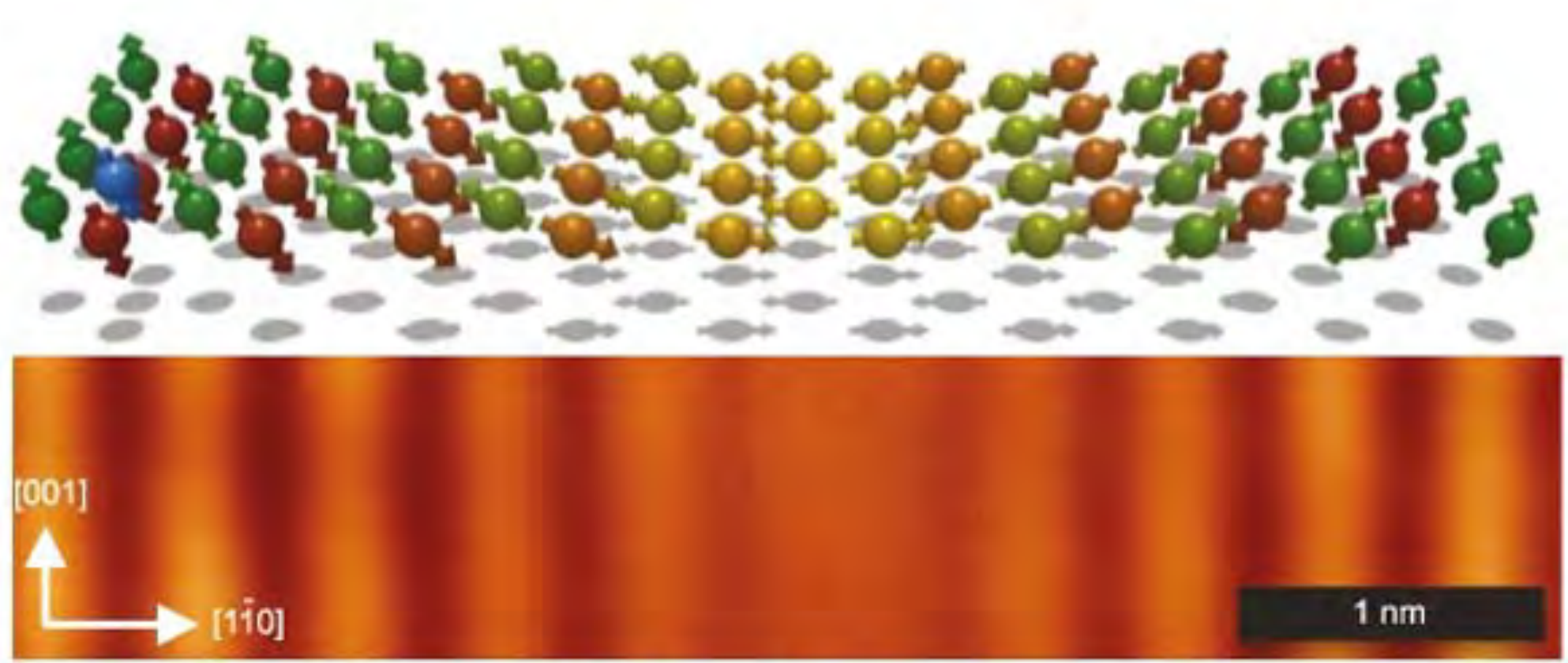

(a)The spins of the antiferromagetic manganese surface in a spin-spiral state.

(b) Out of plane SP-STM image showing the anti-parallel spins.

End / Jump ?

Boris Wolter,.....,Roland Wiesendanger, et al Phys. Rev. Lett. ***109*** *116102*

AMR ?


Advanced
Recovery


AMR
AUSTRALIAN MINIATURE HORSE & PONY REGISTRY


Angry Monkeys
Racing


Alaskan Malamute Rescue


How it Works!

5.1 Anisotropic Magnetoresistance (AMR)

"Normal" Non Crystalline AMR

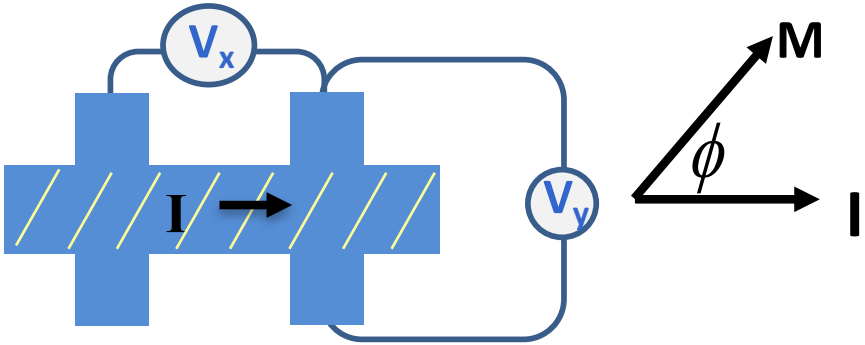

Hall Bar

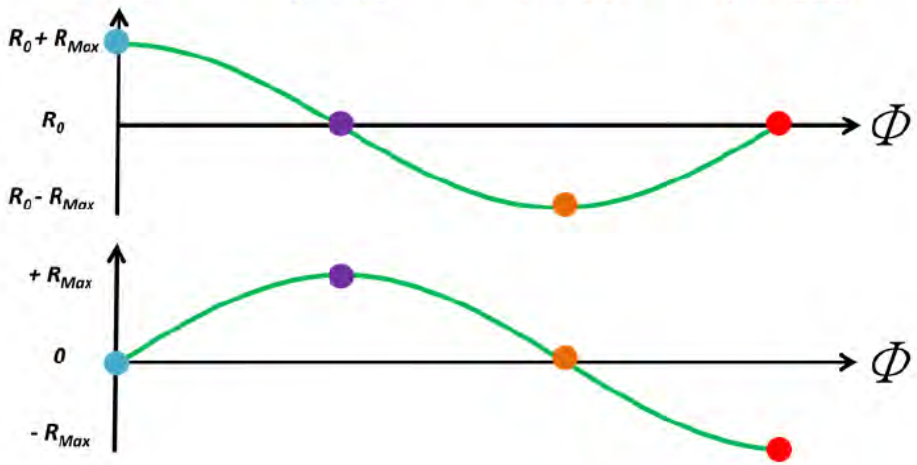

$$\rho_{xx} = \rho_0 + \Delta\rho \cos 2\phi \qquad \rho_{xy} = \Delta\rho \sin 2\phi$$

Resistance depends on relative orientation of Magnetisation and current.

Only contribution for isotropic (e.g. polycrystalline) materials.

FM (Ga,Mn)As: Measured AMR

GaMnAs 5% Mn 25nm epilayer.
Fixed field of 1 Tesla rotated in plane @ 4.2 K

4 Hall Bars along 4 crystal directions

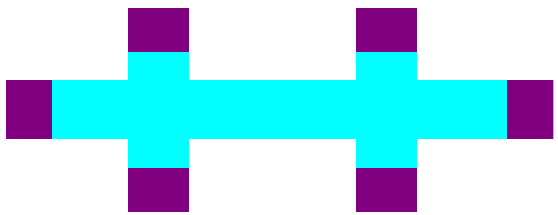

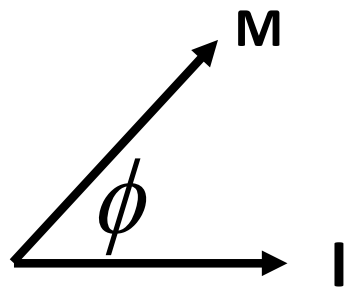

Find size of measured AMR Depends on crystallographic orientation of the Hall bar

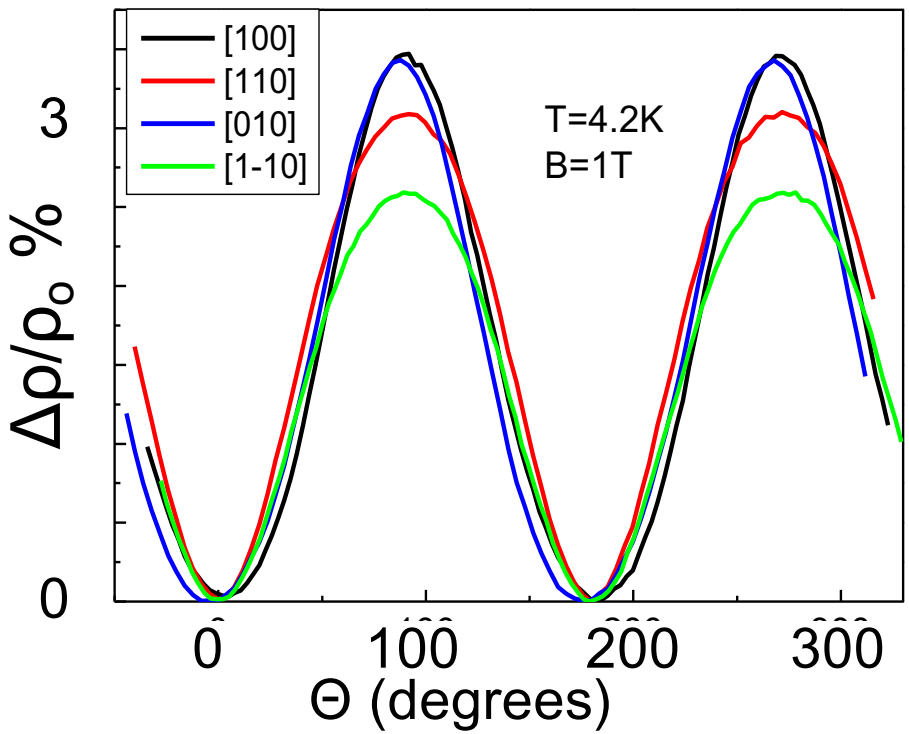

FM (Ga,Mn)As: Measured AMR

Corbino Disk. Current radial.
Zero non-crystalline AMR

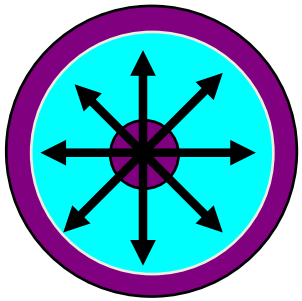

Measured AMR depends on relative orientation of magnetisation and crystallographic axis.

"Small" Bi-axial and uniaxial magneto-crystalline contributions

GaMnAs 5% Mn 25nm epilayer.
1 Tesla field rotated in plane @ 4.2 K

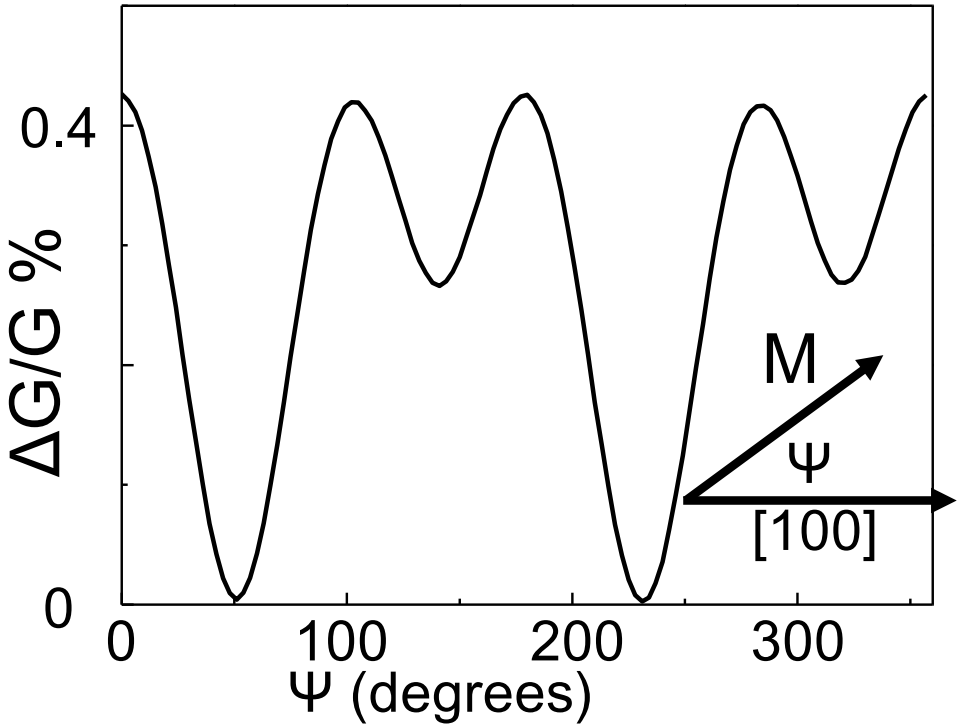

$$\frac{\Delta\rho_{xx}}{\rho_{av}} = C_I \cos 2\phi + C_U \cos 2\psi + C_C \cos 4\psi + C_{I,C} \cos(4\psi - 2\phi) + C_{I,U} \sin(6\psi - 2\phi) + \ldots$$

$$\frac{\Delta\rho_{xy}}{\rho_{av}} = C_I \sin 2\phi + C_{I,C} \sin(4\psi - 2\phi) + C_{I,U} \cos(6\psi - 2\phi) + \ldots.$$

Rushforth et al., PRL 99, 147207 (2007)

Antiferromagnetic AMR: FeRh

FeRh: AF to FM transition at ~400K.

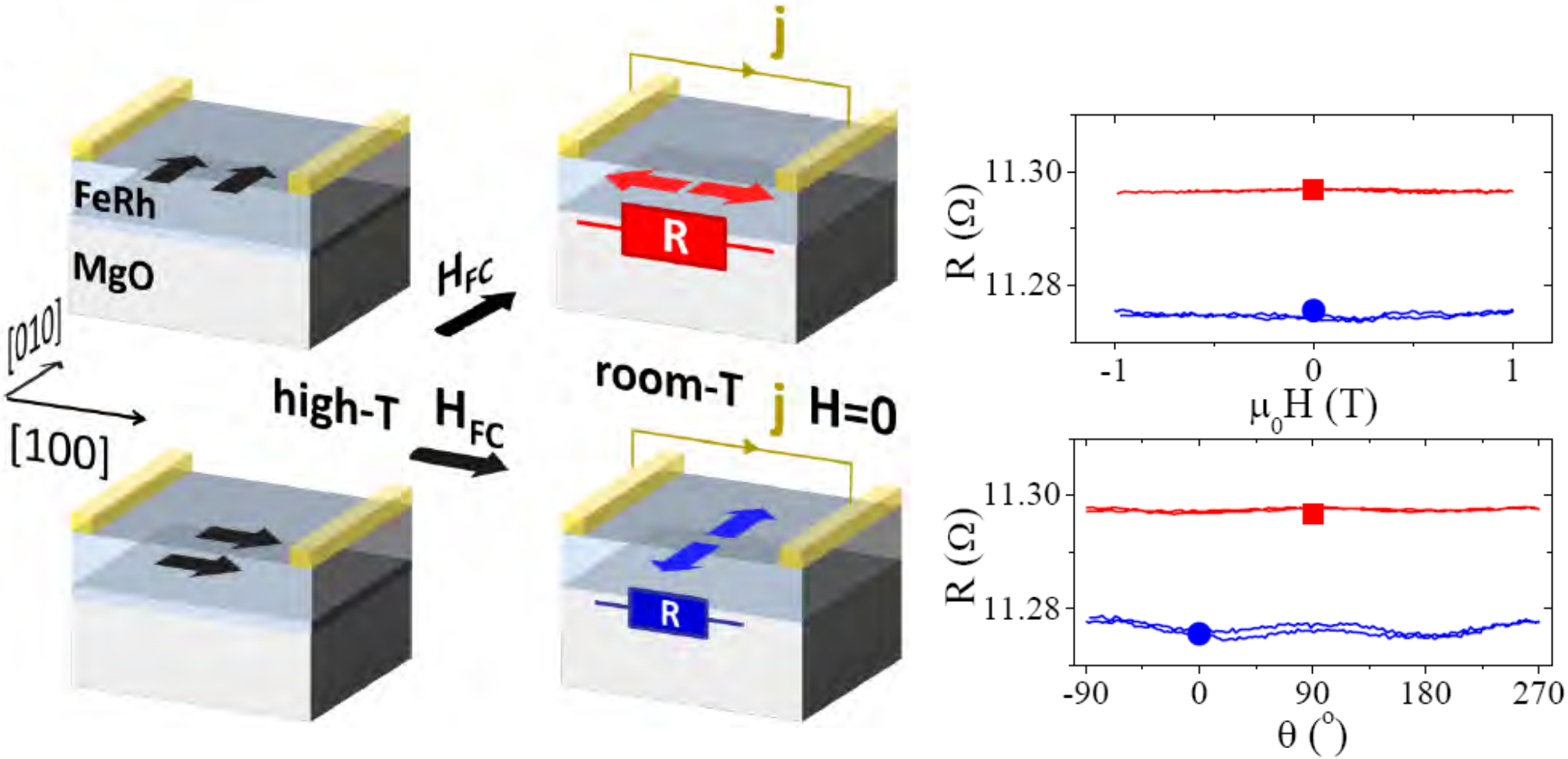

Cool in field through the FM to AF transition temperature:
Spins flop into direction perpendicular to applied field.

Marti, et al. Nature Mater. (2014)

Antiferromagnetic AMR: α-MnTe

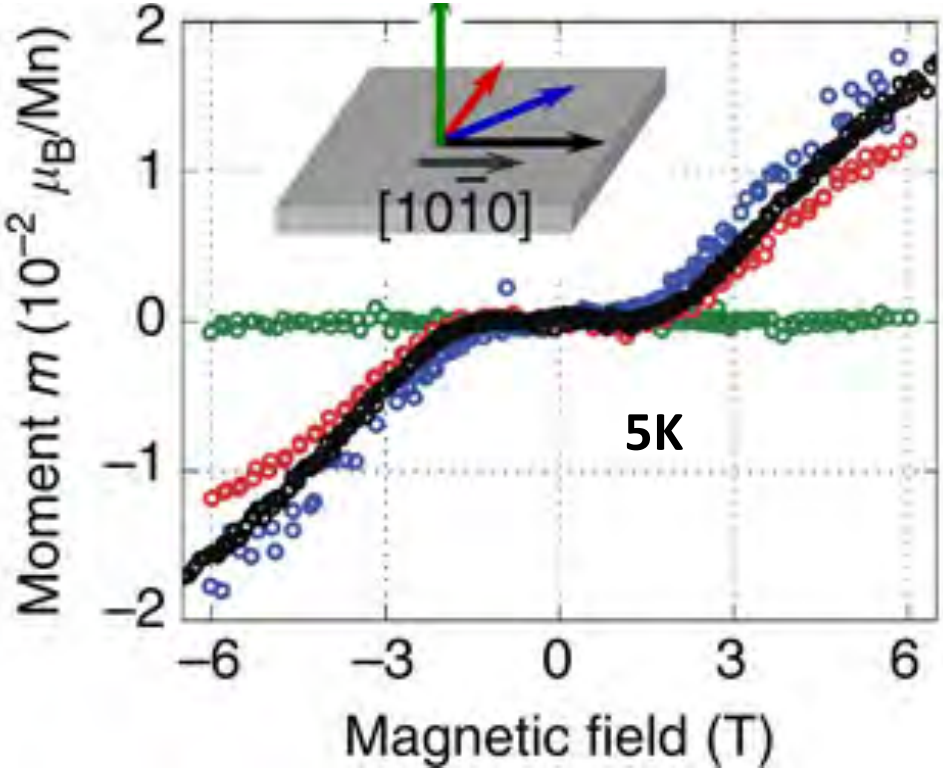

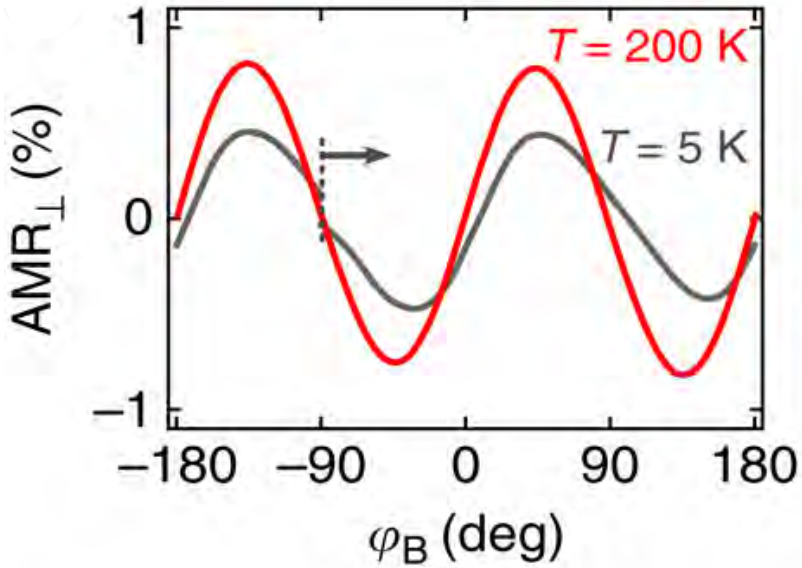

2 Tesla field rotated in plane

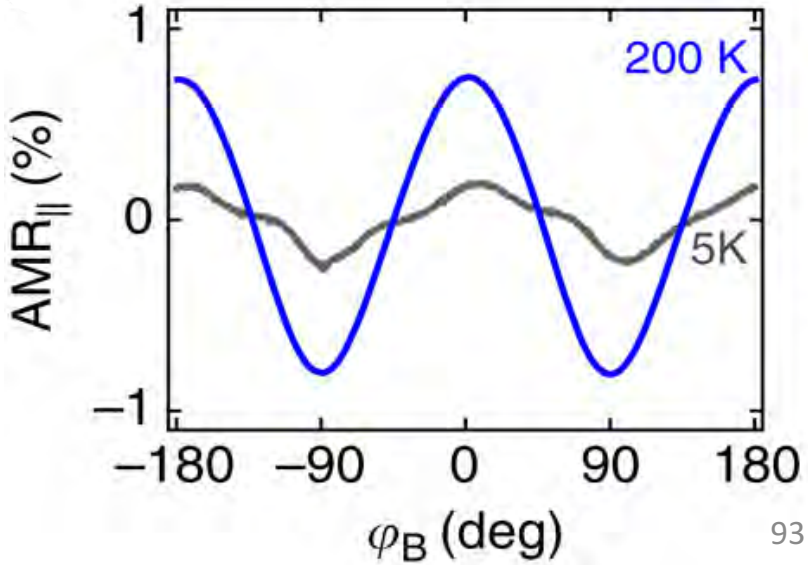

Applied field leads to Spin flop plus domain modification

Kriegner, et al. Nature Commun. '16

Antiferromagnetic AMR: α-MnTe

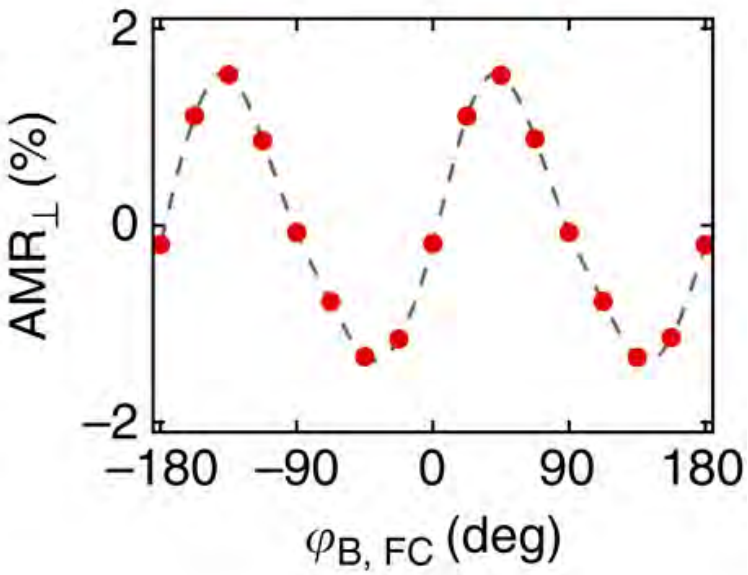

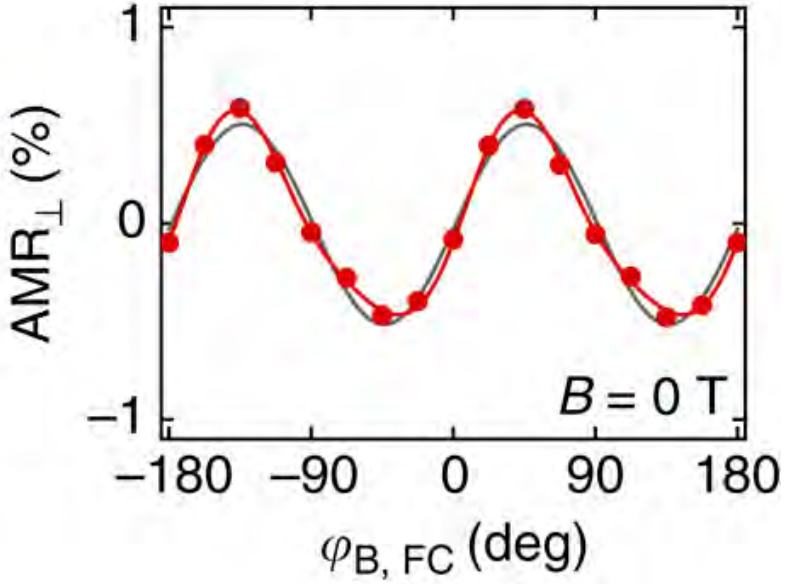

Cooled in 2 Tesla field from 350K to 200K then field left on.

Cooled in 2 Tesla field from 350K to 200K then field removed.

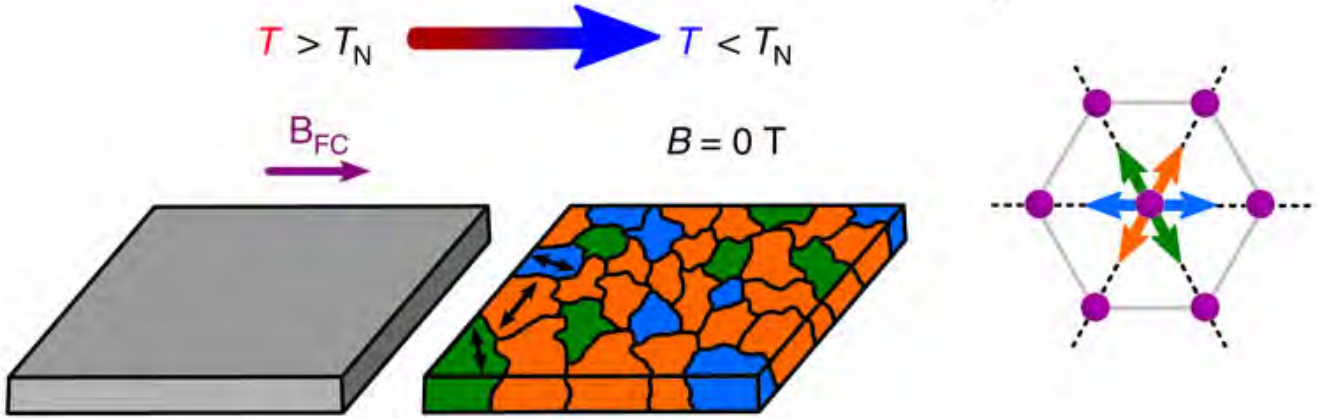

Kriegner, et al. Nature Commun. '16

5.2 Tunnelling Anisotropic Magnetoresistance (TAMR)

Single magnetic contact. Tunnelling density of states depends on relative orientation of magnetisation and crystal axes due to spin-orbit interaction.

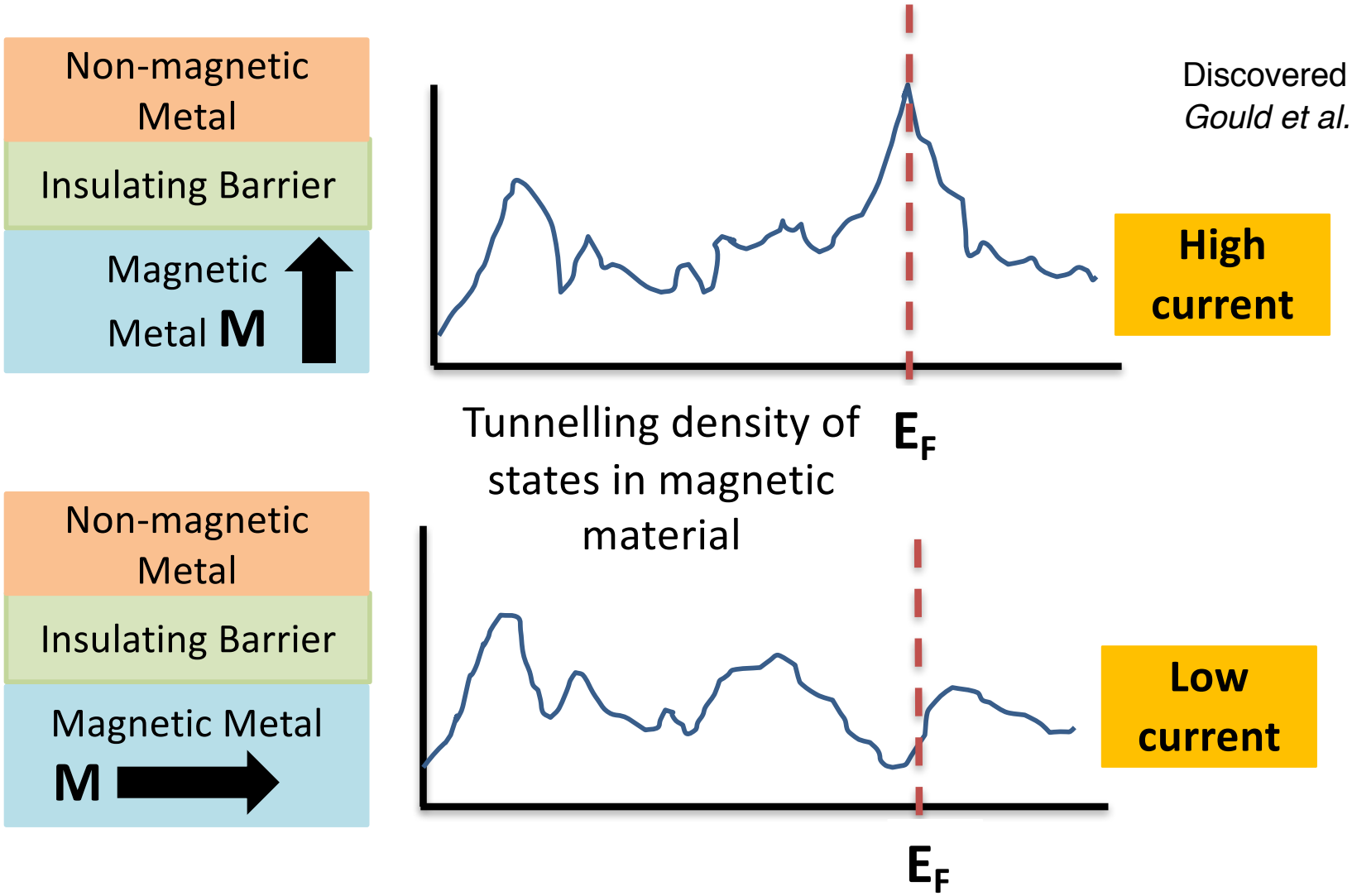

Discovered in GaMnAs
Gould et al. 2004

Antiferromagnetic TAMR

Exchange bias used to control AFM moments

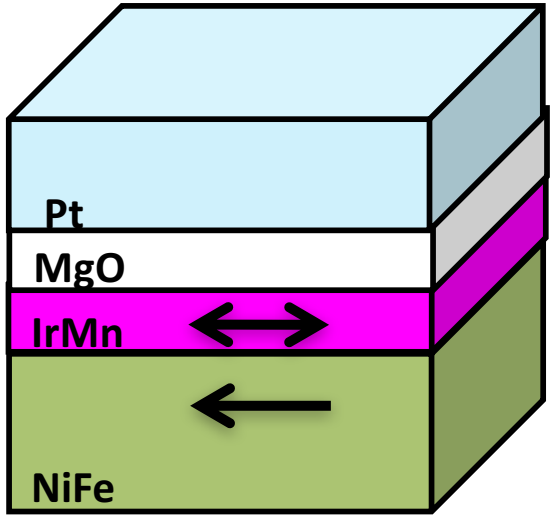

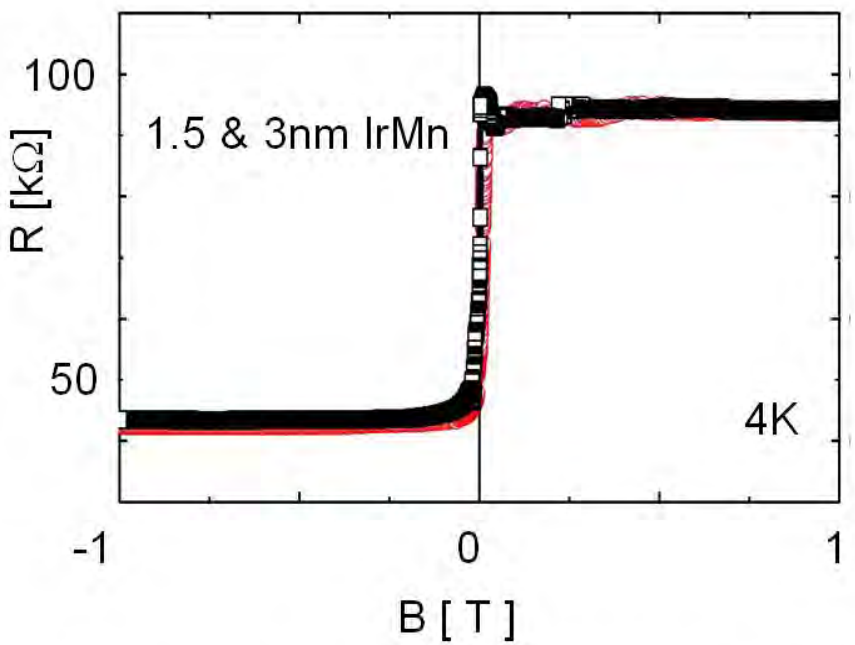

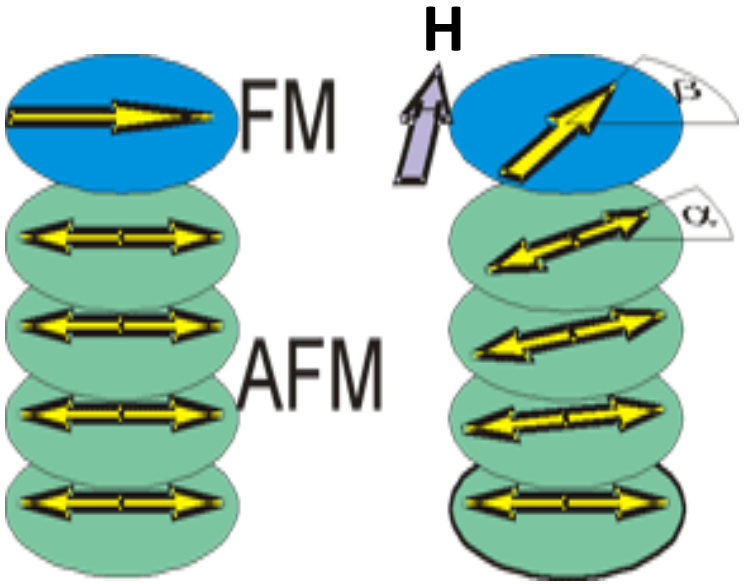

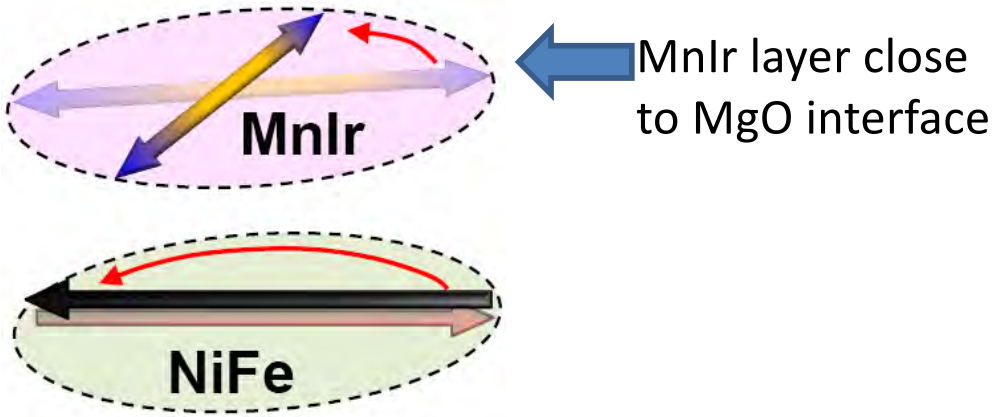

Park et al. Nature Mat. 2011, PRL 2012 Wang et al. PRL 2012:

The End

The Detective Dick Tracy (1930s)